Supporting Information

for

Heterogenous preparations of solution-processable cobalt phthalocyanines for carbon dioxide reduction electrocatalysis

Elahe Tajbakhsh, Declan McKearney, Daniel B. Leznoff,* and Jeffrey J. Warren*

Department of Chemistry, Simon Fraser University, 8888 University Drive, Burnaby BC V5A 1S6, Canada, dleznoff@sfu.ca, jjwarren@sfu.ca

Contents

Experimental details

Syntheses

The 1,4,8,11,15,18,22,25-octaalkoxyphthalocyanine cobalt (II) complexes (^{RO}PcCo, where R = normal butyl, and sec-butyl) were prepared and characterized by previously reported synthetic procedures; the R = 2-ethylhexyl species are reported herein. The synthesis of ^{nBuO}PcCo and ^{secBuO}PcCo starts by functionalizing 2,3-dicyanohydroquinone with butylether groups by heating the phthalonitrile, 1-bromobutane or 2-bromobutane respectively, and potassium carbonate in dimethylformamide (DMF).[1,2] Then, by using metal-templating methods, the functionalized phthalonitrile was cyclized around lithium by refluxing the mixture in ROH solvent (R = n-butyl, and sec-butyl). After filtration of the mixture using chloroform, glacial acetic acid was added. The chloroform fraction was washed 3 x with water, and dried over magnesium sulfate.[3] Finally, the functionalized phthalocyanine was metalated using Co(II) acetate in the appropriate alcohol solvent (1-butanol for the n-butoxy-substituted system and 2-butanol for the sec-butoxy-substituted system) and refluxed for 2h to obtain the final products ^{nBuO}PcCo and ^{secBuO}PcCo.[3] These were then purified over silica with a 1:10 acetone:CH_2Cl_2 eluent.

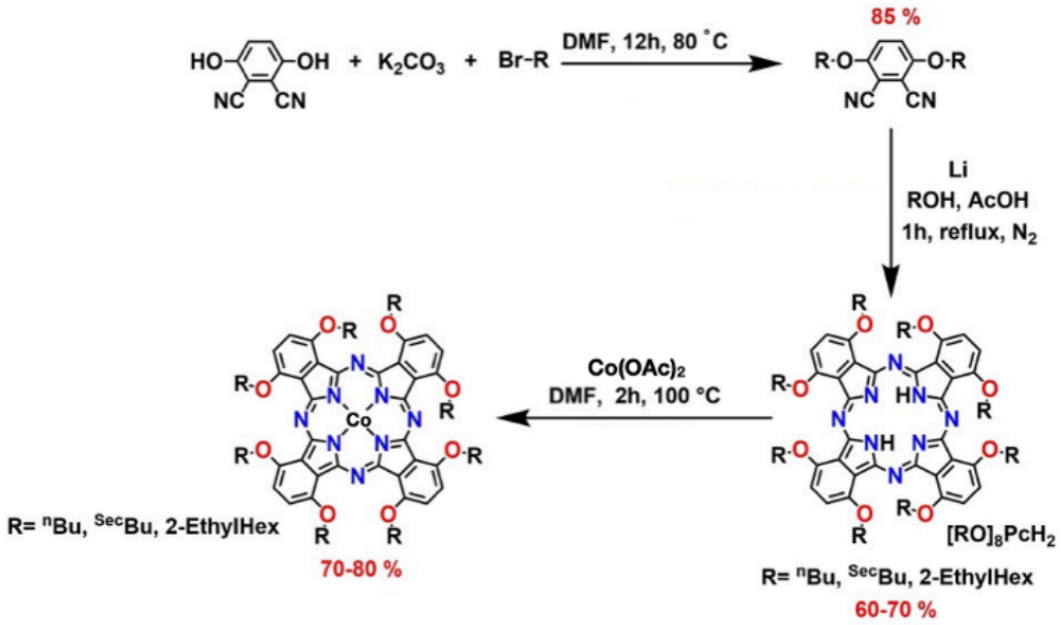

Figure S1. Synthetic scheme for the syntheses of ^{nBuO}PcCo, ^{secBuO}PcCo, and ^{EtHexO}PcCo.

Aggregation of ^{RO}CoPc complexes in solution

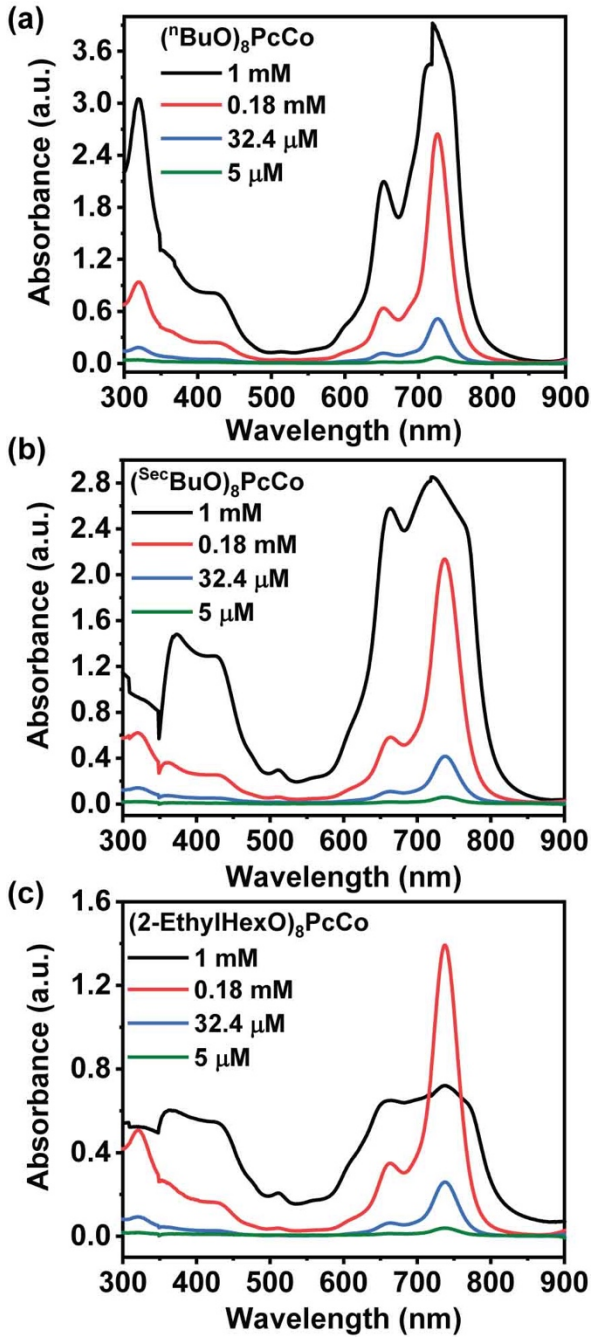

Figure S2. Concentration-dependent UV-Vis spectra of: (a) ^{nBuO}PcCo, (b) ^{secBuO}PcCo, and (c) ^{EtHexO}PcCo in toluene using a 0.1 cm length cuvette. Note that absorbance values above 2 are omitted from any analysis. The discontinuity at ca. 350 nm is from lamp-switching.

Cyclic Voltammetry (CV) experiments

Homogeneous cyclic voltammograms

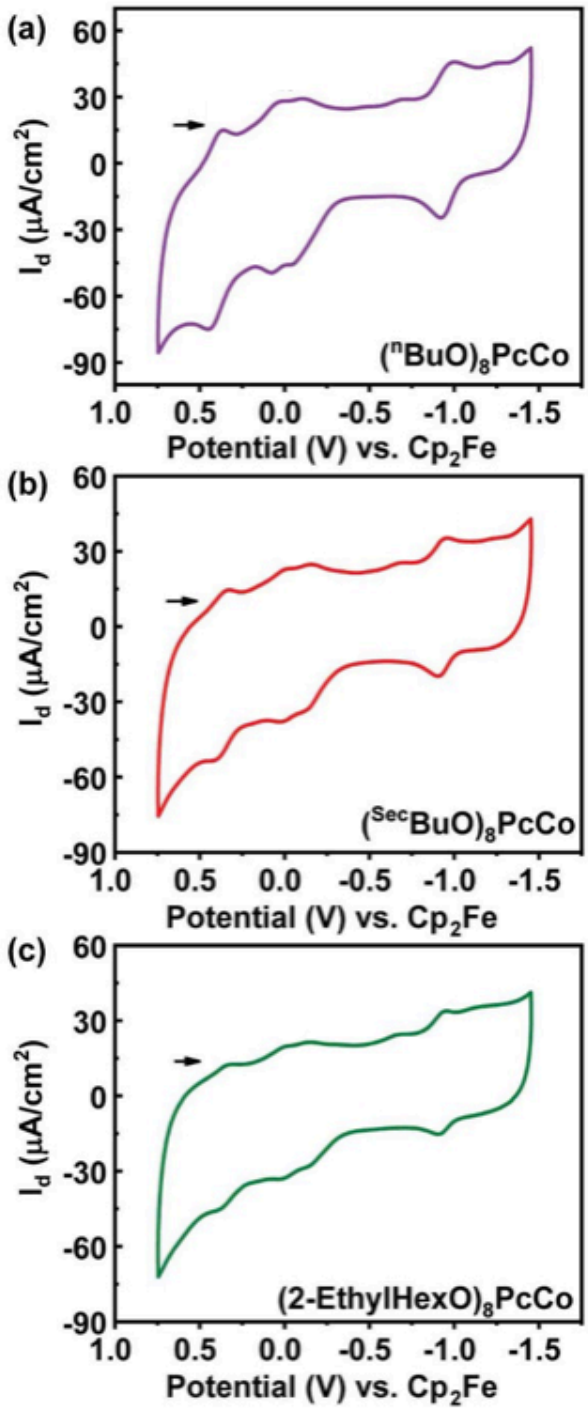

Figure S3. Homogeneous CVs of 0.2 mM solution of of (a) ^{nBuO}PcCo, (b) ^{secBuO}PcCo, and (c) ^{EtHexO}PcCo in benzonitrile with 0.1 M [^{n}Bu$_4$N]PF_6 as supporting electrolyte. The arrow indicates the direction of the scan.

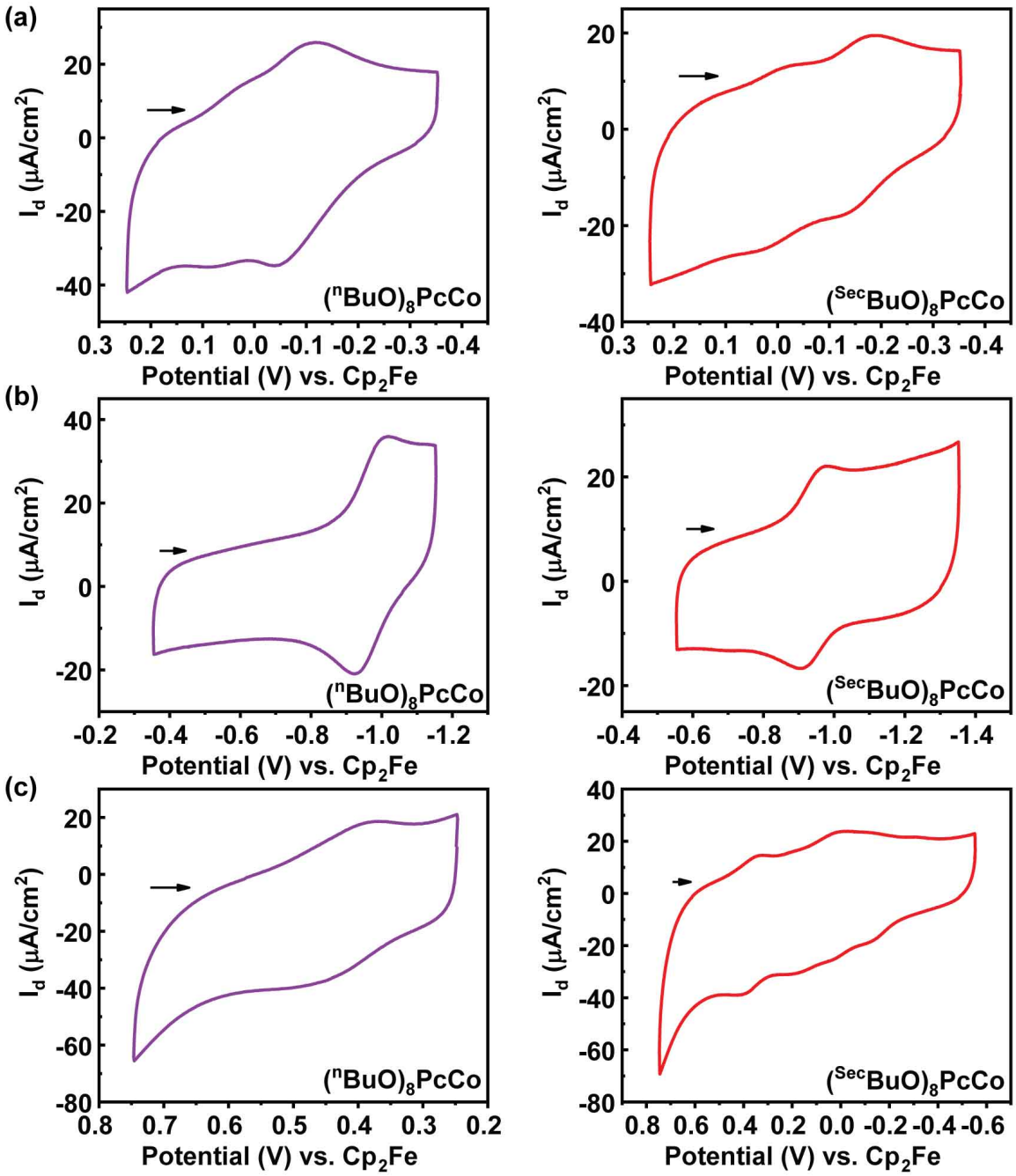

Figure S4. Homogeneous CVs of 0.2 mM solutions of ^{nBuO}PcCo on the left (purple) and ^{secBuO}PcCo on the right (red) in different potential ranges. The CVs were obtained in benzonitrile and using 0.1 M $[^nBu_4N]PF_6$ as supporting electrolyte. The arrow indicates the direction of the scan.

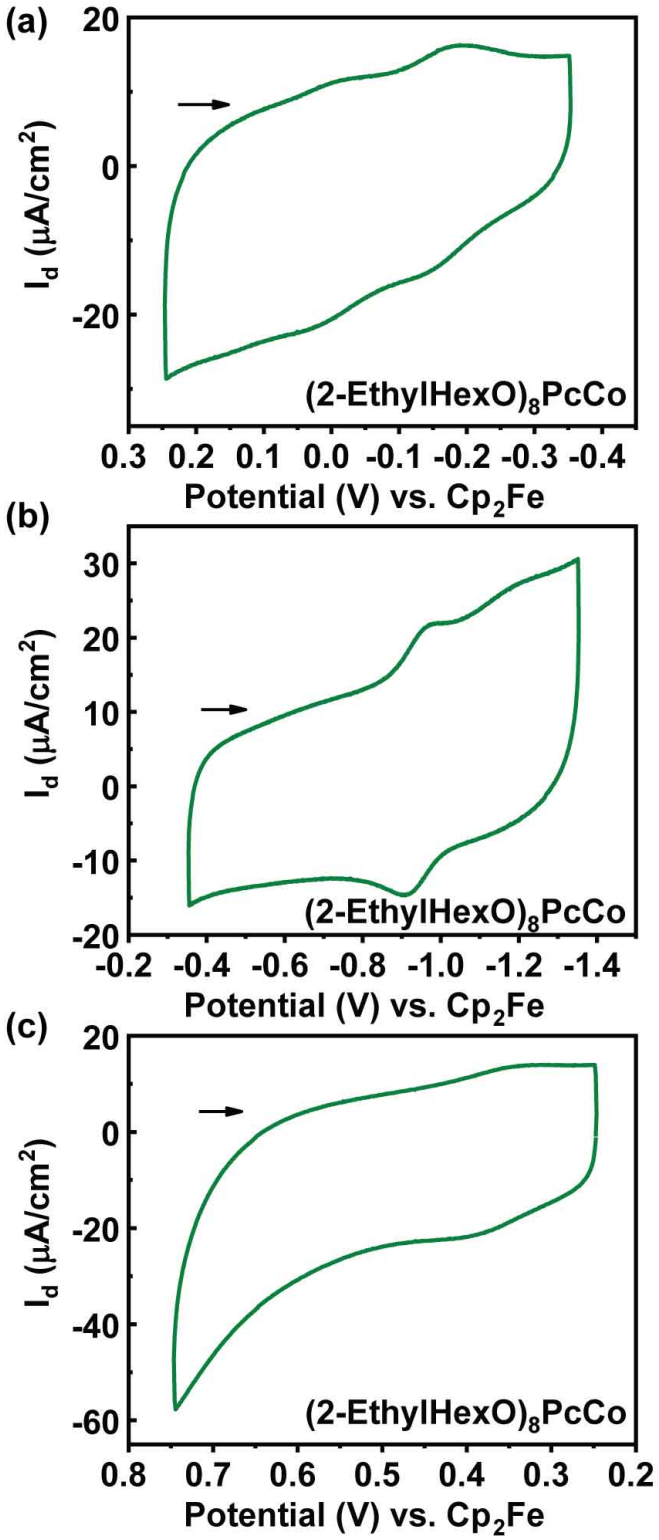

Figure S5. Homogeneous CVs of 0.2 mM solutions of ^{EtHexO}PcCo in different potential ranges. The CVs were obtained in benzonitrile and using 0.1 M [^{n}Bu$_4$N]PF$_6$ as supporting electrolyte. Arrow indicates the direction of the scan.

Heterogeneous CVs

Substituted ^{RO}PcCo complexes were coated onto BPG electrodes from six stock solutions in toluene at concentrations of 1 mM, 0.18 mM, 32.4 μM, 5 μM, 1 μM, and 0.18 μM. The solution (5μL) was applied to each electrode surface and allowed to evaporate at room temperature until the surface appeared dry. To ensure more complete solvent removal, a gentle air flow and heat were applied once the drop had visibly dried. CVs of the bare electrode also were obtained. CVs of bare electrodes (Figure S41) have negligible CO_2 reduction activity compared to the ^{RO}PcCo compounds.

CVs of ^{nBuO}PcCo, ^{secBuO}PcCo, and ^{EtHexO}PcCo were obtained in the 6 different loadings. Figure S5 to S40 show the complete set of CVs of these compounds for three triplicate runs. For each run, a new working electrode and electrochemical cell was prepared each time. For reporting electrochemical features, and for the analysis of data, the second cycle was used due to the instability of the catalyst films during the first cycle. This instability is common and can arise from re-structuring of the film on sweeping the potential or from reductive exfoliation of the graphite.[4]

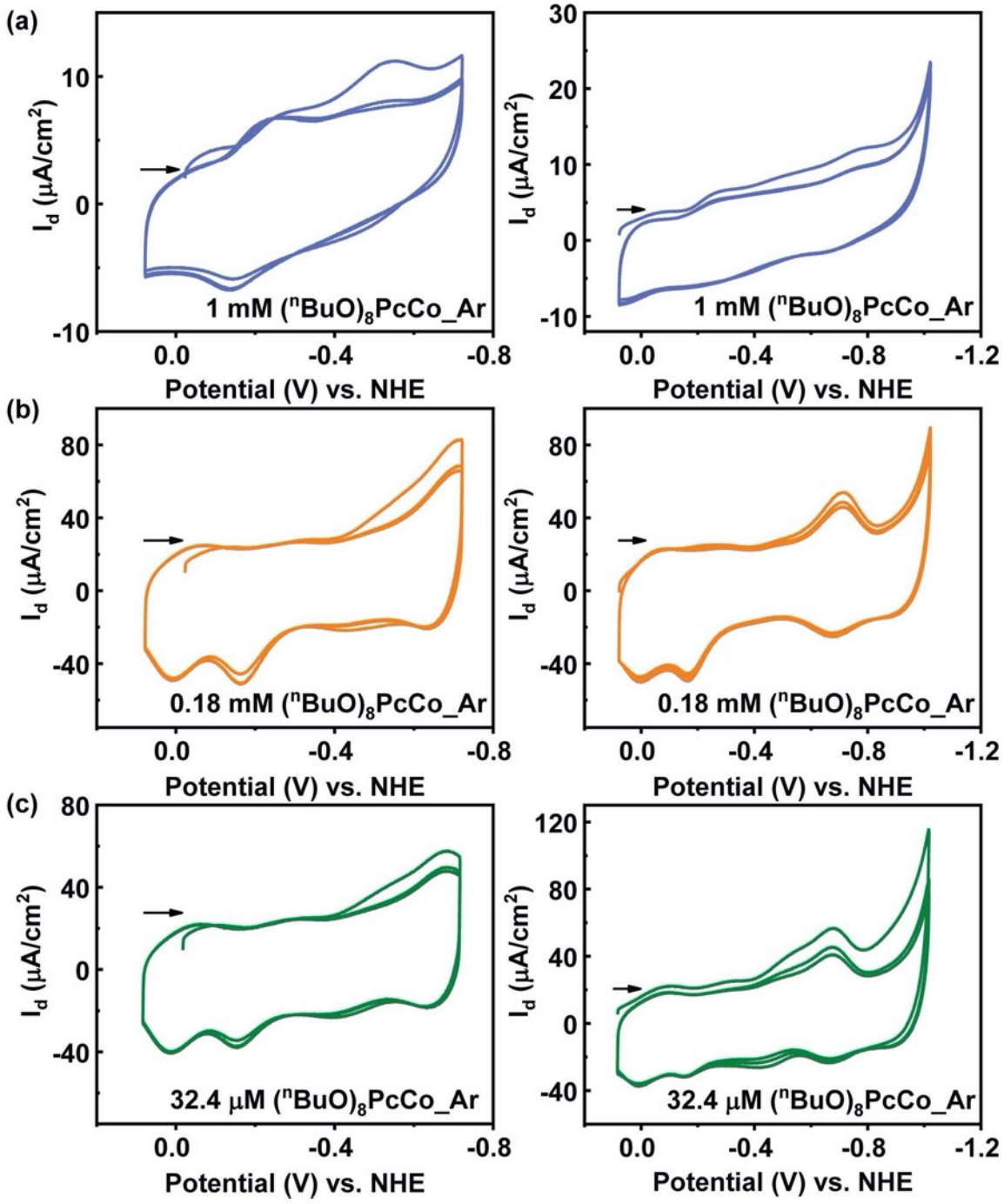

Figure S6. Run 1 CVs of ^{nBuO}PcCo under Ar atmosphere in concentrations of (a) 1 mM, (b) 0.18 mM, and (c) 32.4 μM stock solutions used to coat working electrodes. On the left scan of more narrow potential window and on the right more broader potential window are observed. The arrow shown in the plots indicates the scan direction.

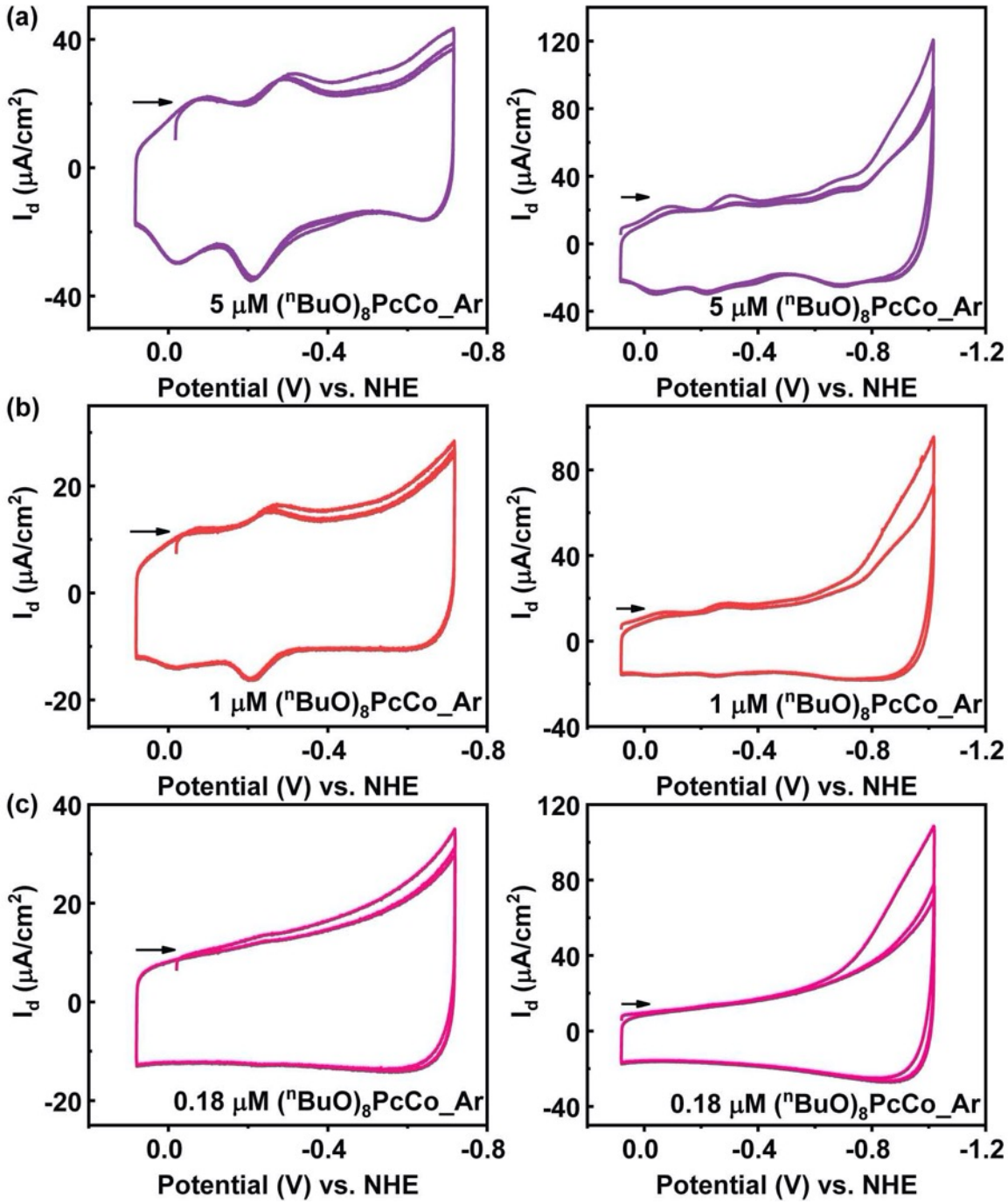

Figure S7. Run 1 CVs of ^{nBuO}PcCo under Ar atmosphere in concentrations of (a) 5 μM, (b) 1 μM, and (c) 0.18 μM stock solutions used to coat working electrodes. On the left scan of more narrow potential window and on the right more broader potential window are observed. The arrow shown in the plots indicates the scan direction.

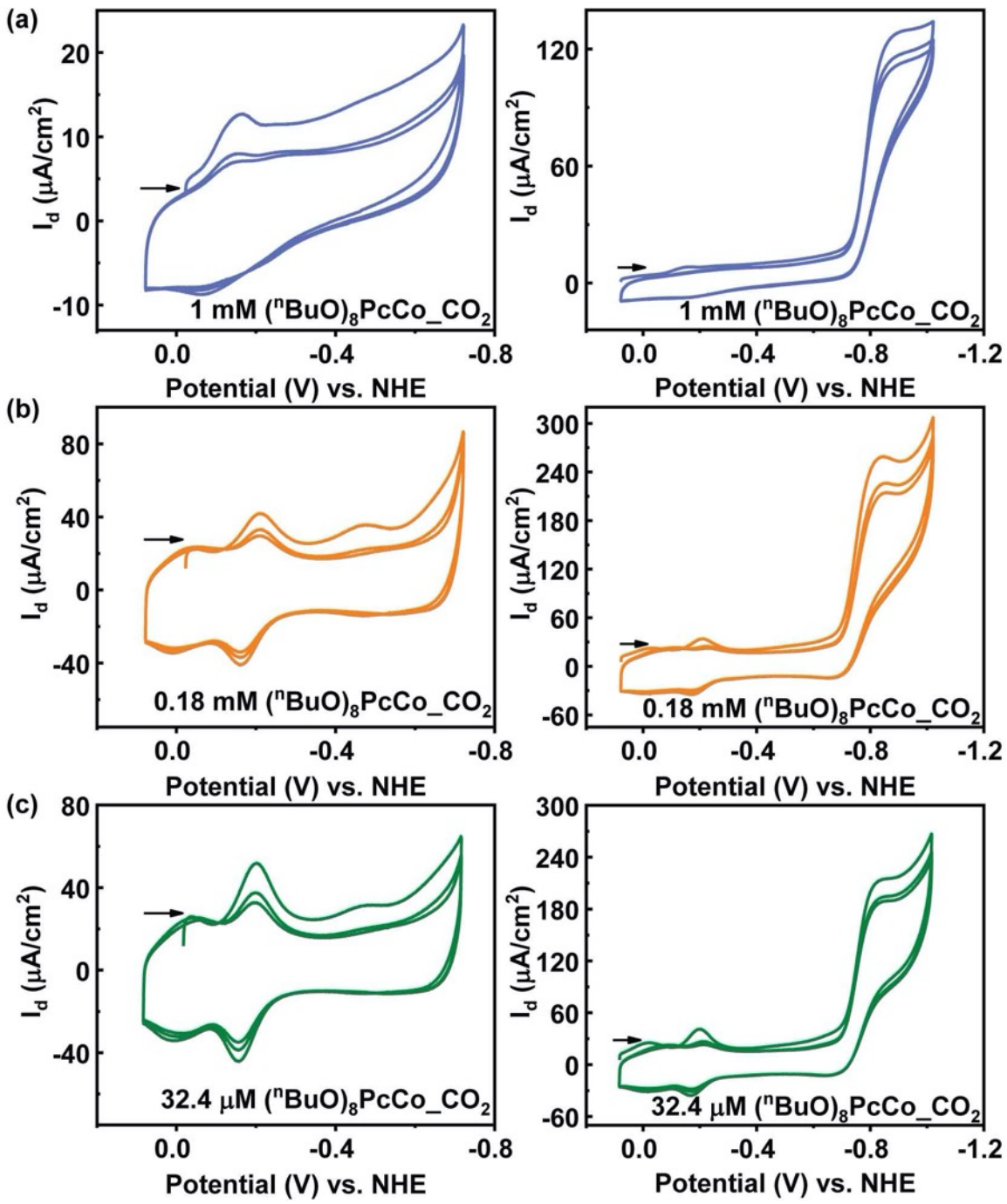

Figure S8. Run 1 CVs of ^{nBuO}PcCo under CO_2 atmosphere in concentrations of (a) 1 mM, (b) 0.18 mM, and (c) 32.4 μM stock solutions used to coat working electrodes. On the left scan of more narrow potential window and on the right more broader potential window are observed. The arrow shown in the plots indicates the scan direction.

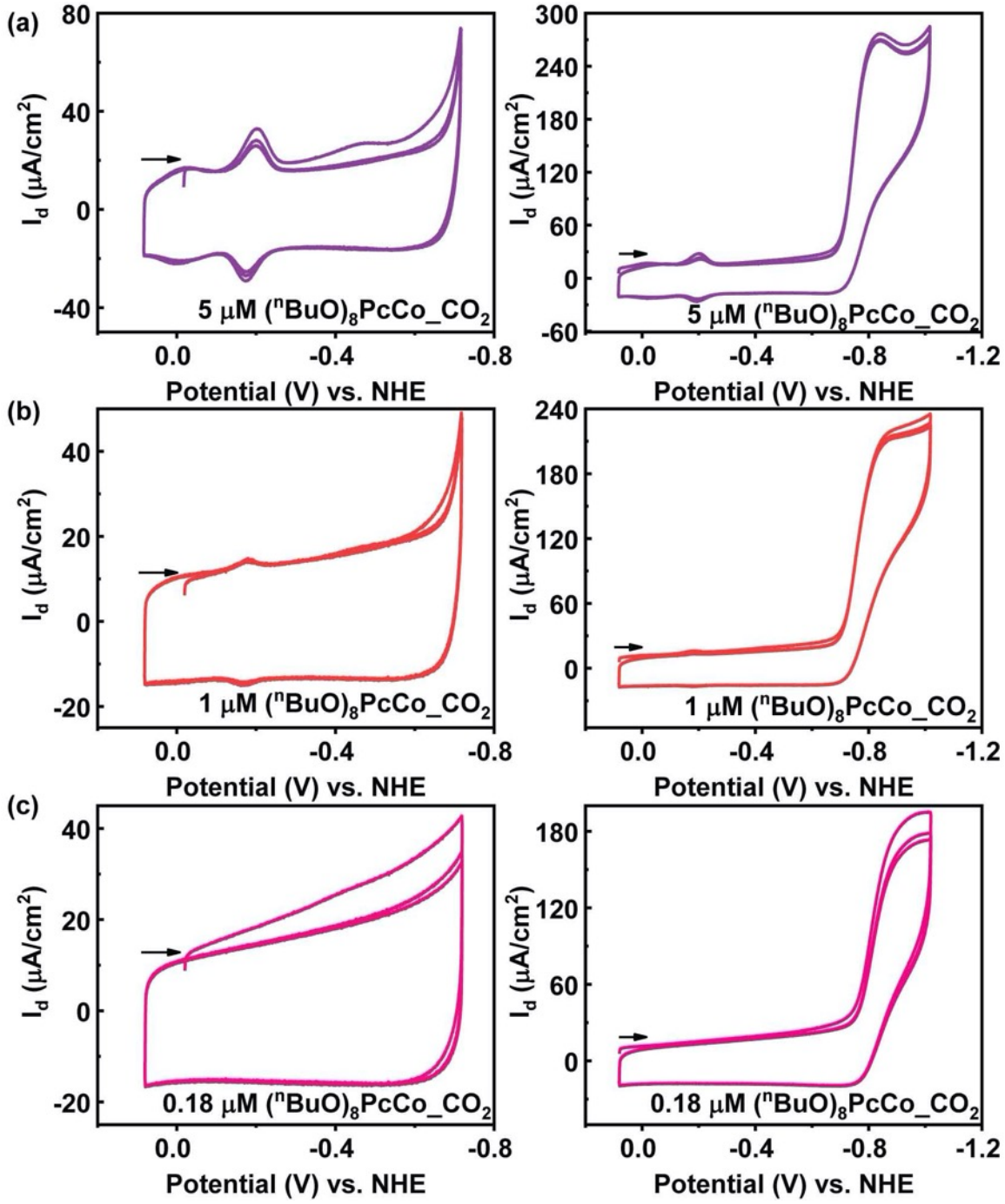

Figure S9. Run 1 CVs of ^{nBuO}PcCo under CO_2 atmosphere in concentrations of (a) 5 μM, (b) 1 μM, and (c) 0.18 μM stock solutions used to coat working electrodes. On the left scan of more narrow potential window and on the right more broader potential window are observed. The arrow shown in the plots indicates the scan direction.

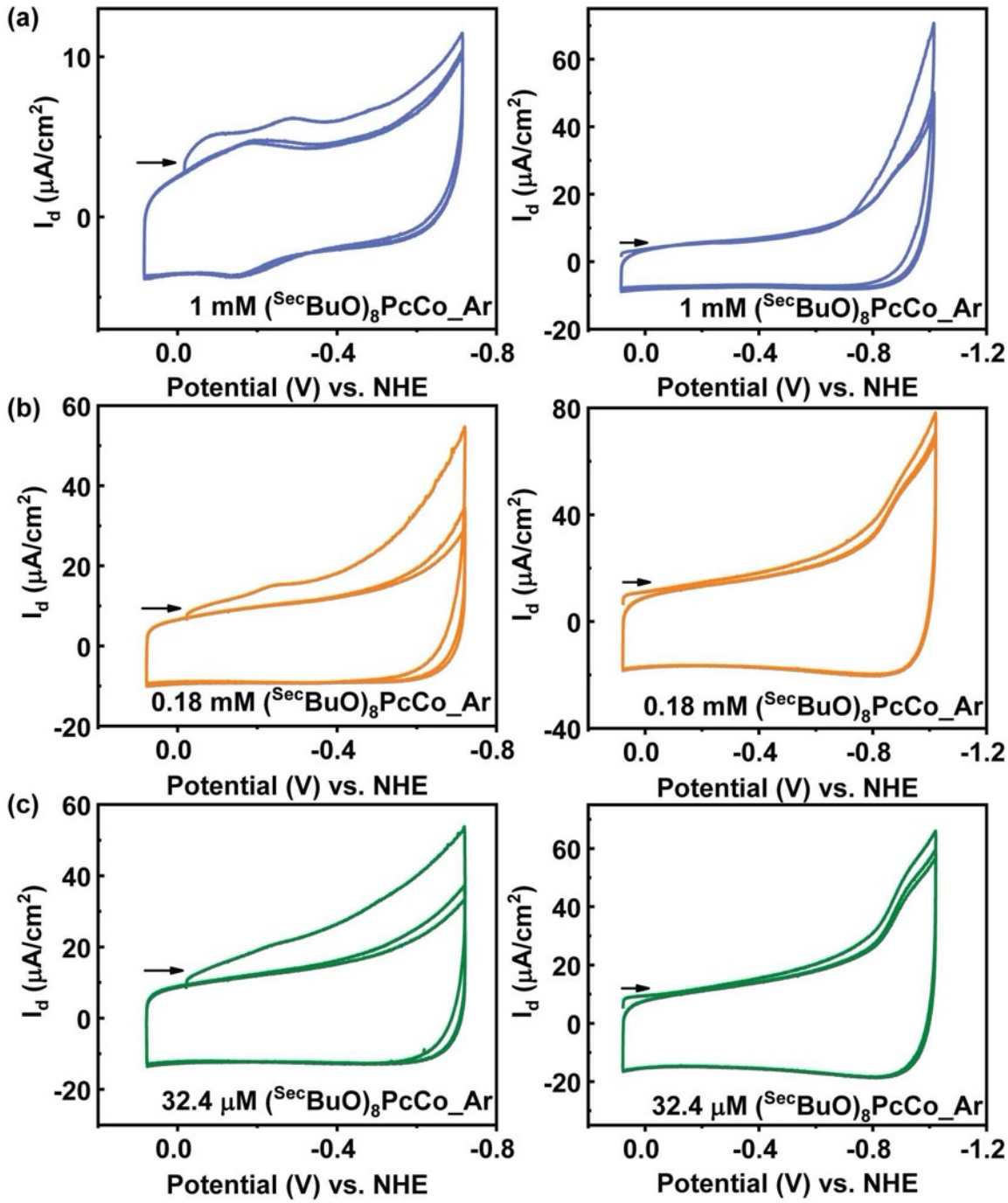

Figure S10. Run 1 CVs of ^{secBuO}PcCo under Ar atmosphere in concentrations of (a) 1 mM, (b) 0.18 mM, and (c) 32.4 μM stock solutions used to coat working electrodes. On the left scan of more narrow potential window and on the right more broader potential window are observed. The arrow shown in the plots indicates the scan direction.

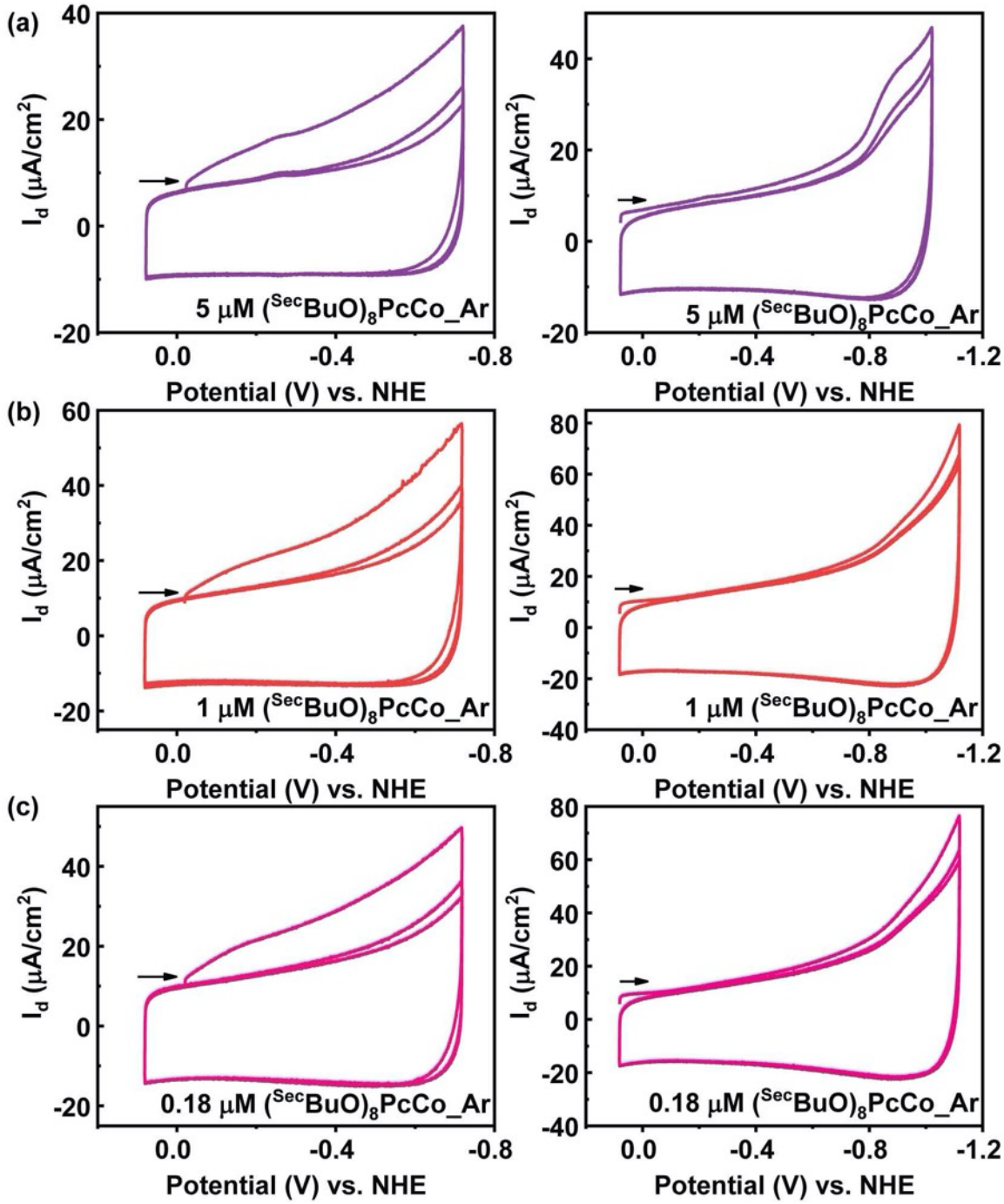

Figure S11. Run 1 CVs of ^{secBuO}PcCo under Ar atmosphere in concentrations of (a) 5 μM, (b) 1 μM, and (c) 0.18 μM stock solutions used to coat working electrodes. On the left scan of more narrow potential window and on the right more broader potential window are observed. The arrow shown in the plots indicates the scan direction.

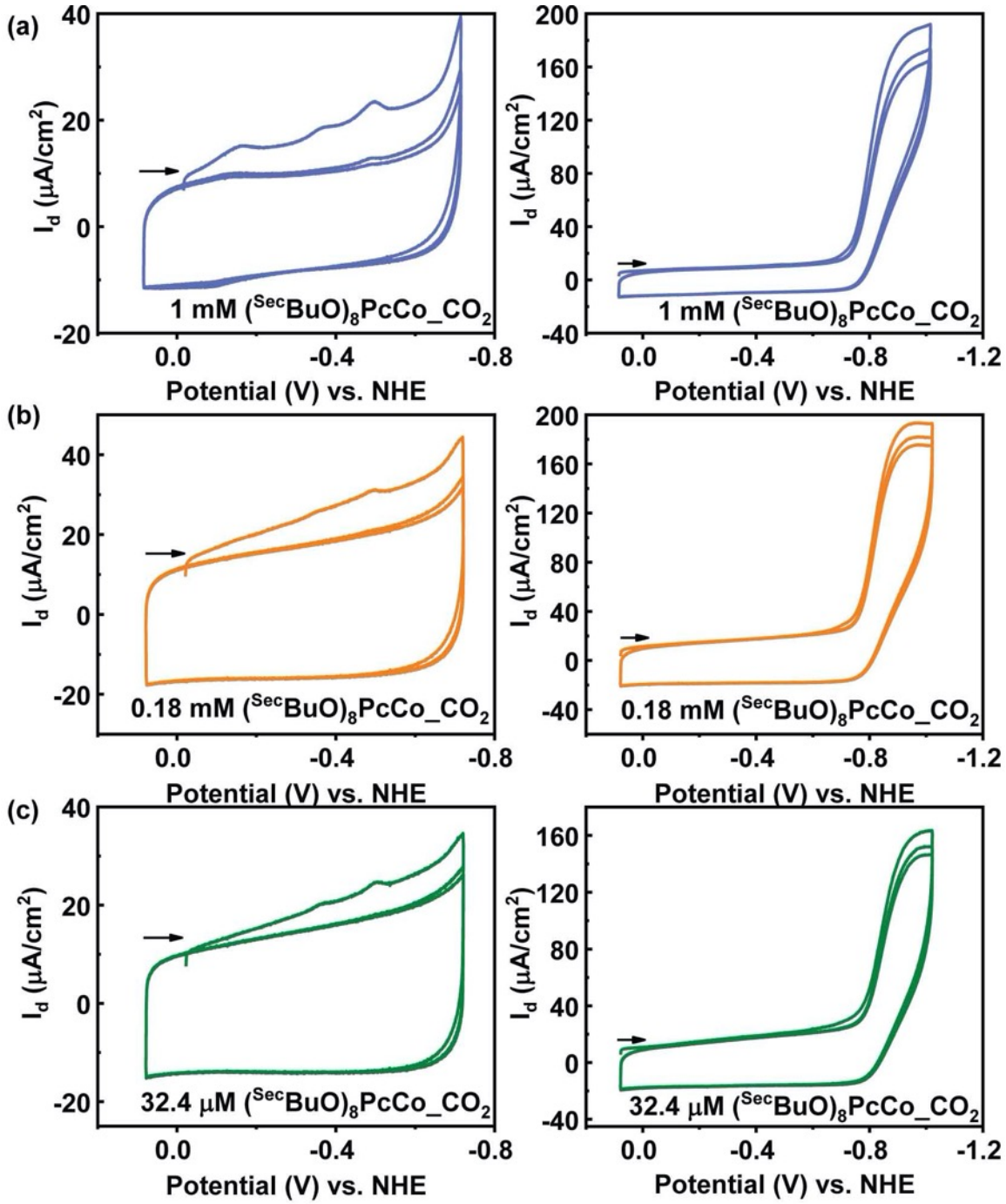

Figure S12. Run 1 CVs of ^{secBuO}PcCo under CO_2 atmosphere in concentrations of (a) 1 mM, (b) 0.18 mM, and (c) 32.4 µM stock solutions used to coat working electrodes. On the left scan of more narrow potential window and on the right more broader potential window are observed. The arrow shown in the plots indicates the scan direction.

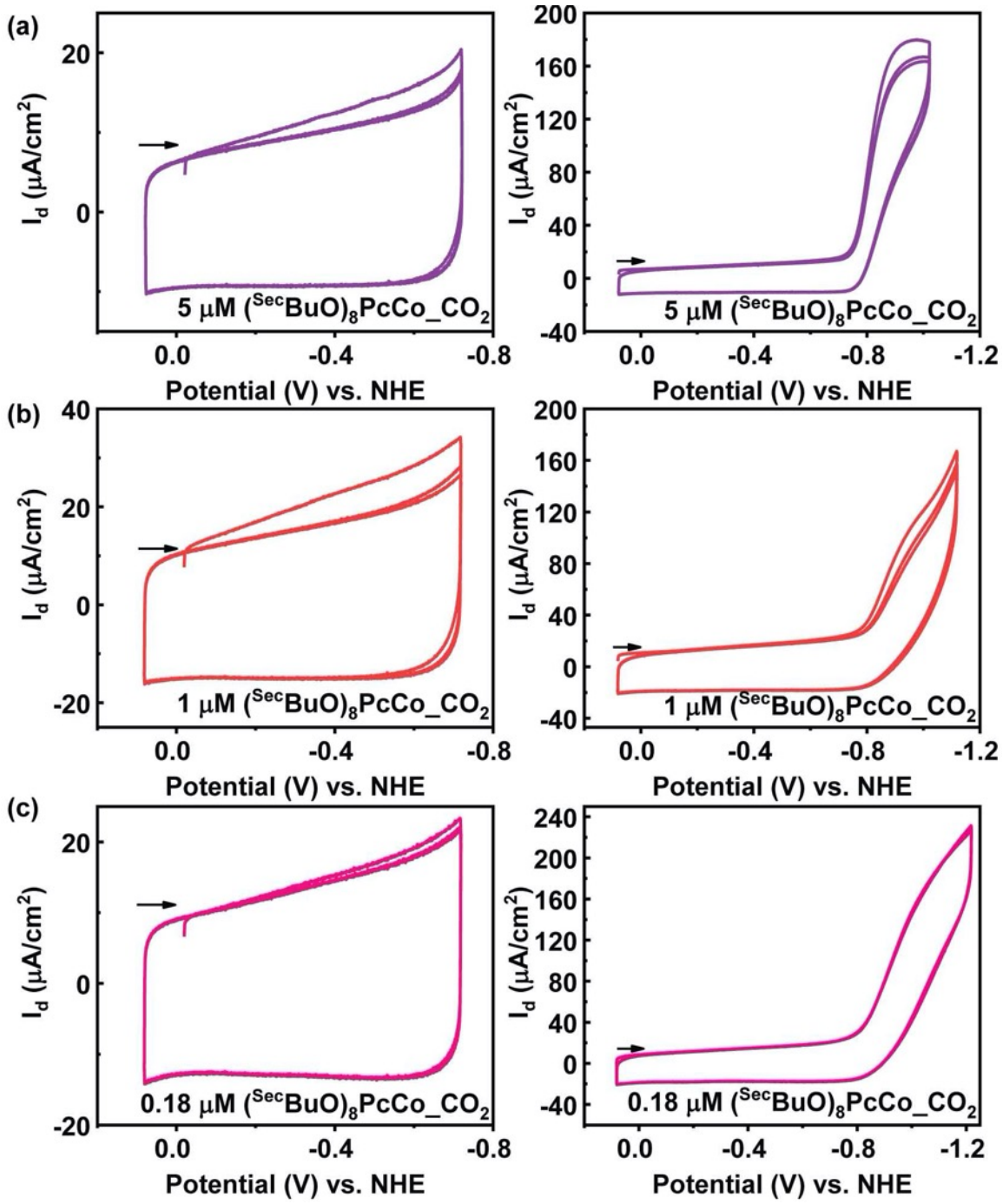

Figure S13. Run 1 CVs of ^{secBuO}PcCo under CO_2 atmosphere in concentrations of (a) 5 μM, (b) 1 μM, and (c) 0.18 μM stock solutions used to coat working electrodes. On the left scan of more narrow potential window and on the right more broader potential window are observed. The arrow shown in the plots indicates the scan direction.

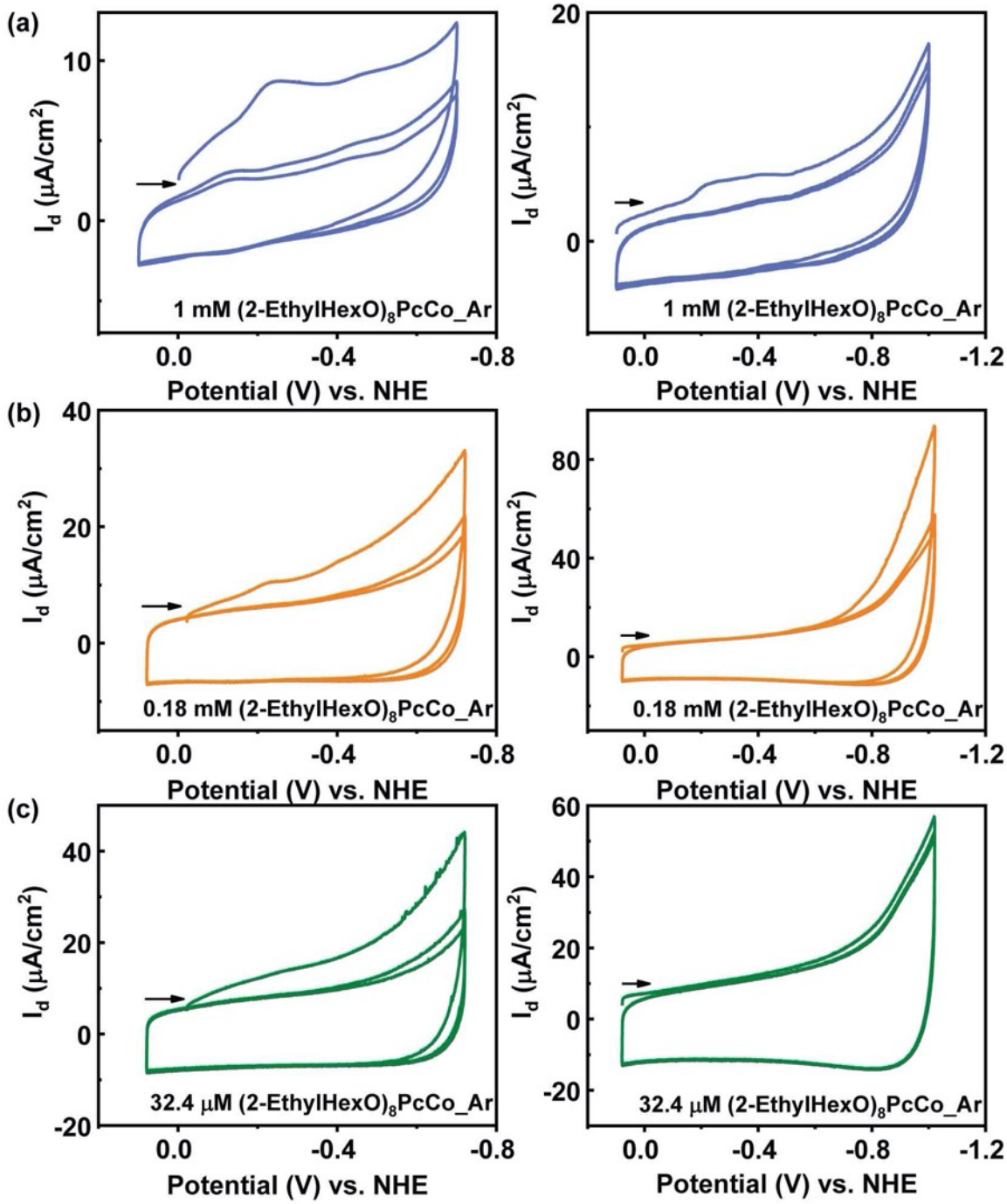

Figure S14. Run 1 CVs of ^{EtHexO}PcCo under Ar atmosphere in concentrations of (a) 1 mM, (b) 0.18 mM, and (c) 32.4 μM stock solutions used to coat working electrodes. On the left scan of more narrow potential window and on the right more broader potential window are observed. The arrow shown in the plots indicates the scan direction.

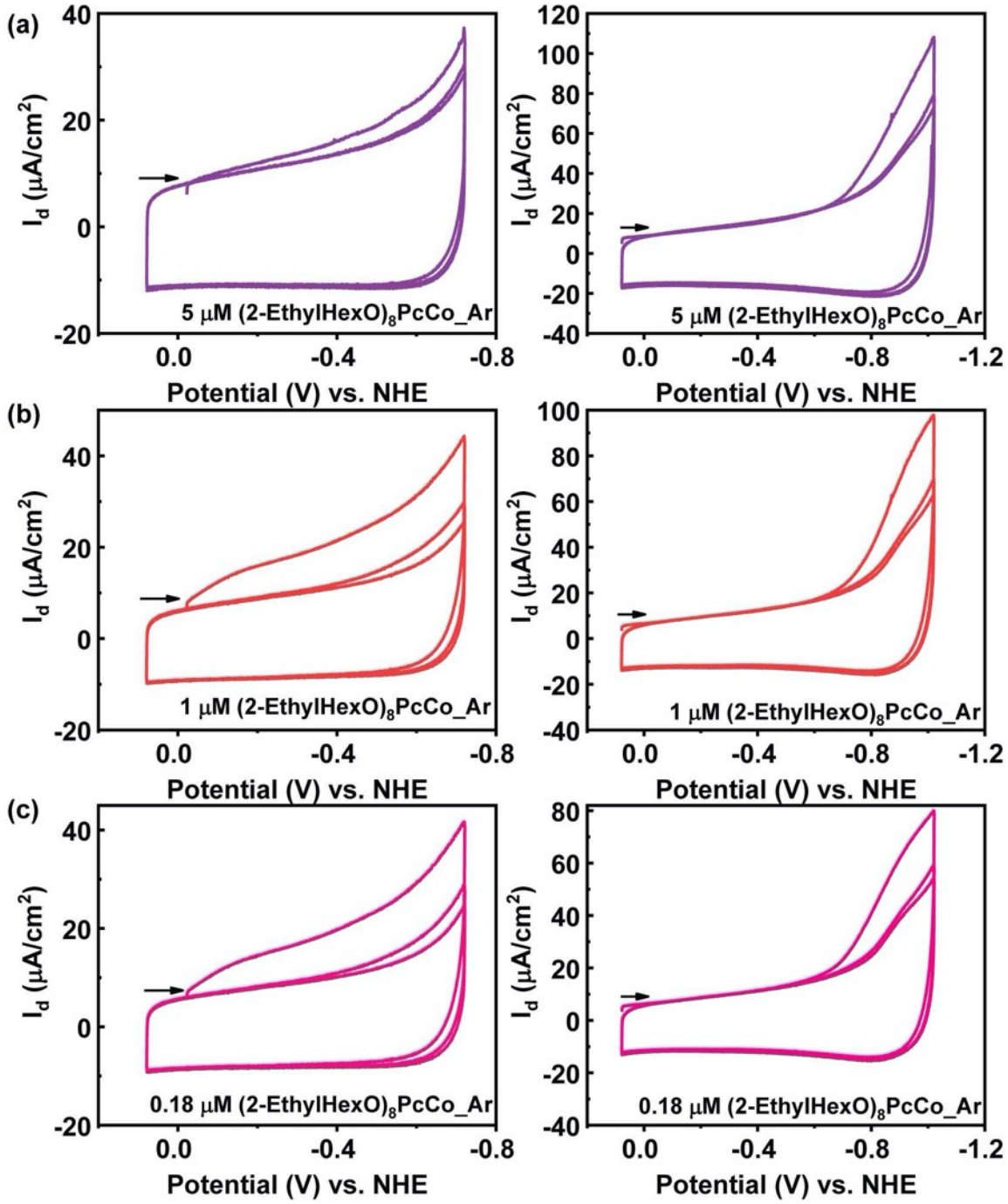

Figure S15. Run 1 CVs of ^{EtHexO}PcCo under Ar atmosphere in concentrations of (a) 5 μM, (b) 1 μM, and (c) 0.18 μM stock solutions used to coat working electrodes. On the left scan of more narrow potential window and on the right more broader potential window are observed. The arrow shown in the plots indicates the scan direction.

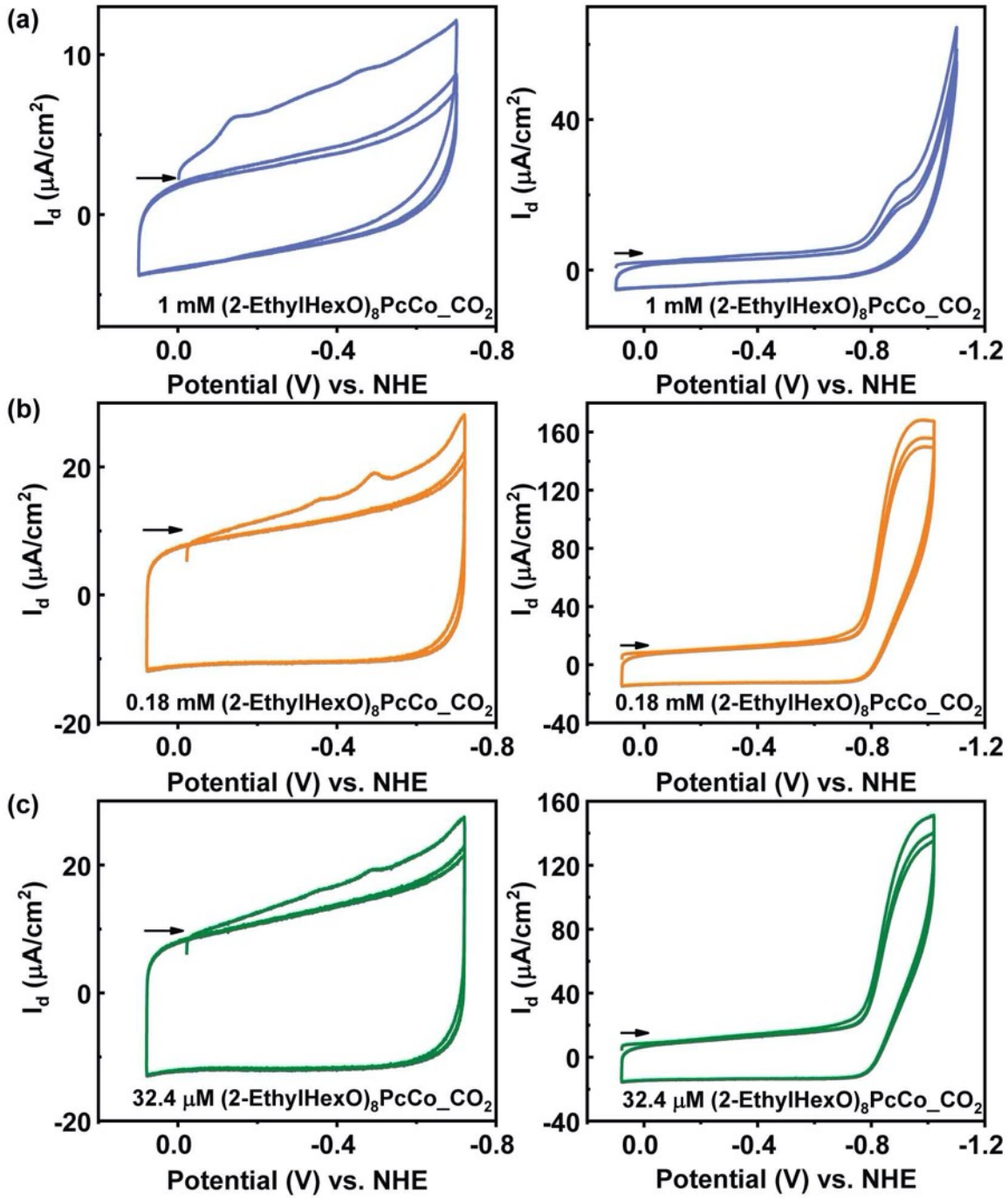

Figure S16. Run 1 CVs of ^{EtHexO}PcCo under CO_2 atmosphere in concentrations of (a) 1 mM, (b) 0.18 mM, and (c) 32.4 μM stock solutions used to coat working electrodes. On the left scan of more narrow potential window and on the right more broader potential window are observed. The arrow shown in the plots indicates the scan direction.

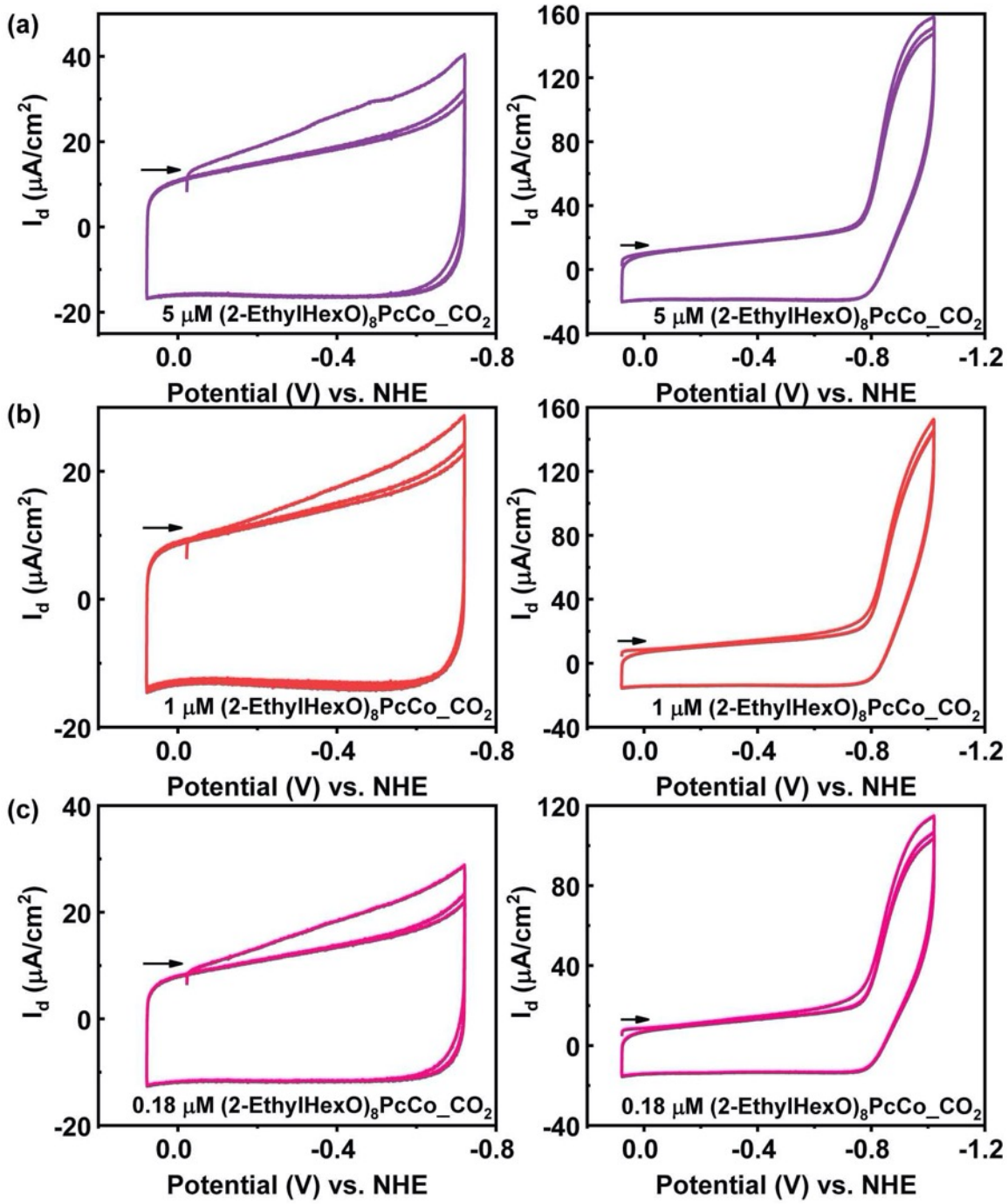

Figure S17. Run 1 CVs of ^{EtHexO}PcCo under CO_2 atmosphere in concentrations of (a) 5 μM, (b) 1 μM, and (c) 0.18 μM stock solutions used to coat working electrodes. On the left scan of more narrow potential window and on the right more broader potential window are observed. The arrow shown in the plots indicates the scan direction.

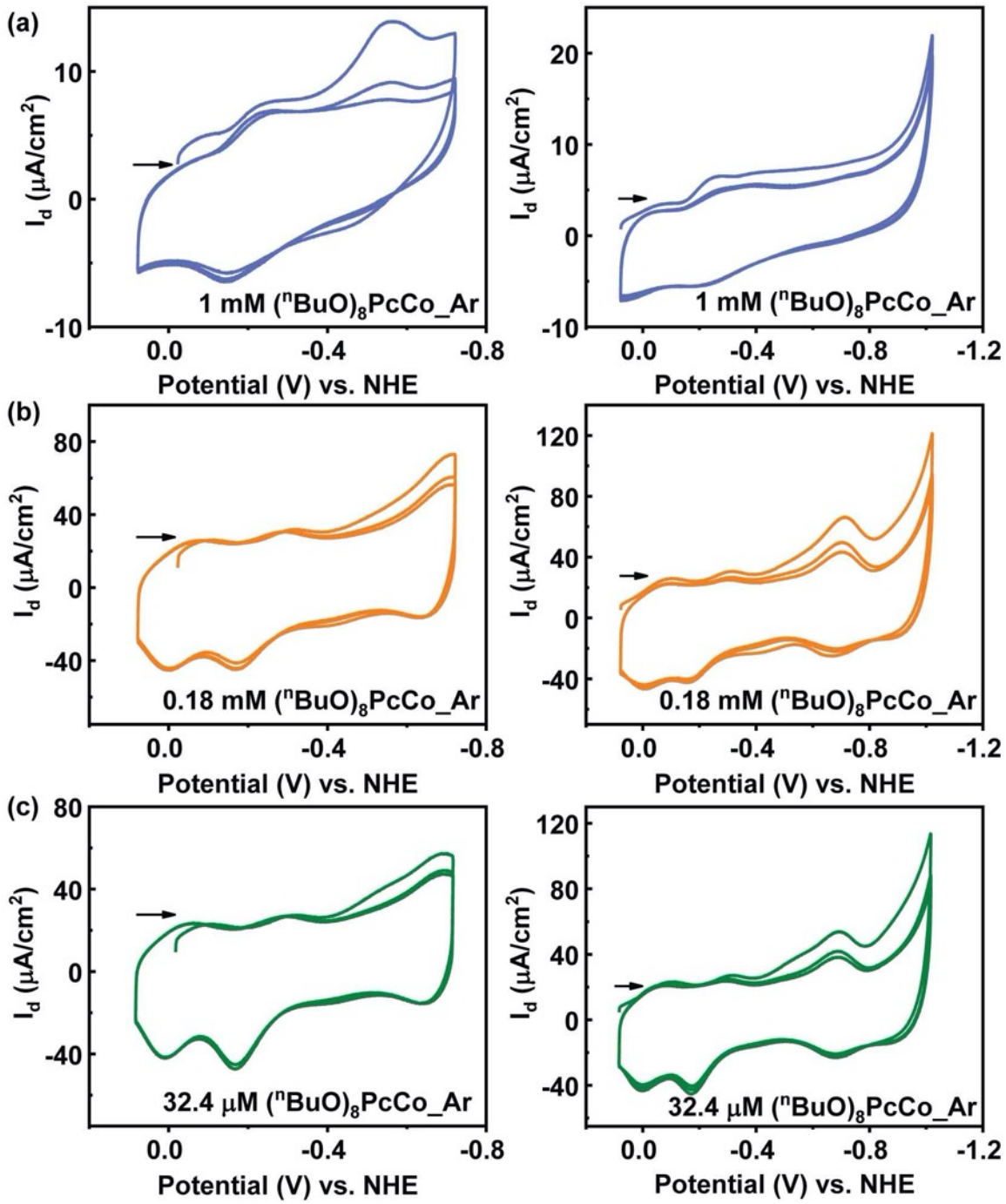

Figure S18. Run 2 CVs of ^{nBuO}PcCo under Ar atmosphere in concentrations of (a) 1 mM, (b) 0.18 mM, and (c) 32.4 μM stock solutions used to coat working electrodes. On the left, scan of more narrow potential windows and on the right, more broader potential windows are observed. The arrow shown in the plots indicates the scan direction.

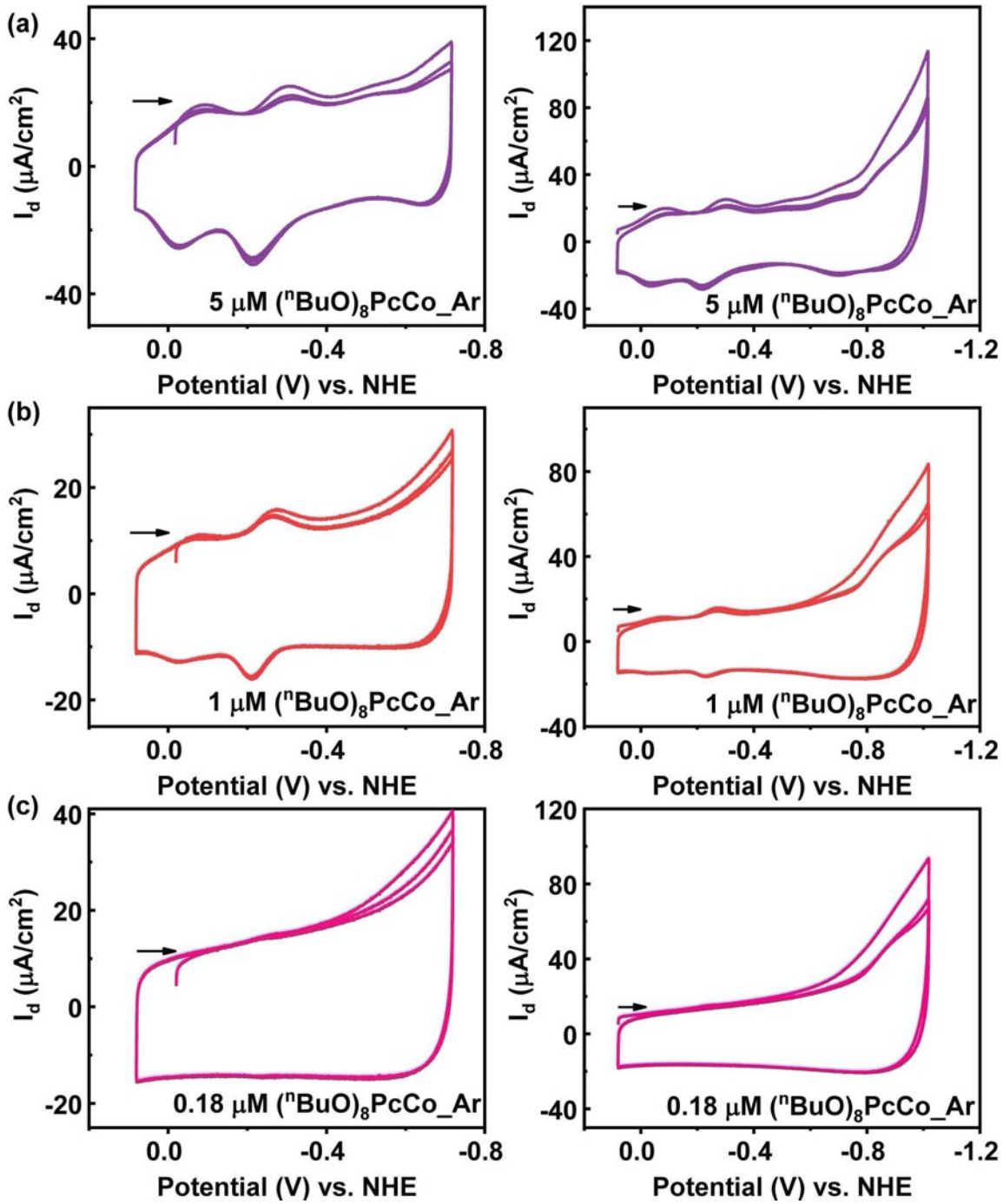

Figure S19. Run 2 CVs of ^{nBuO}PcCo under Ar atmosphere in concentrations of (a) 5 μM, (b) 1 μM, and (c) 0.18 μM stock solutions used to coat working electrodes. On the left, scan of more narrow potential windows and on the right, more broader potential window are observed. The arrow shown in the plots indicates the scan direction.

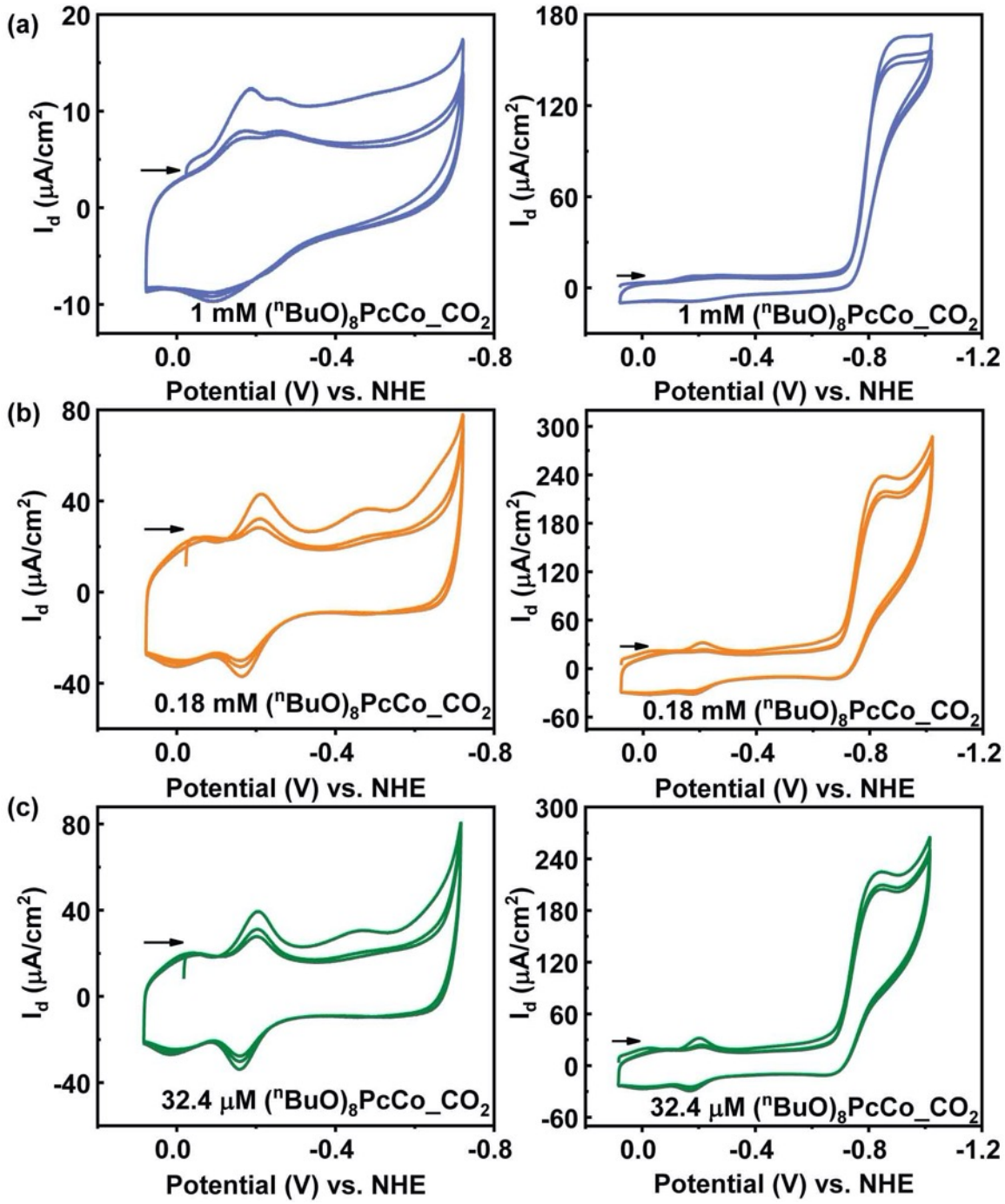

Figure S20. Run 2 CVs of ^{nBuO}PcCo under CO_2 atmosphere in concentrations of (a) 1 mM, (b) 0.18 mM, and (c) 32.4 μM stock solutions used to coat working electrodes. On the left, scan of more narrow potential windows and on the right, more broader potential windows are observed. The arrow shown in the plots indicates the scan direction.

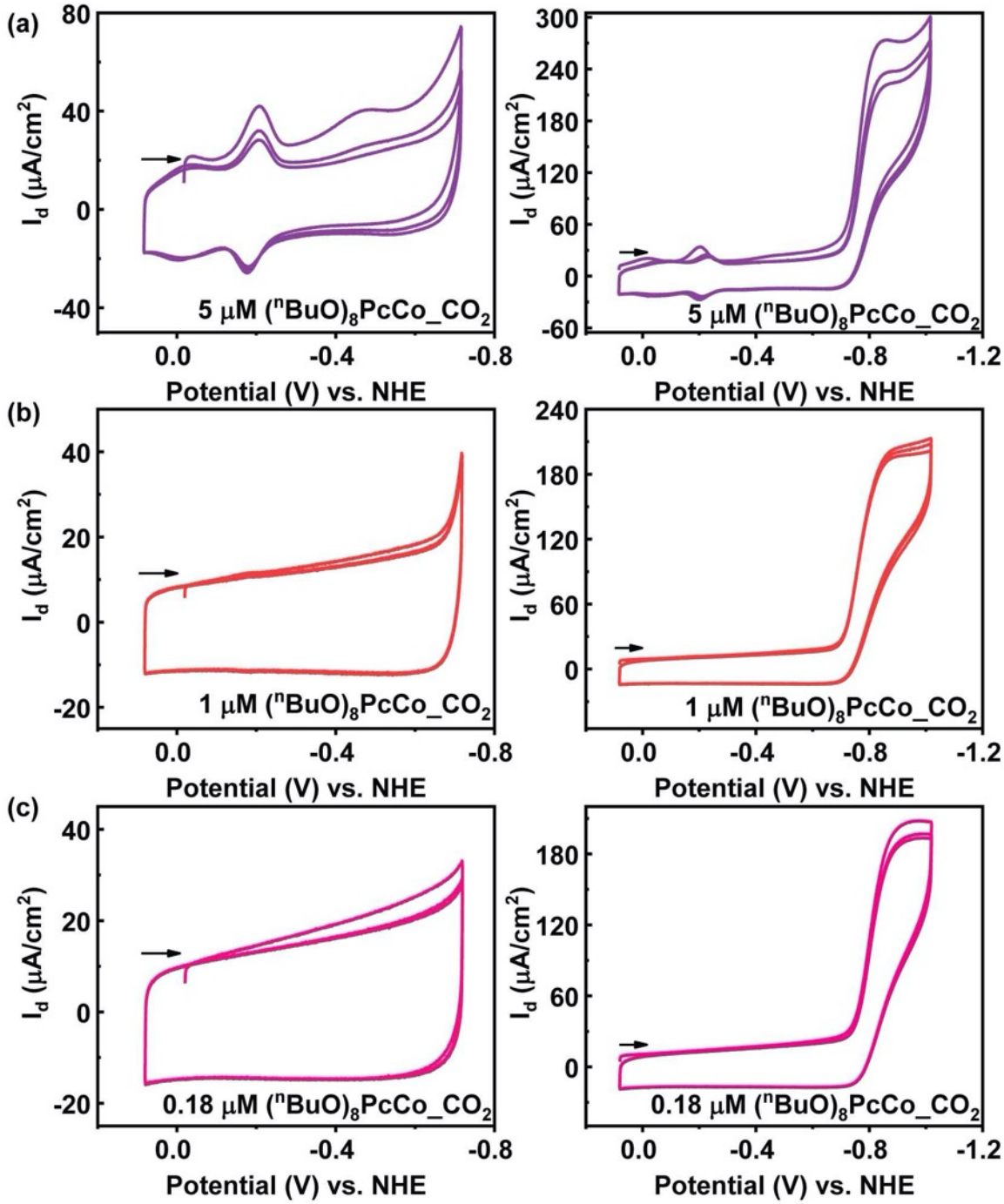

Figure S21. Run 2 CVs of ^{nBuO}PcCo under CO_2 atmosphere in concentrations of (a) 5 μM, (b) 1 μM, and (c) 0.18 μM stock solutions used to coat working electrodes. On the left, scan of more narrow potential windows and on the right, more broader potential windows are observed. The arrow shown in the plots indicates the scan direction.

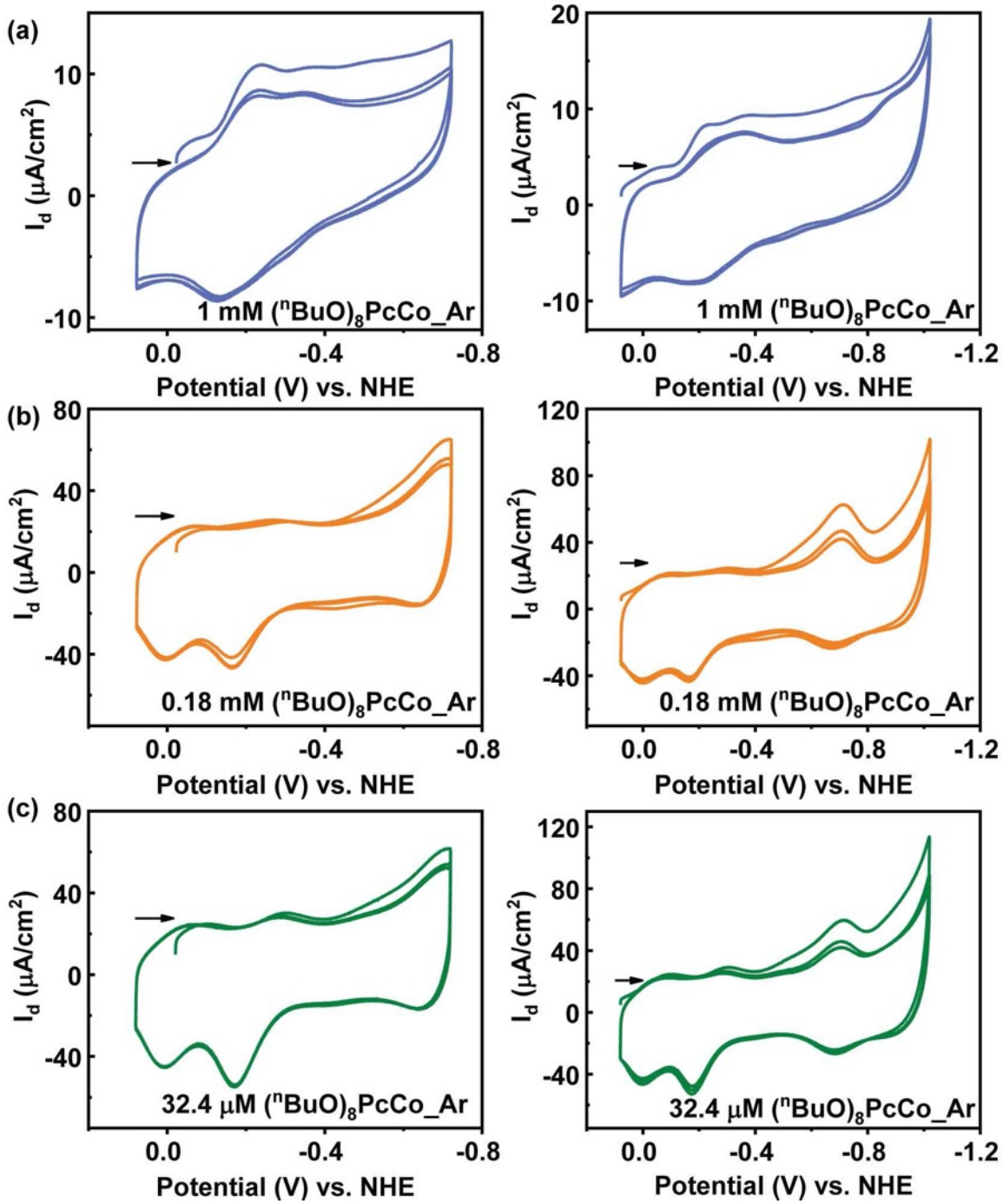

Figure S22. Run 3 CVs of ^{nBuO}PcCo under Ar atmosphere in concentrations of (a) 1 mM, (b) 0.18 mM, and (c) 32.4 μM stock solutions used to coat working electrodes. On the left, scan of more narrow potential windows and on the right, more broader potential windows are observed. The arrow shown in the plots indicates the scan direction.

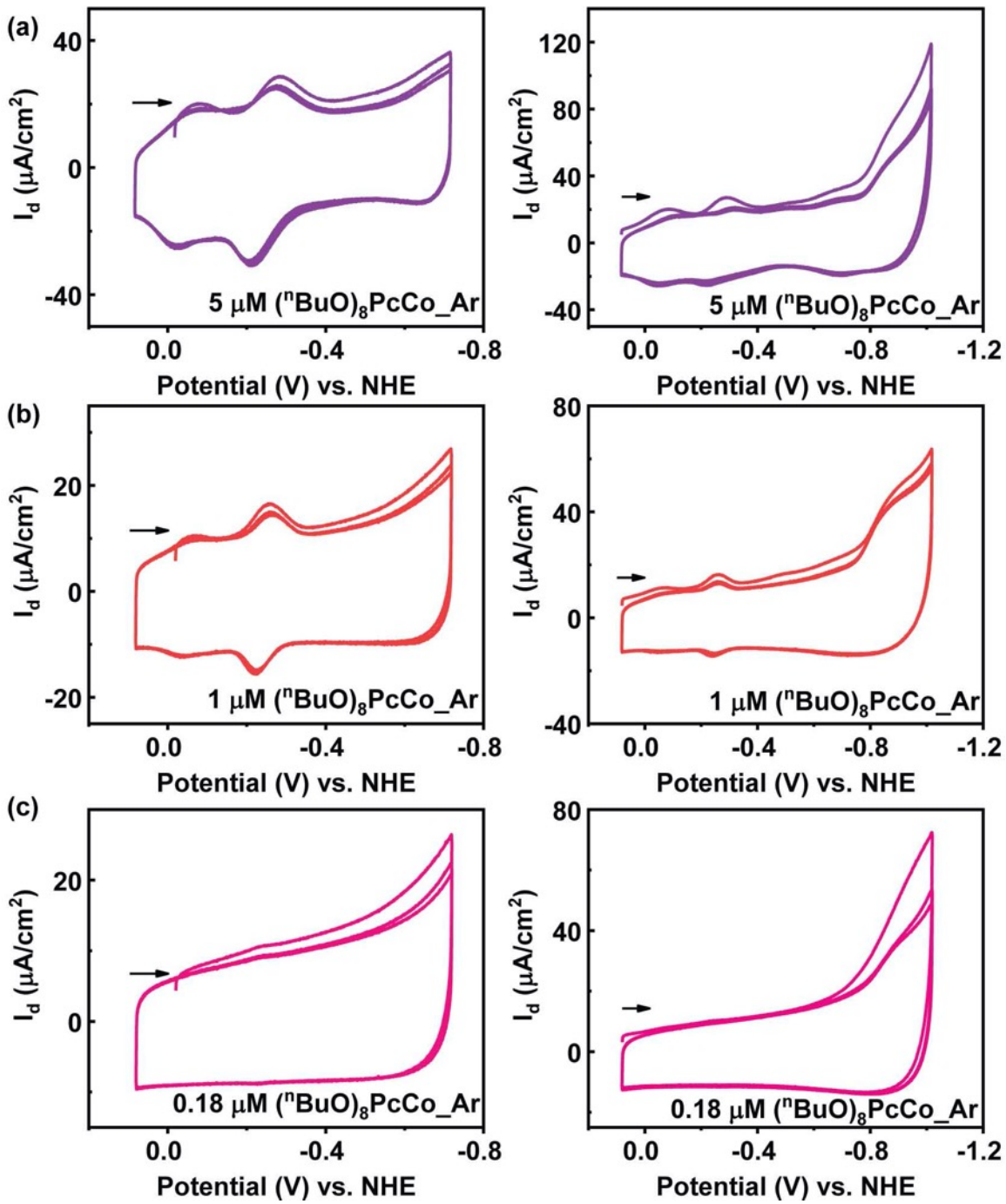

Figure S23. Run 3 CVs of ^{nBuO}PcCo under Ar atmosphere in concentrations of (a) 5 μM, (b) 1 μM, and (c) 0.18 μM stock solutions used to coat working electrodes. On the left, scan of more narrow potential windows and on the right, more broader potential windows are observed. The arrow shown in the plots indicates the scan direction.

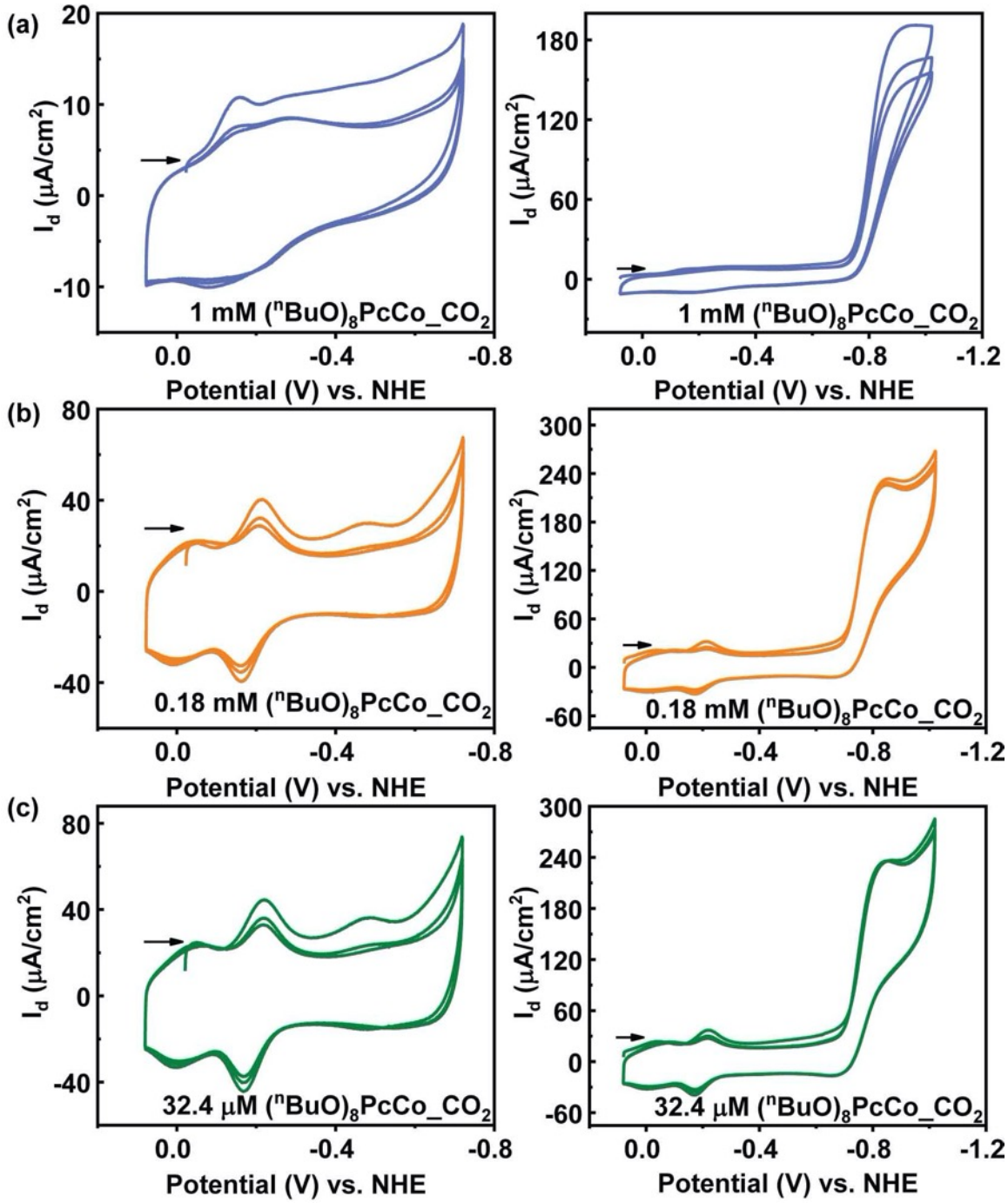

Figure S24. Run 3 CVs of ^{nBuO}PcCo under CO_2 atmosphere in concentrations of (a) 1 mM, (b) 0.18 mM, and (c) 32.4 μM stock solutions used to coat working electrodes. On the left, scan of more narrow potential windows and on the right, more broader potential windows are observed. The arrow shown in the plots indicates the scan direction.

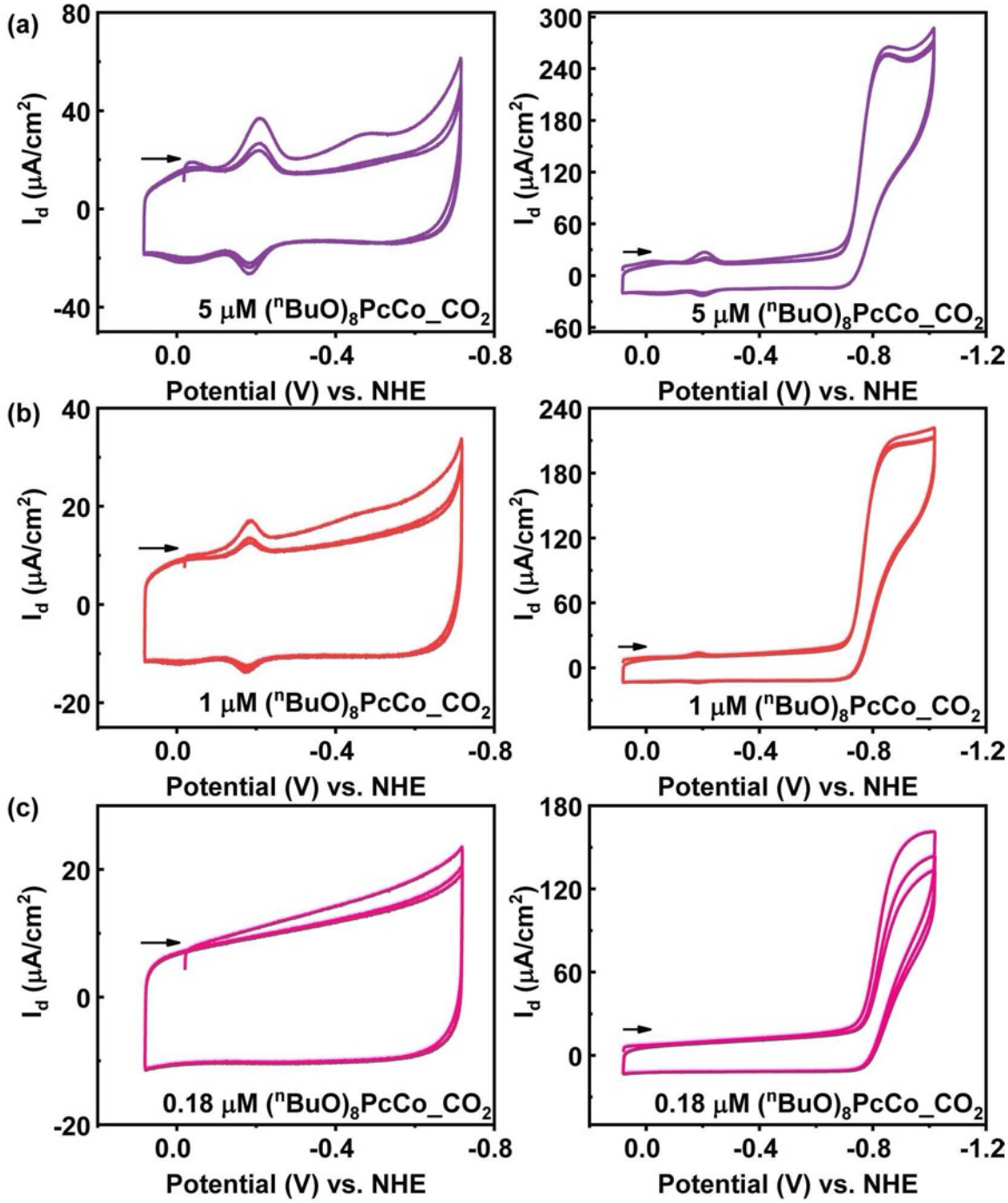

Figure S25. Run 3 CVs of ^{nBuO}PcCo under CO_2 atmosphere in concentrations of (a) 5 μM, (b) 1 μM, and (c) 0.18 μM stock solutions used to coat working electrodes. On the left, scan of more narrow potential windows and on the right, more broader potential windows are observed. The arrow shown in the plots indicates the scan direction.

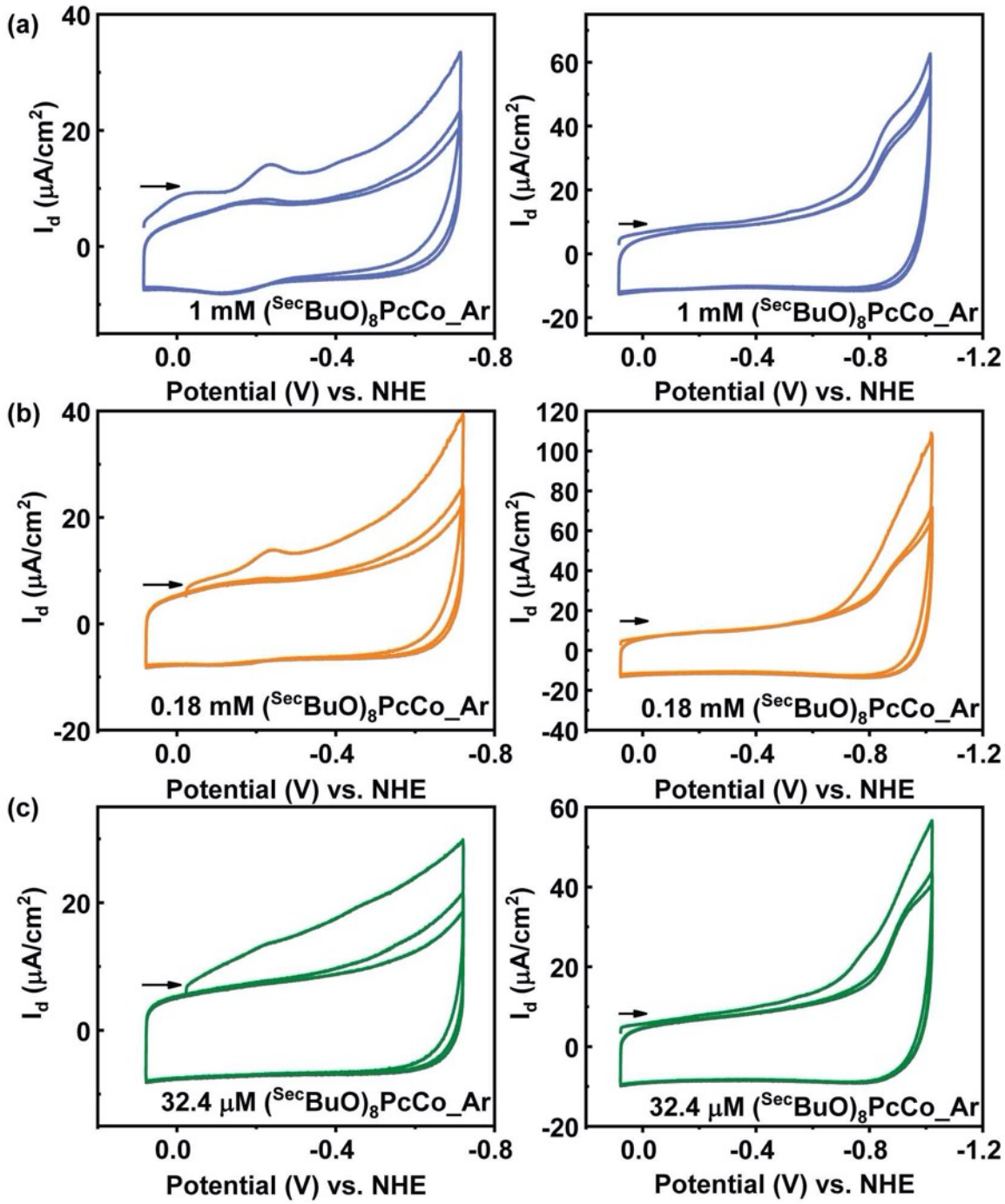

Figure S26. Run 2 CVs of ^{secBuO}PcCo under Ar atmosphere in concentrations of (a) 1 mM, (b) 0.18 mM, and (c) 32.4 μM stock solutions used to coat working electrodes. On the left, scan of more narrow potential windows and on the right, more broader potential windows are observed. The arrow shown in the plots indicates the scan direction.

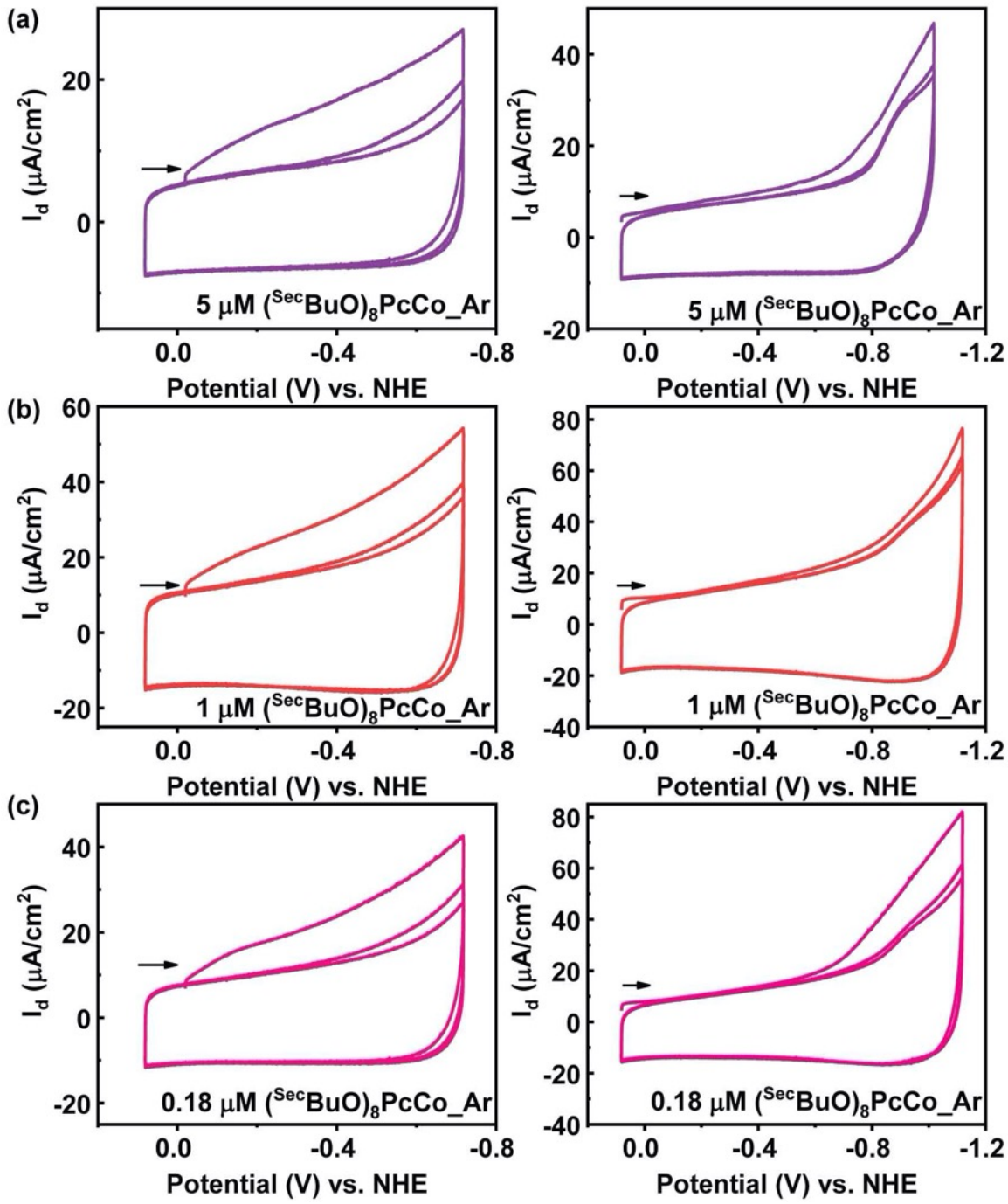

Figure S27. Run 2 CVs of ^{secBuO}PcCo under Ar atmosphere in concentrations of (a) 5 μM, (b) 1 μM, and (c) 0.18 μM stock solutions used to coat working electrodes. On the left, scan of more narrow potential windows and on the right, more broader potential windows are observed. The arrow shown in the plots indicates the scan direction.

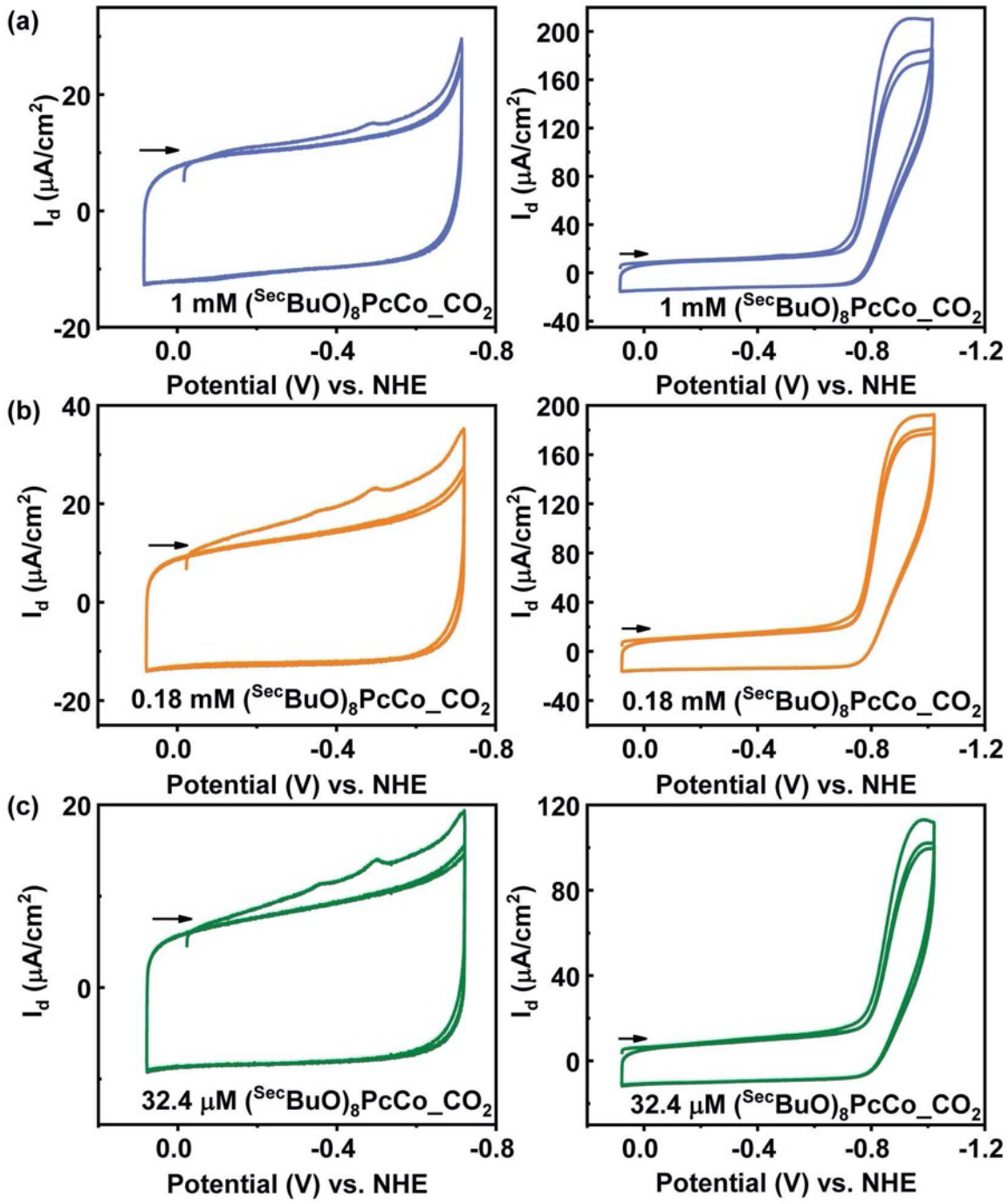

Figure S28. Run 2 CVs of ^{secBuO}PcCo under CO_2 atmosphere in concentrations of (a) 1 mM, (b) 0.18 mM, and (c) 32.4 µM stock solutions used to coat working electrodes. On the left, scan of more narrow potential windows and on the right, more broader potential windows are observed. The arrow shown in the plots indicates the scan direction.

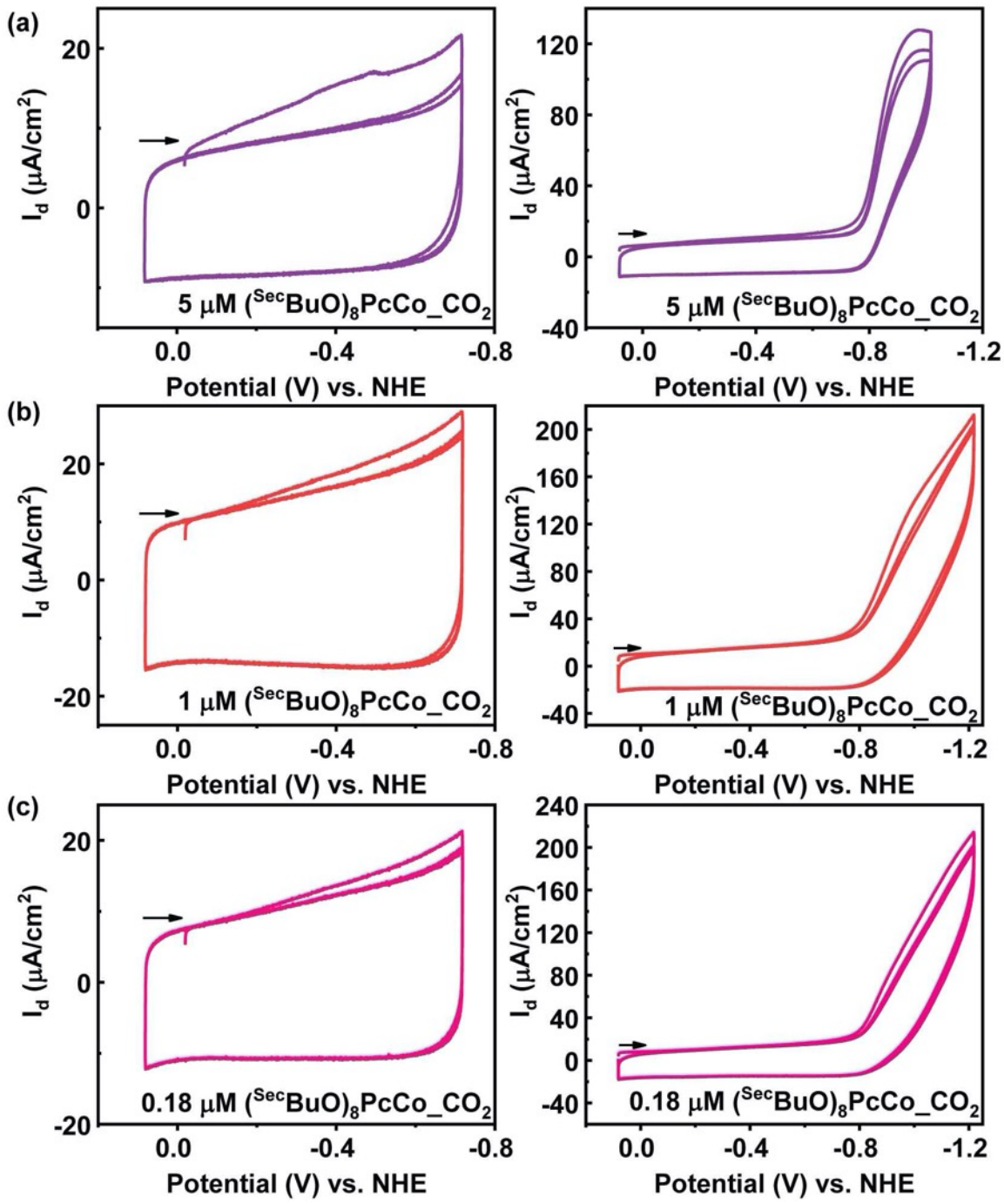

Figure S29. Run 2 CVs of ^{secBuO}PcCo under CO_2 atmosphere in concentrations of (a) 5 μM, (b) 1 μM, and (c) 0.18 μM stock solutions used to coat working electrodes. On the left, scan of more narrow potential windows and on the right, more broader potential windows are observed. The arrow shown in the plots indicates the scan direction.

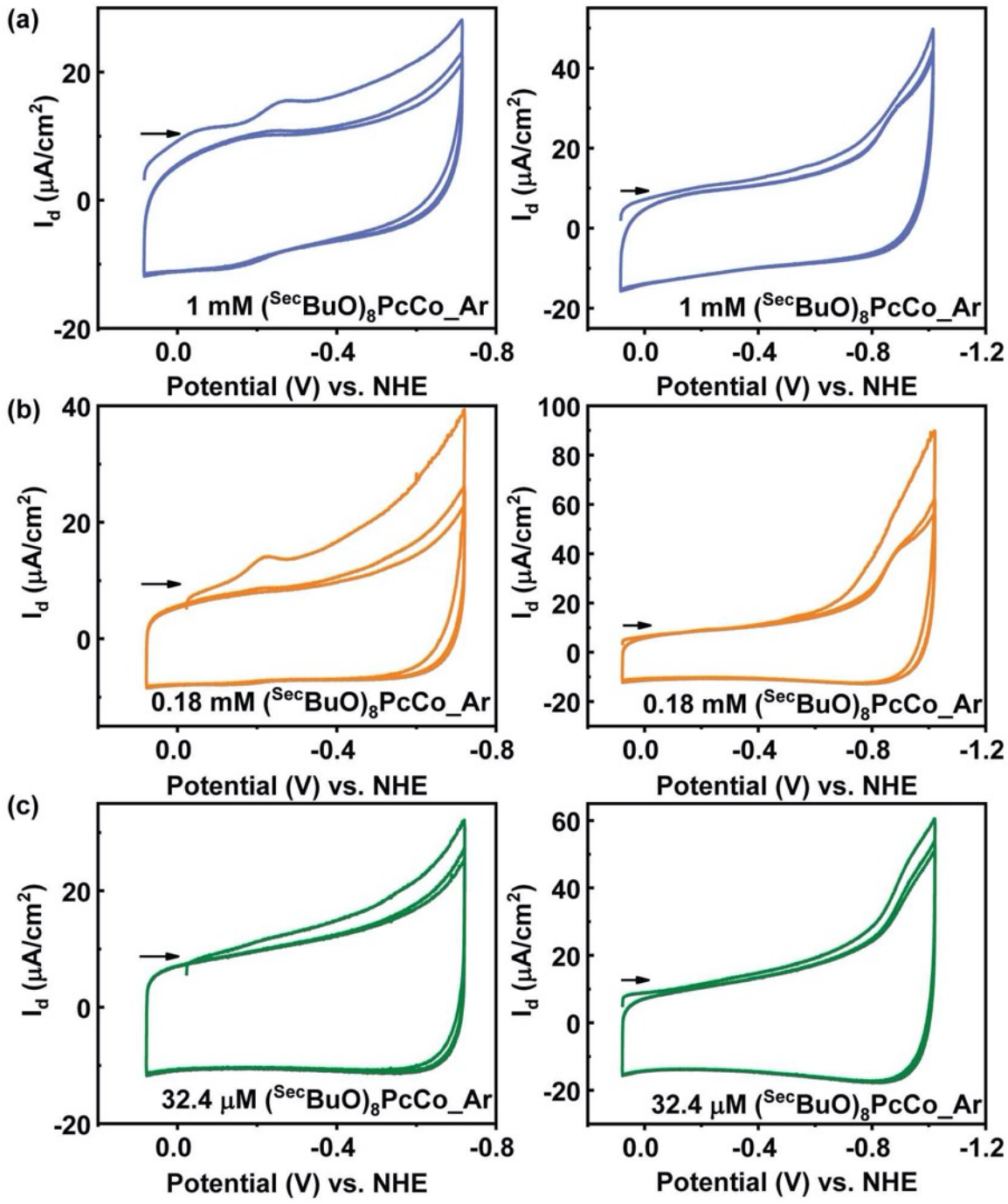

Figure S30. Run 3 CVs of ^{secBuO}PcCo under Ar atmosphere in concentrations of (a) 1 mM, (b) 0.18 mM, and (c) 32.4 µM stock solutions used to coat working electrodes. On the left, scan of more narrow potential windows and on the right, more broader potential windows are observed. The arrow shown in the plots indicates the scan direction.

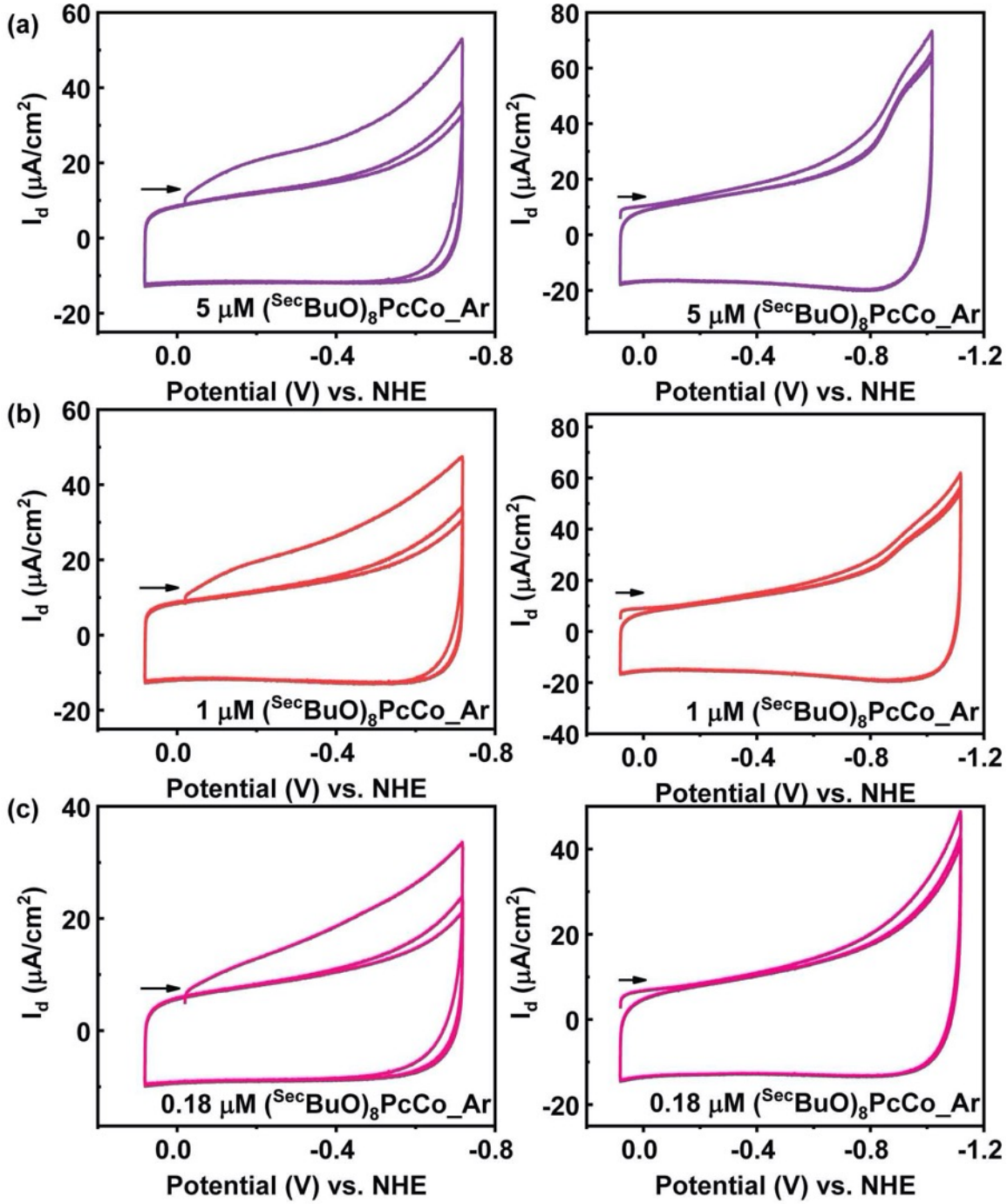

Figure S31. Run 3 CVs of ^{secBuO}PcCo under Ar atmosphere in concentrations of (a) 5 μM, (b) 1 μM, and (c) 0.18 μM stock solutions used to coat working electrodes. On the left, scan of more narrow potential windows and on the right, more broader potential windows are observed. The arrow shown in the plots indicates the scan direction.

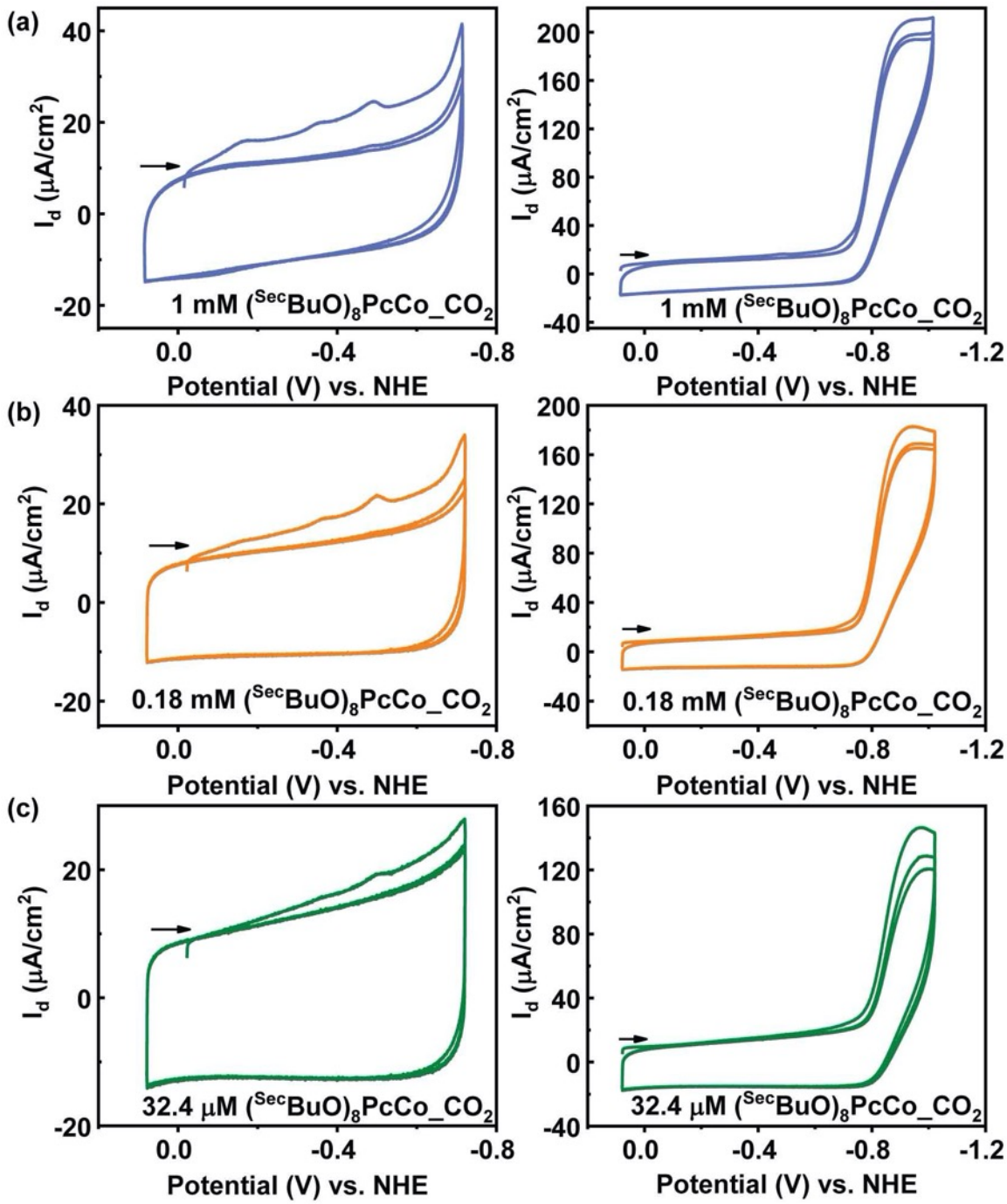

Figure S32. Run 3 CVs of ^{secBuO}PcCo under CO_2 atmosphere in concentrations of (a) 1 mM, (b) 0.18 mM, and (c) 32.4 µM stock solutions used to coat working electrodes. On the left, scan of more narrow potential windows and on the right, more broader potential windows are observed. The arrow shown in the plots indicates the scan direction.

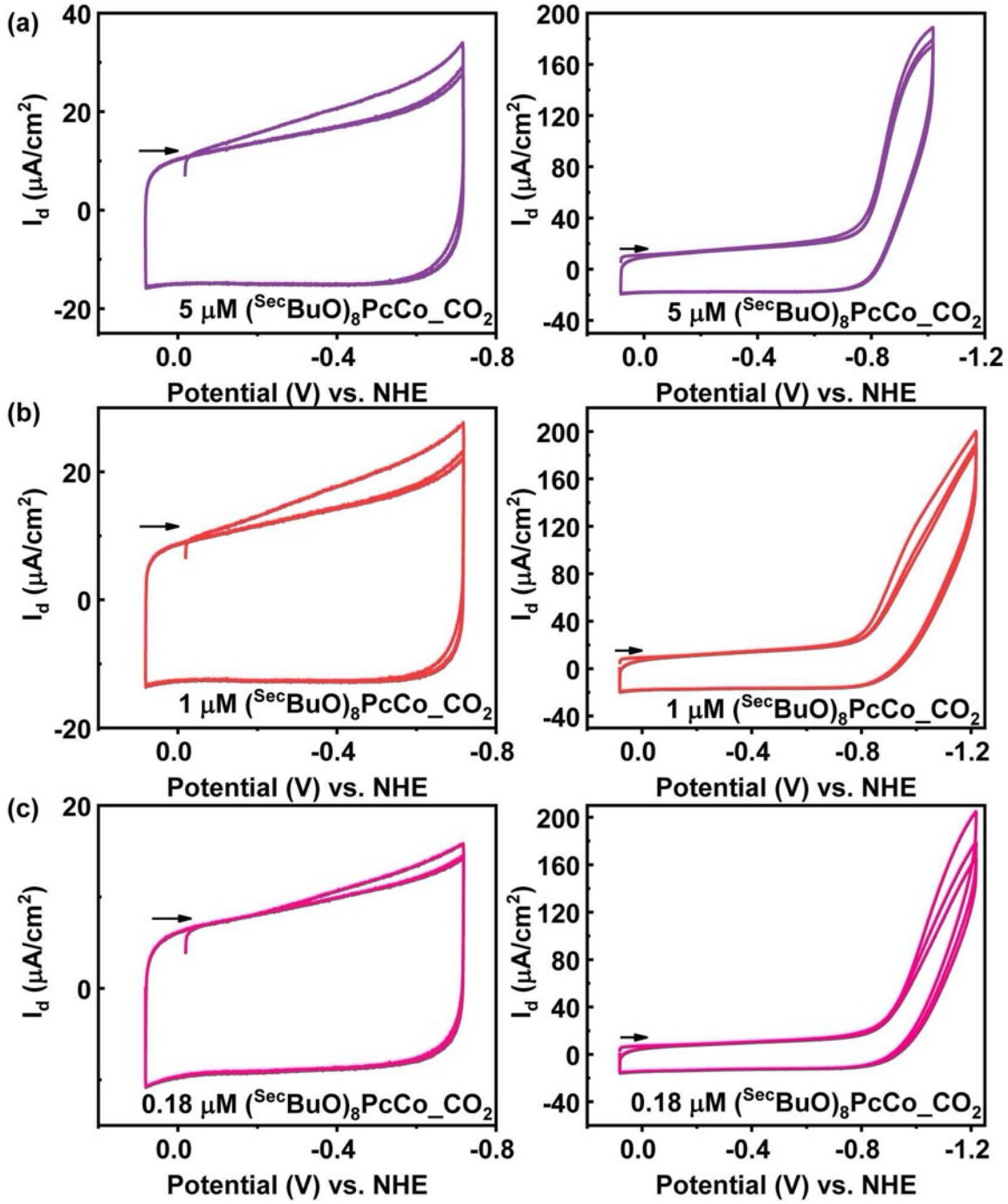

Figure S33. Run 3 CVs of ^{secBuO}PcCo under CO_2 atmosphere in concentrations of (a) 5 μM, (b) 1 μM, and (c) 0.18 μM stock solutions used to coat working electrodes. On the left, scan of more narrow potential windows and on the right, more broader potential windows are observed. The arrow shown in the plots indicates the scan direction.

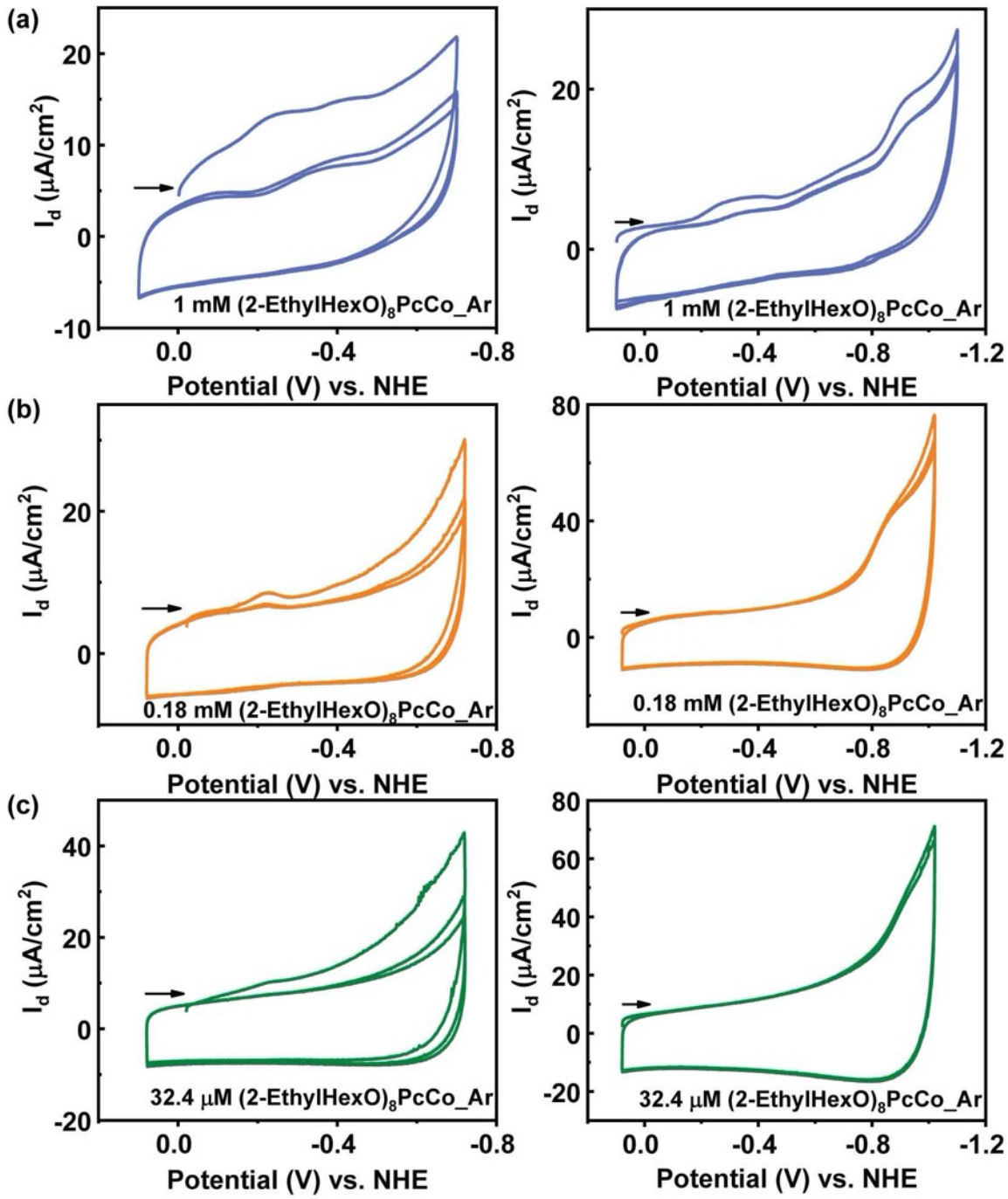

Figure S34. Run 2 CVs of ^{EtHexO}PcCo under Ar atmosphere in concentrations of (a) 1 mM, (b) 0.18 mM, and (c) 32.4 μM stock solutions used to coat working electrodes. On the left, scan of more narrow potential windows and on the right, more broader potential windows are observed. The arrow shown in the plots indicates the scan direction.

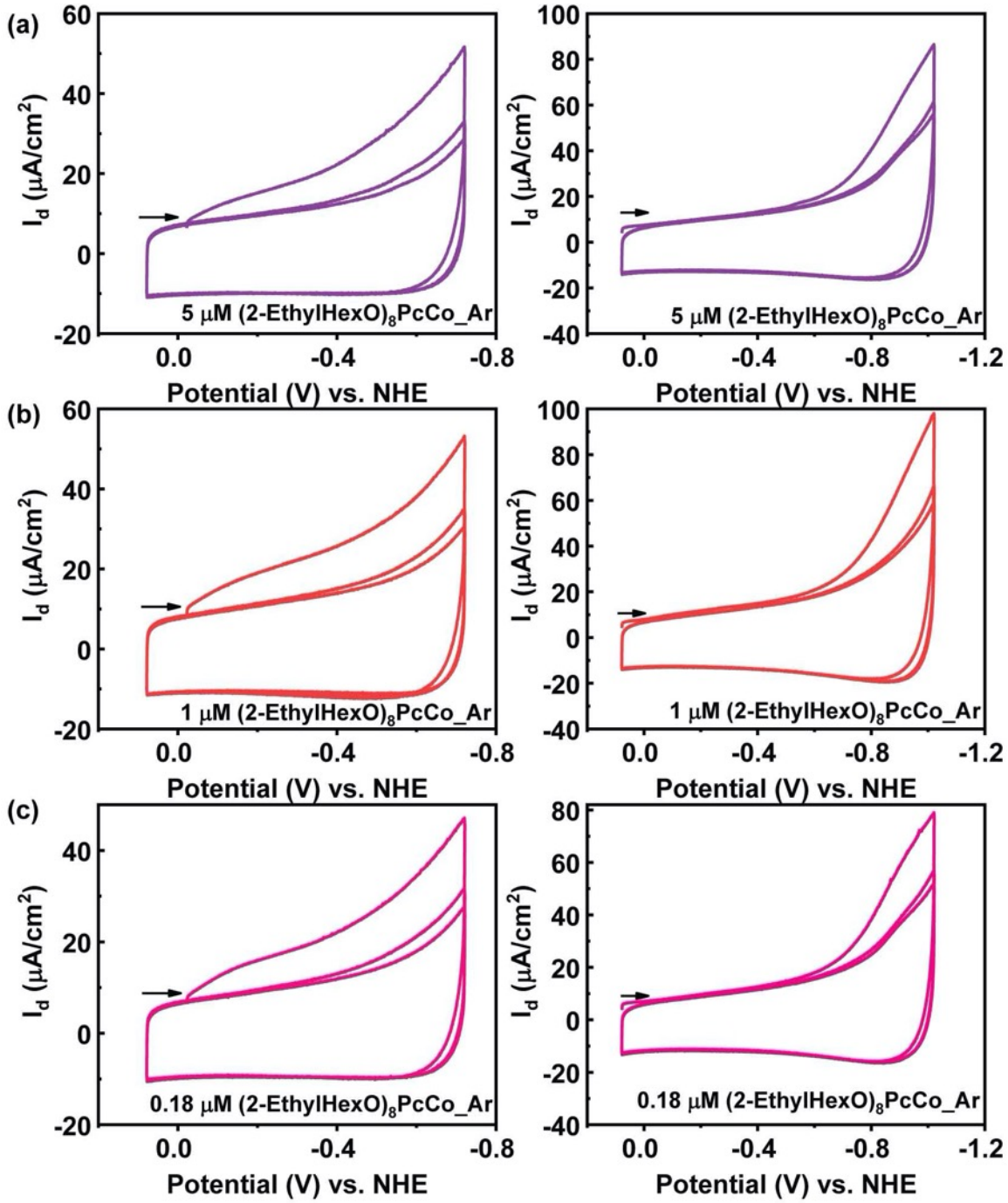

Figure S35. Run 2 CVs of [EtHexO]PcCo under Ar atmosphere in concentrations of (a) 5 μM, (b) 1 μM, and (c) 0.18 μM stock solutions used to coat working electrodes. On the left, scan of more narrow potential windows and on the right, more broader potential windows are observed. The arrow shown in the plots indicates the scan direction.

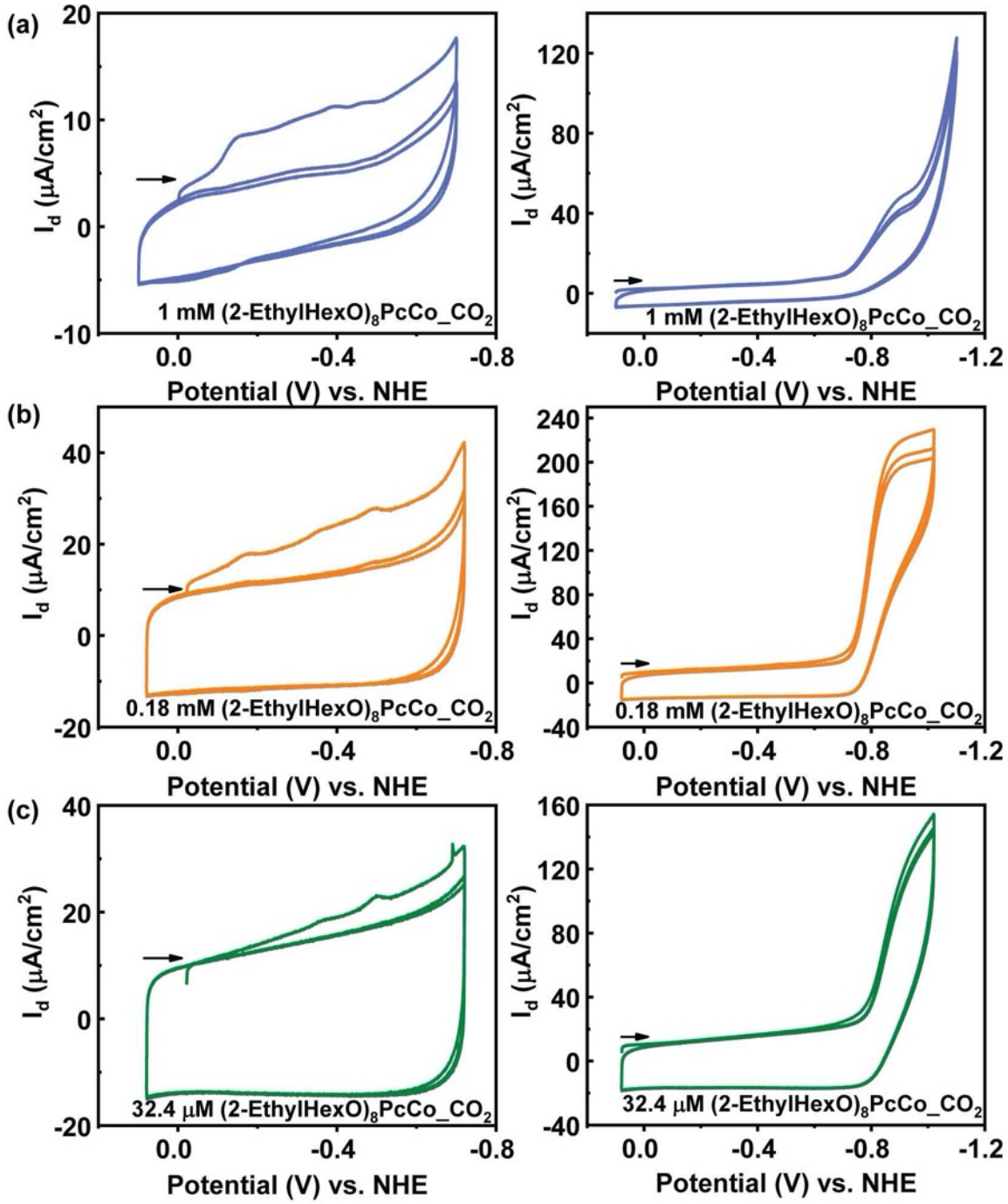

Figure S36. Run 2 CVs of ^{EtHexO}PcCo under CO_2 atmosphere in concentrations of (a) 1 mM, (b) 0.18 mM, and (c) 32.4 μM stock solutions used to coat working electrodes. On the left, scan of more narrow potential windows and on the right, more broader potential windows are observed. The arrow shown in the plots indicates the scan direction.

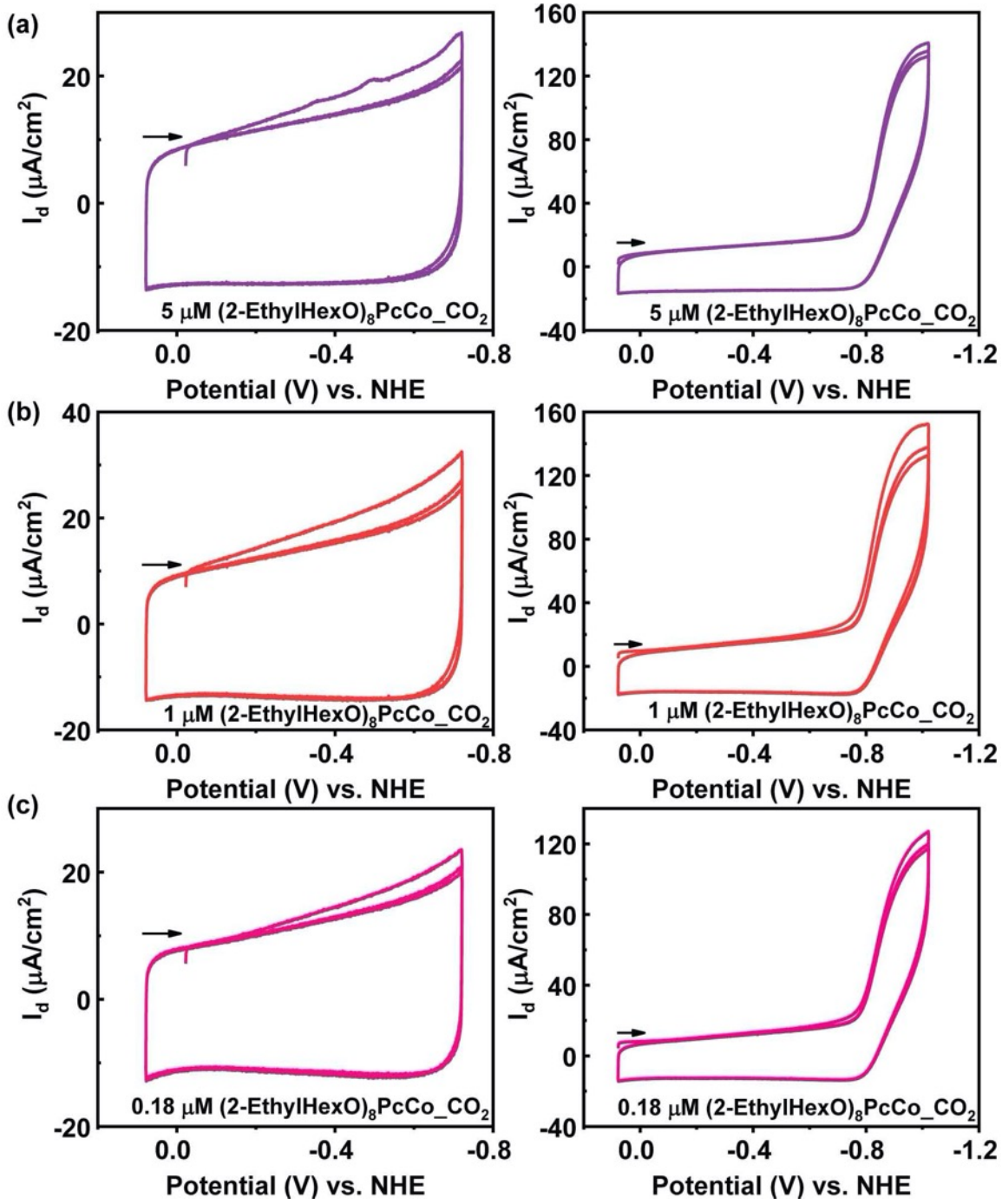

Figure S37. Run 2 CVs of ^{EtHexO}PcCo under CO_2 atmosphere in concentrations of (a) 5 μM, (b) 1 μM, and (c) 0.18 μM stock solutions used to coat working electrodes. On the left, scan of more narrow potential windows and on the right, more broader potential windows are observed. The arrow shown in the plots indicates the scan direction.

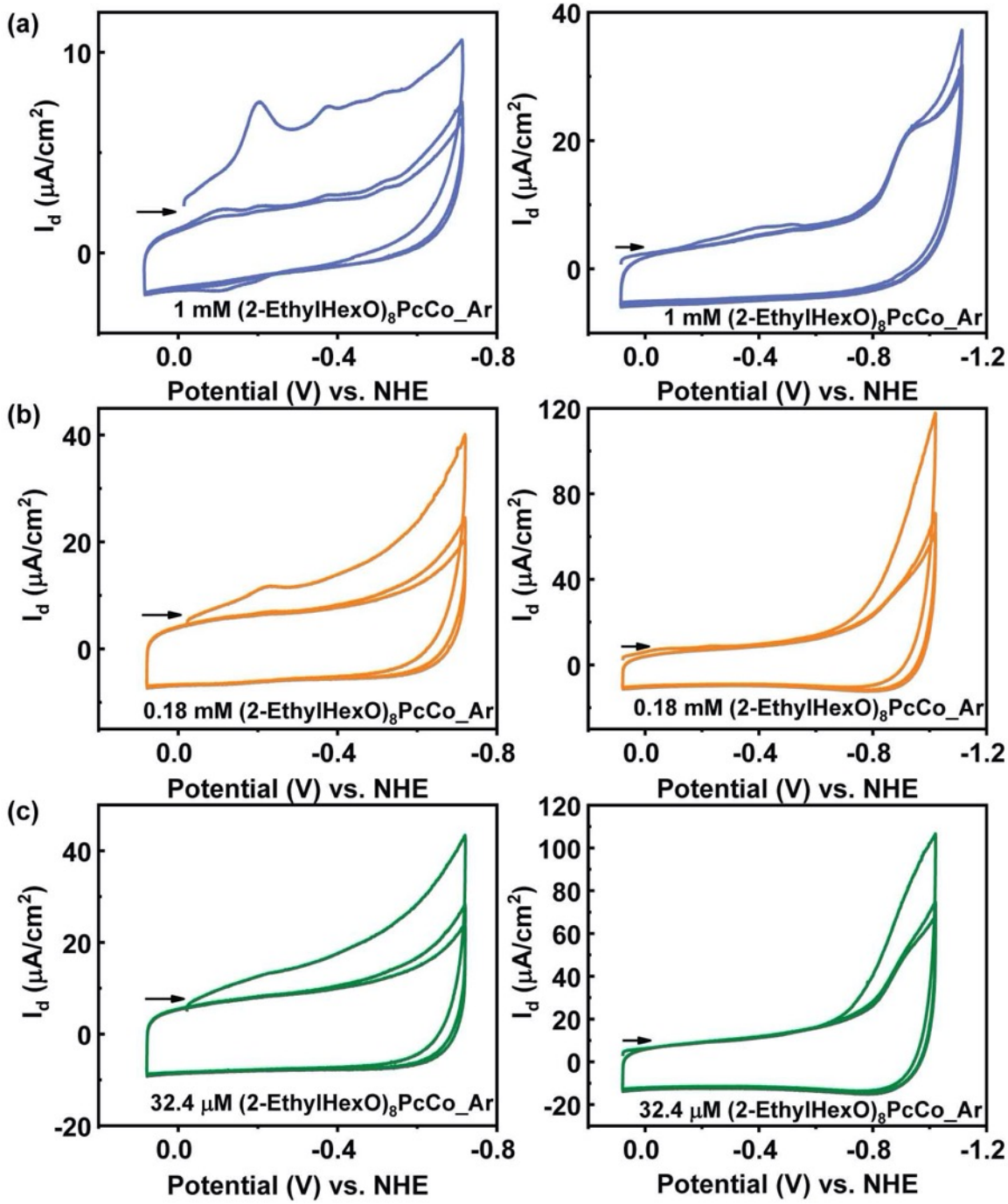

Figure S38. Run 3 CVs of ^{EtHexO}PcCo under Ar atmosphere in concentrations of (a) 1 mM, (b) 0.18 mM, and (c) 32.4 μM stock solutions used to coat working electrodes. On the left, scan of more narrow potential windows and on the right, more broader potential windows are observed. The arrow shown in the plots indicates the scan direction.

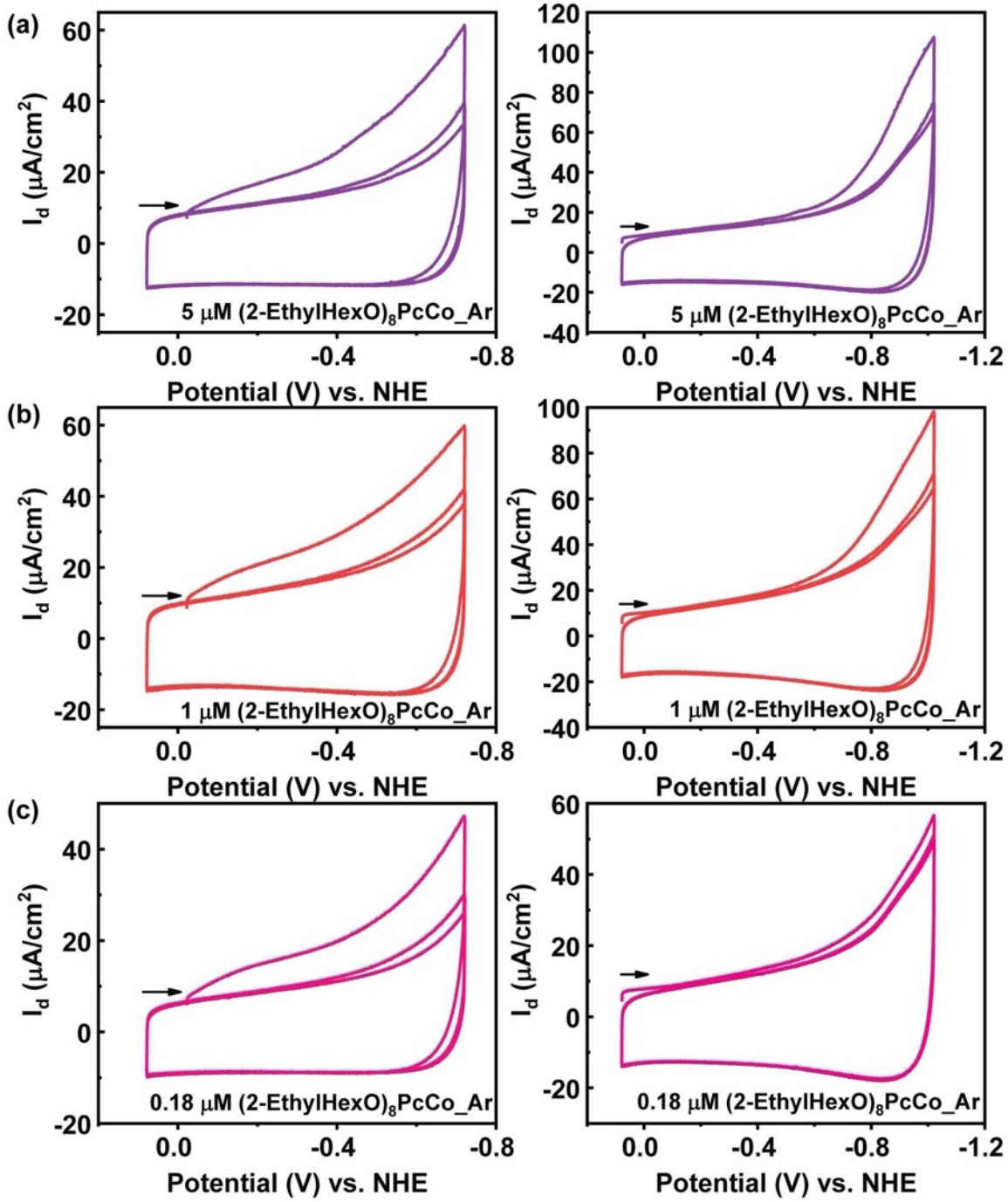

Figure S39. Run 3 CVs of ^{EtHexO}PcCo under Ar atmosphere in concentrations of (a) 5 μM, (b) 1 μM, and (c) 0.18 μM stock solutions used to coat working electrodes. On the left, scan of more narrow potential windows and on the right, more broader potential windows are observed. The arrow shown in the plots indicates the scan direction.

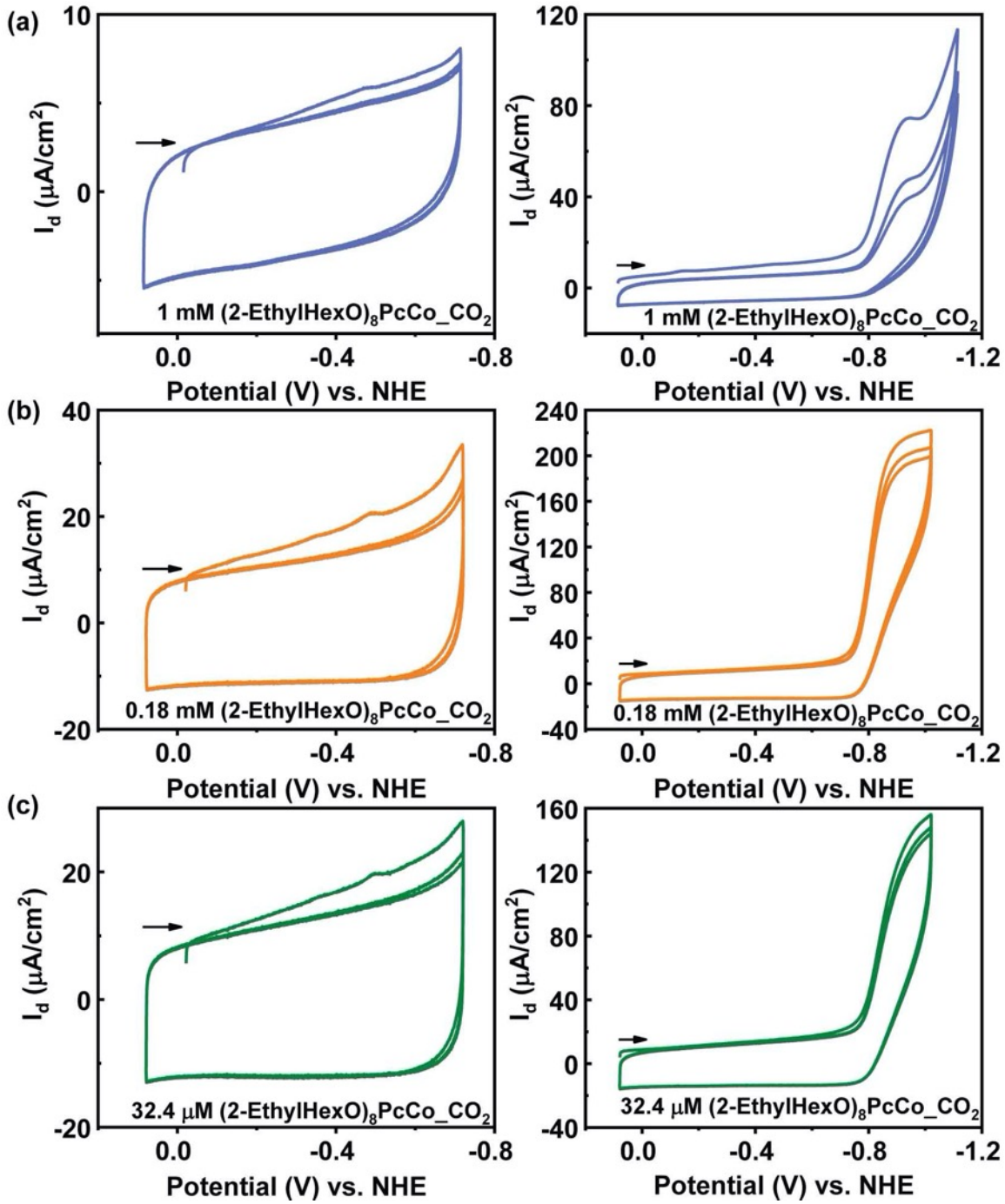

Figure S40. Run 3 CVs of ^{EtHexO}PcCo under CO_2 atmosphere in concentrations of (a) 1 mM, (b) 0.18 mM, and (c) 32.4 μM stock solutions used to coat working electrodes. On the left, scan of more narrow potential windows and on the right, more broader potential windows are observed. The arrow shown in the plots indicates the scan direction.

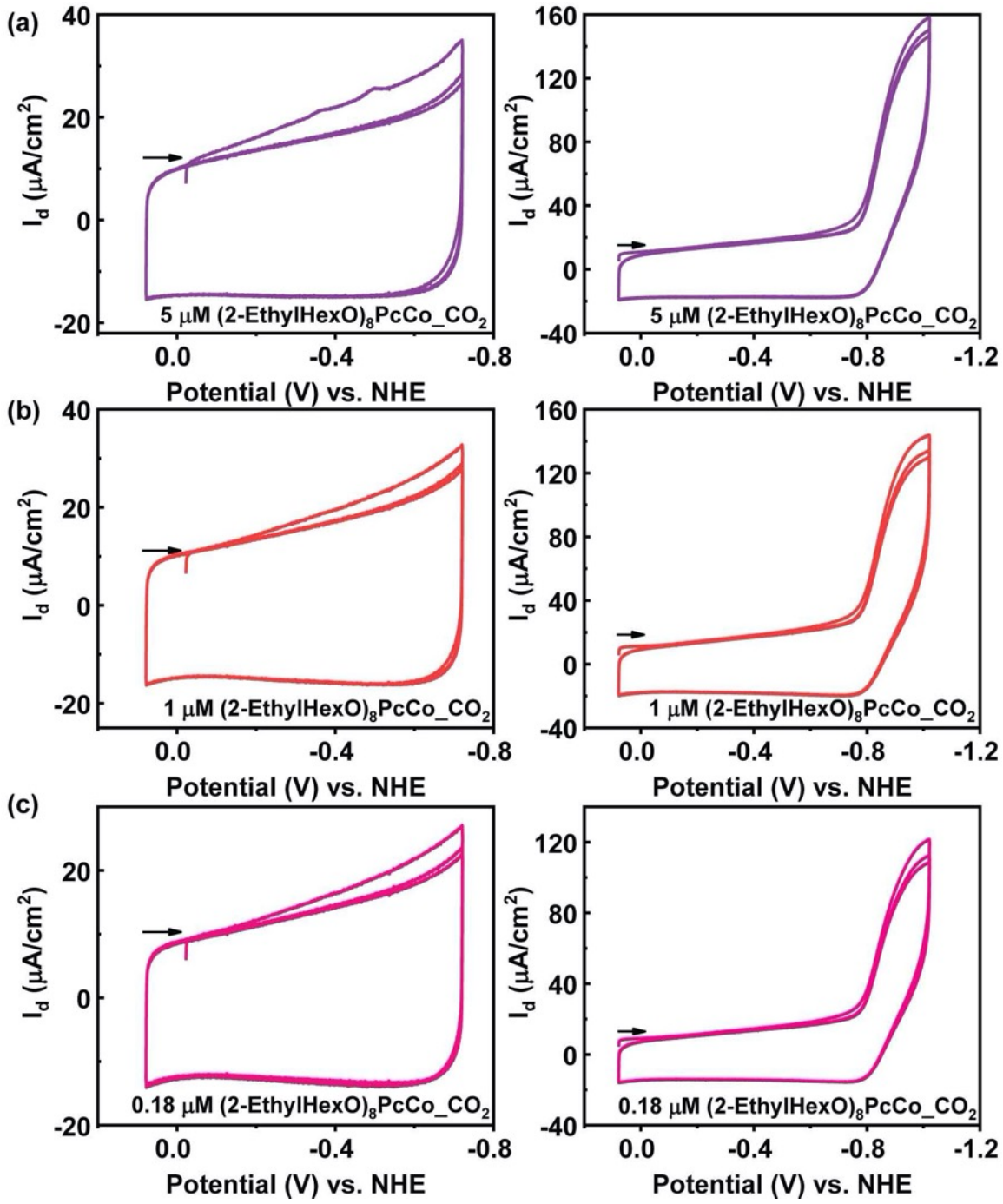

Figure S41. Run 3 CVs of ^{EtHexO}PcCo under CO_2 atmosphere in concentrations of (a) 5 μM, (b) 1 μM, and (c) 0.18 μM stock solutions used to coat working electrodes. On the left, scan of more narrow potential windows and on the right, more broader potential windows are observed. The arrow shown in the plots indicates the scan direction.

Bare electrode CV and CPE

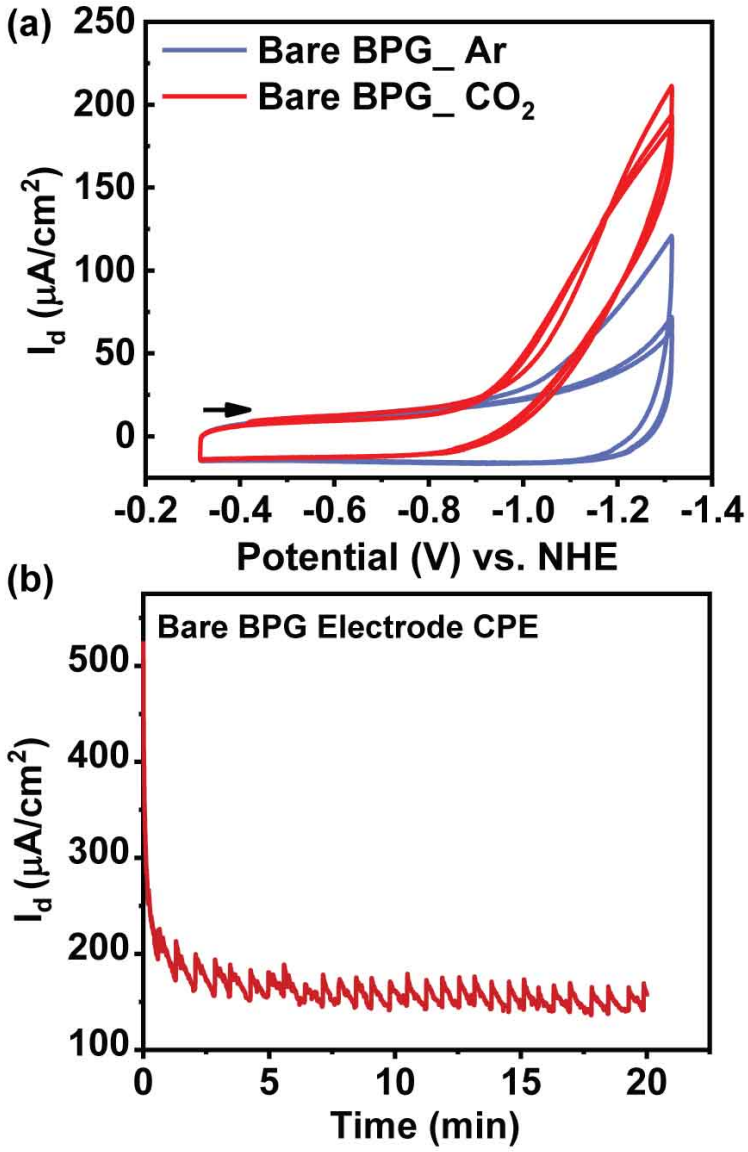

Figure S42. (a) Cyclic Voltammogram for bare BPG electrode under Ar (Blue) and under CO_2 (red) atmosphere. The arrow shown in the plots indicates the scan direction. (b) CPE of bare BPG electrode run for 20 min.

Scan Rate Dependant CVs of ^{RO}PcCo Complexes

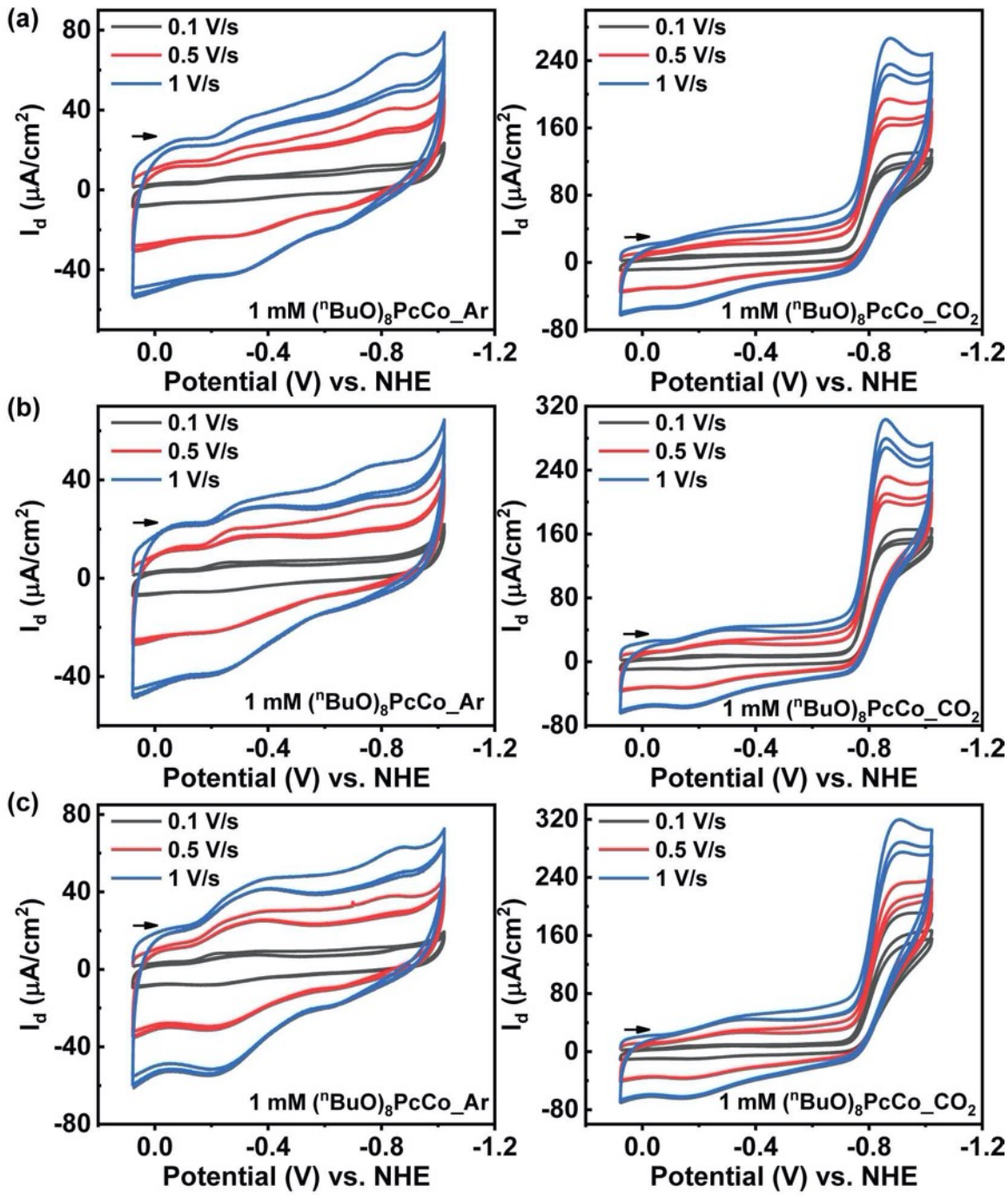

Figure S43. (a) Run 1, (b) Run 2, and (c) Run 3 Scan rate dependent CVs of ^{nBuO}PcCo in 1 mM concentration stock solution used to coat working electrodes. On the left the rate dependent CVs are under Ar and on the right the rate dependent CVs are under CO_2 atmosphere. The arrow shown in the plots indicates the scan direction.

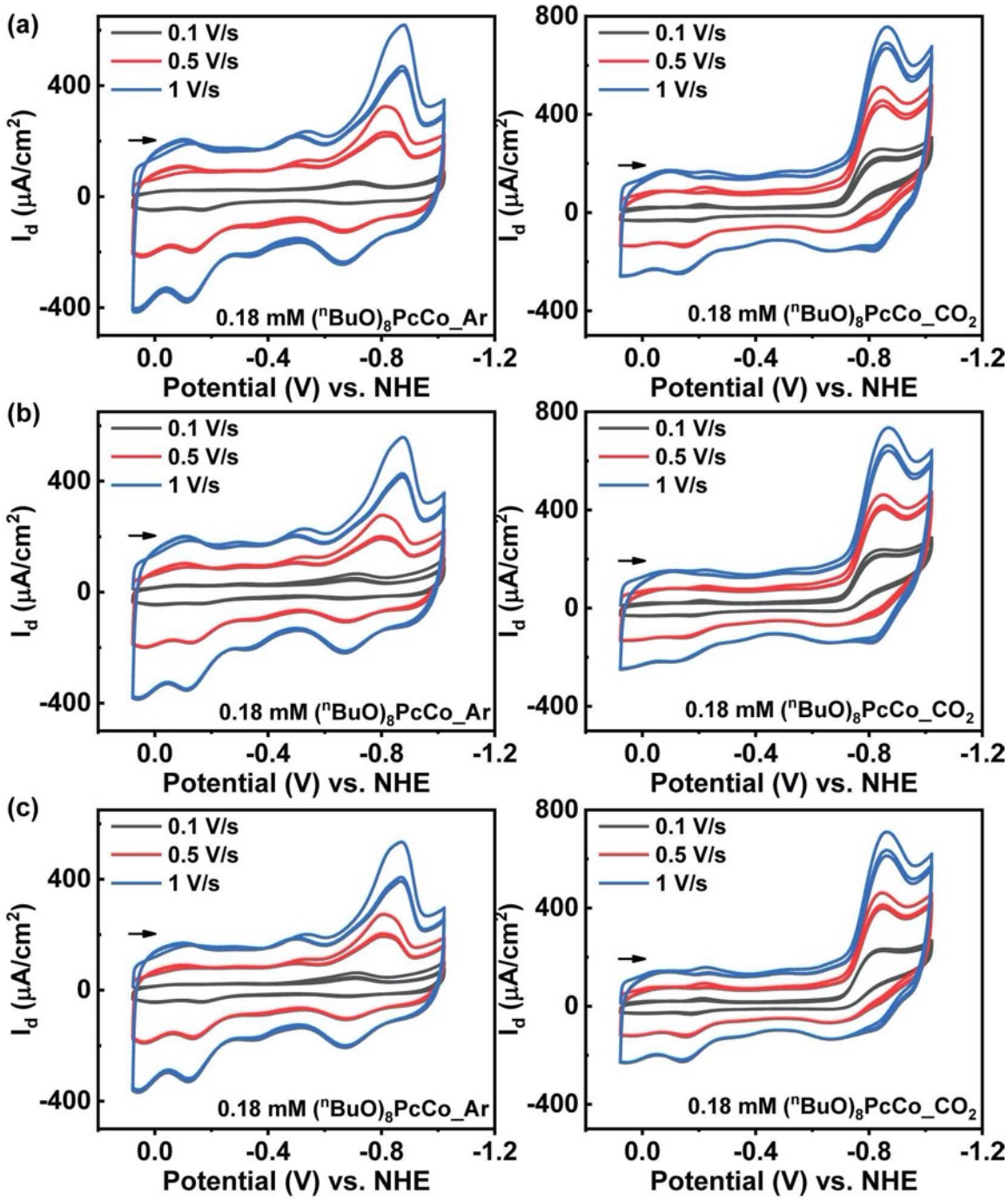

Figure S44. (a) Run 1, (b) Run 2, and (c) Run 3 Scan rate dependent CVs of ^{nBuO}PcCo in 0.18 mM concentration stock solution used to coat working electrodes. On the left the rate dependent CVs are under Ar and on the right the rate dependent CVs are under CO_2 atmosphere. The arrow shown in the plots indicates the scan direction.

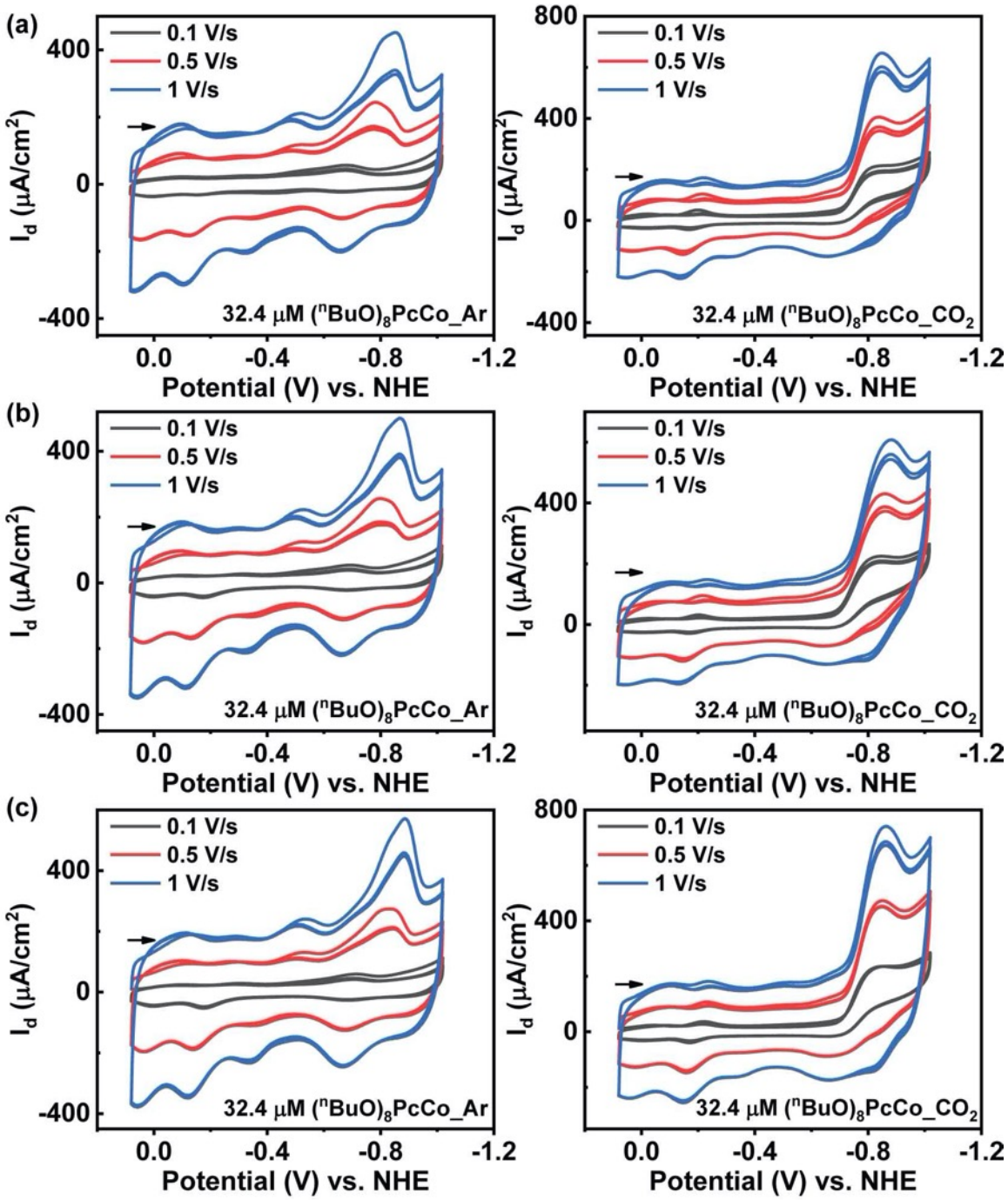

Figure S45. (a) Run 1, (b) Run 2, and (c) Run 3 Scan rate dependent CVs of ^{nBuO}PcCo in 32.4 μM concentration stock solution used to coat working electrodes. On the left the rate dependent CVs are under Ar and on the right the rate dependent CVs are under CO_2 atmosphere. The arrow shown in the plots indicates the scan direction.

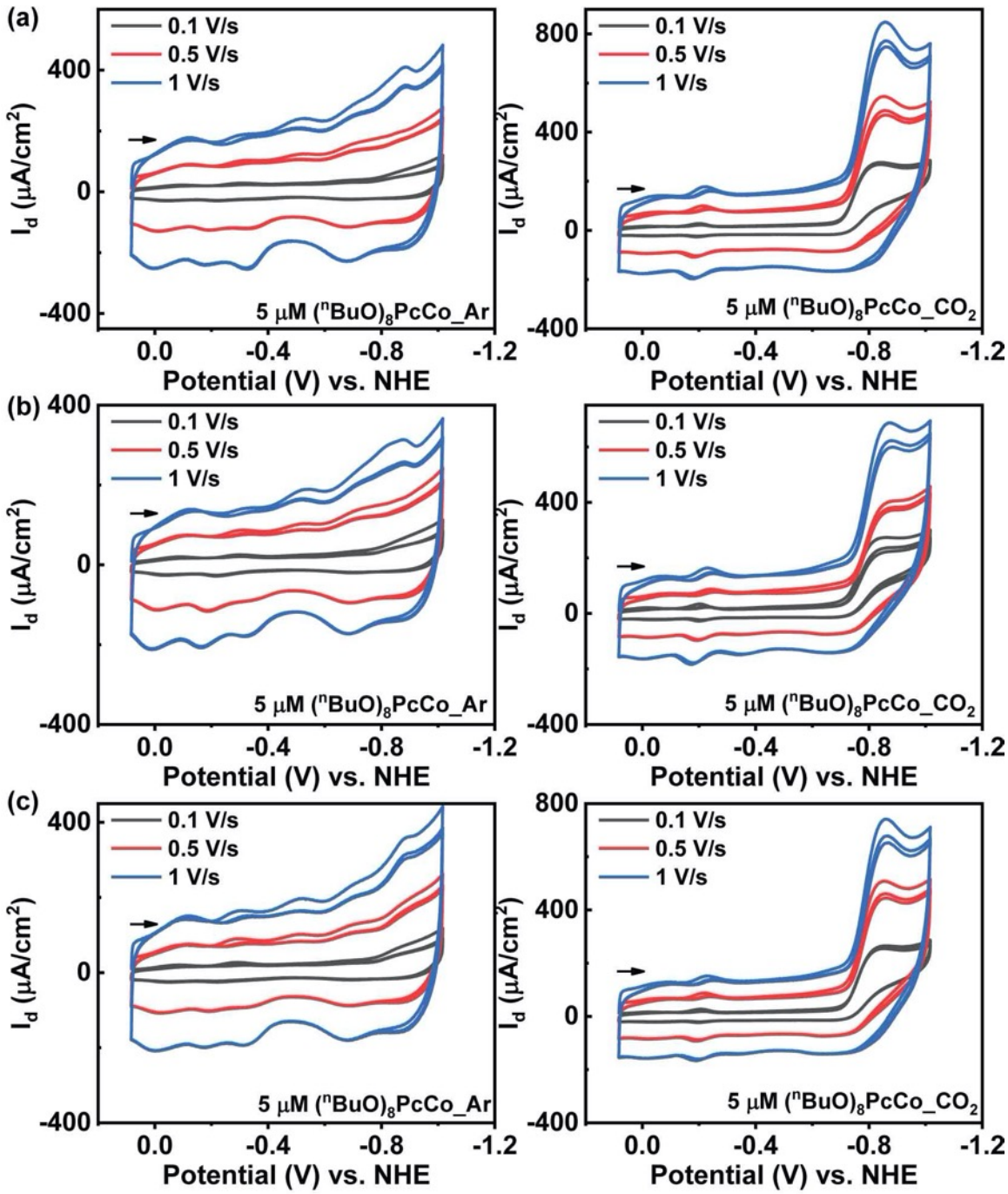

Figure S46. (a) Run 1, (b) Run 2, and (c) Run 3 Scan rate dependent CVs of ^{nBuO}PcCo in 5 μM concentration stock solution used to coat working electrodes. On the left the rate dependent CVs are under Ar and on the right the rate dependent CVs are under CO_2 atmosphere. The arrow shown in the plots indicates the scan direction.

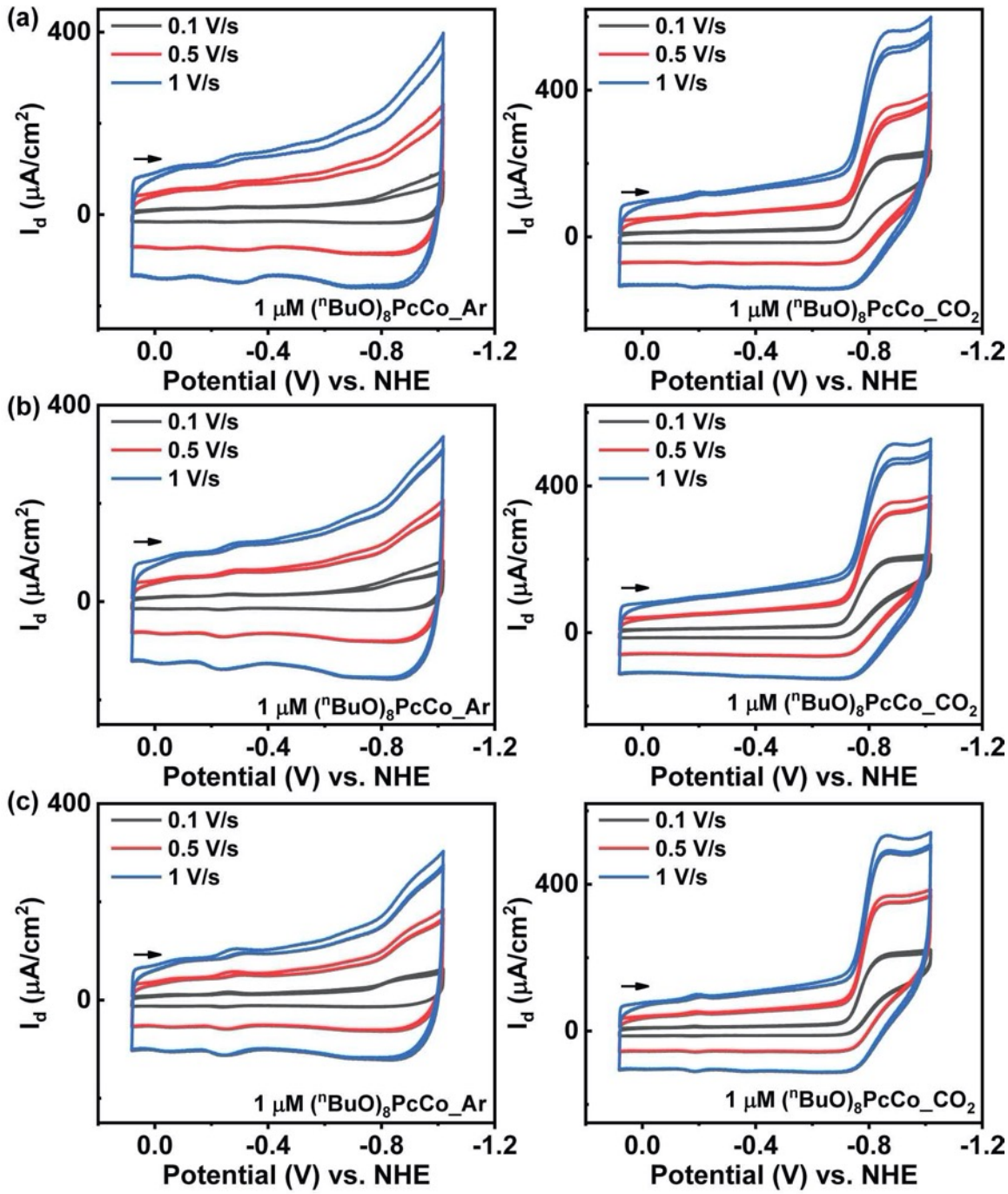

Figure S47. (a) Run 1, (b) Run 2, and (c) Run 3 Scan rate dependent CVs of ^{nBuO}PcCo in 1 μM concentration stock solution used to coat working electrodes. On the left the rate dependent CVs are under Ar and on the right the rate dependent CVs are under CO_2 atmosphere. The arrow shown in the plots indicates the scan direction.

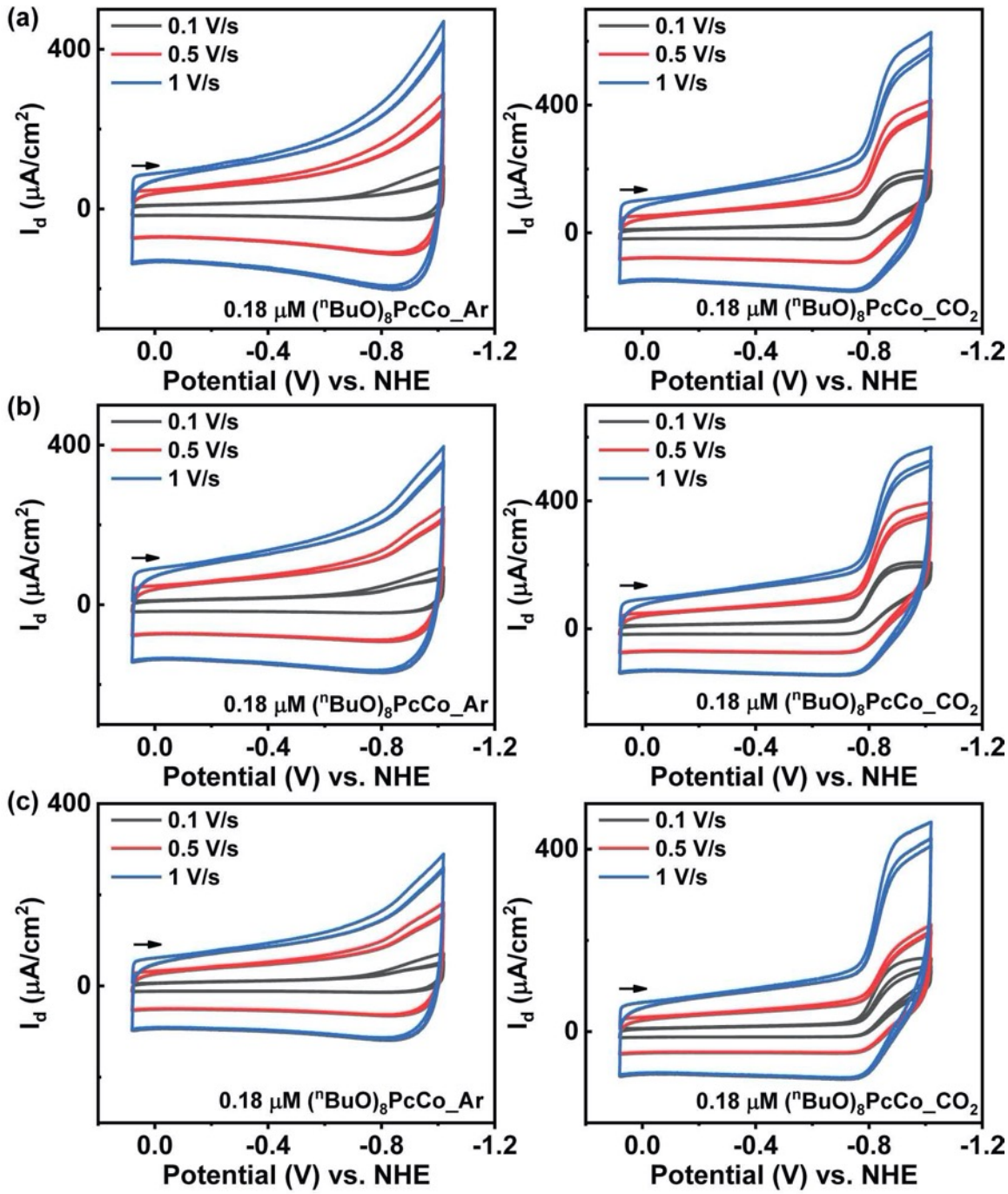

Figure S48. (a) Run 1, (b) Run 2, and (c) Run 3 Scan rate dependent CVs of ^{nBuO}PcCo in 0.18 μM concentration stock solution used to coat working electrodes. On the left the rate dependent CVs are under Ar and on the right the rate dependent CVs are under CO_2 atmosphere. The arrow shown in the plots indicates the scan direction.

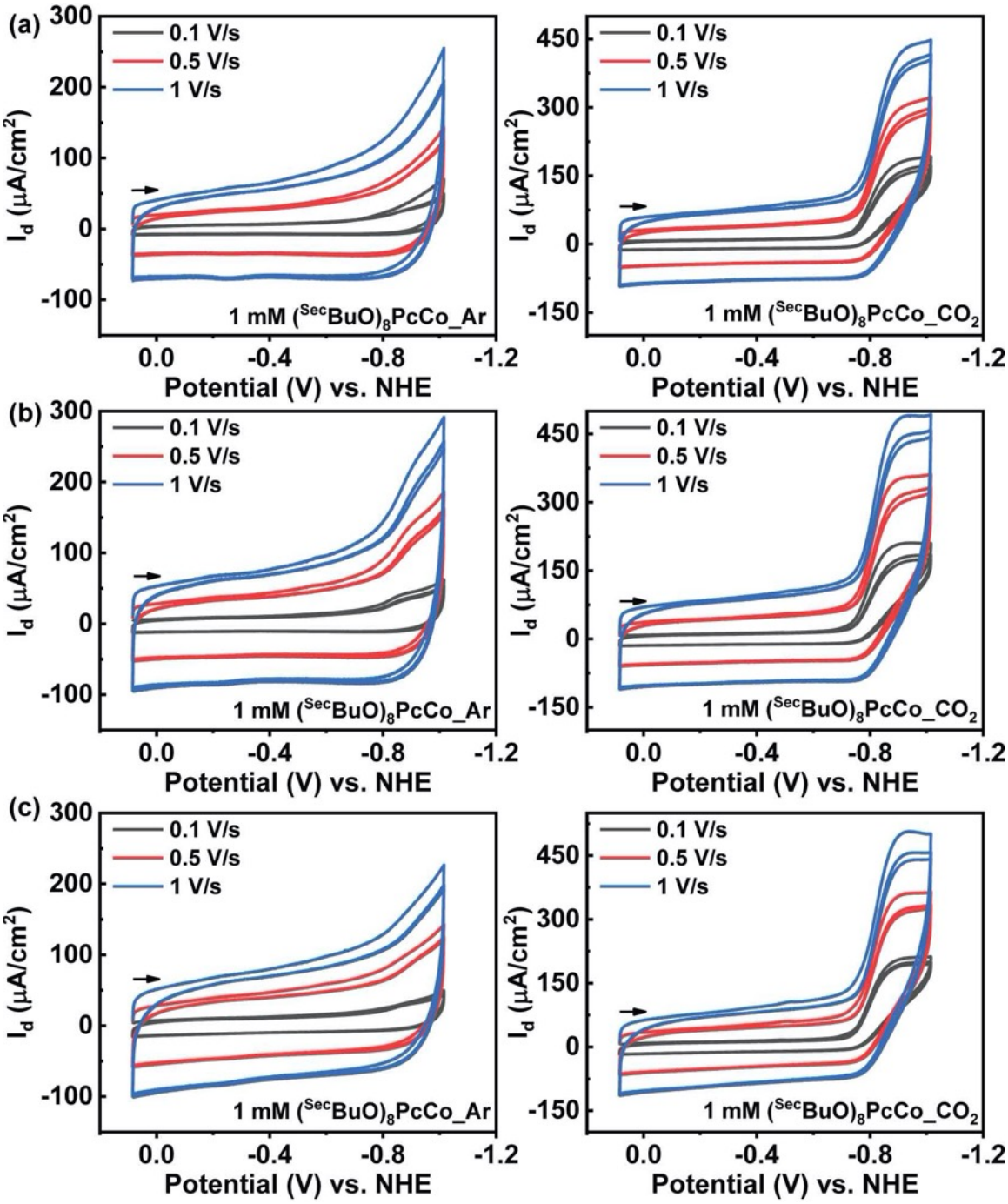

Figure S49. (a) Run 1, (b) Run 2, and (c) Run 3 Scan rate dependent CVs of ^{nBuO}PcCo in 1 mM concentration stock solution used to coat working electrodes. On the left the rate dependent CVs are under Ar and on the right the rate dependent CVs are under CO_2 atmosphere. The arrow shown in the plots indicates the scan direction.

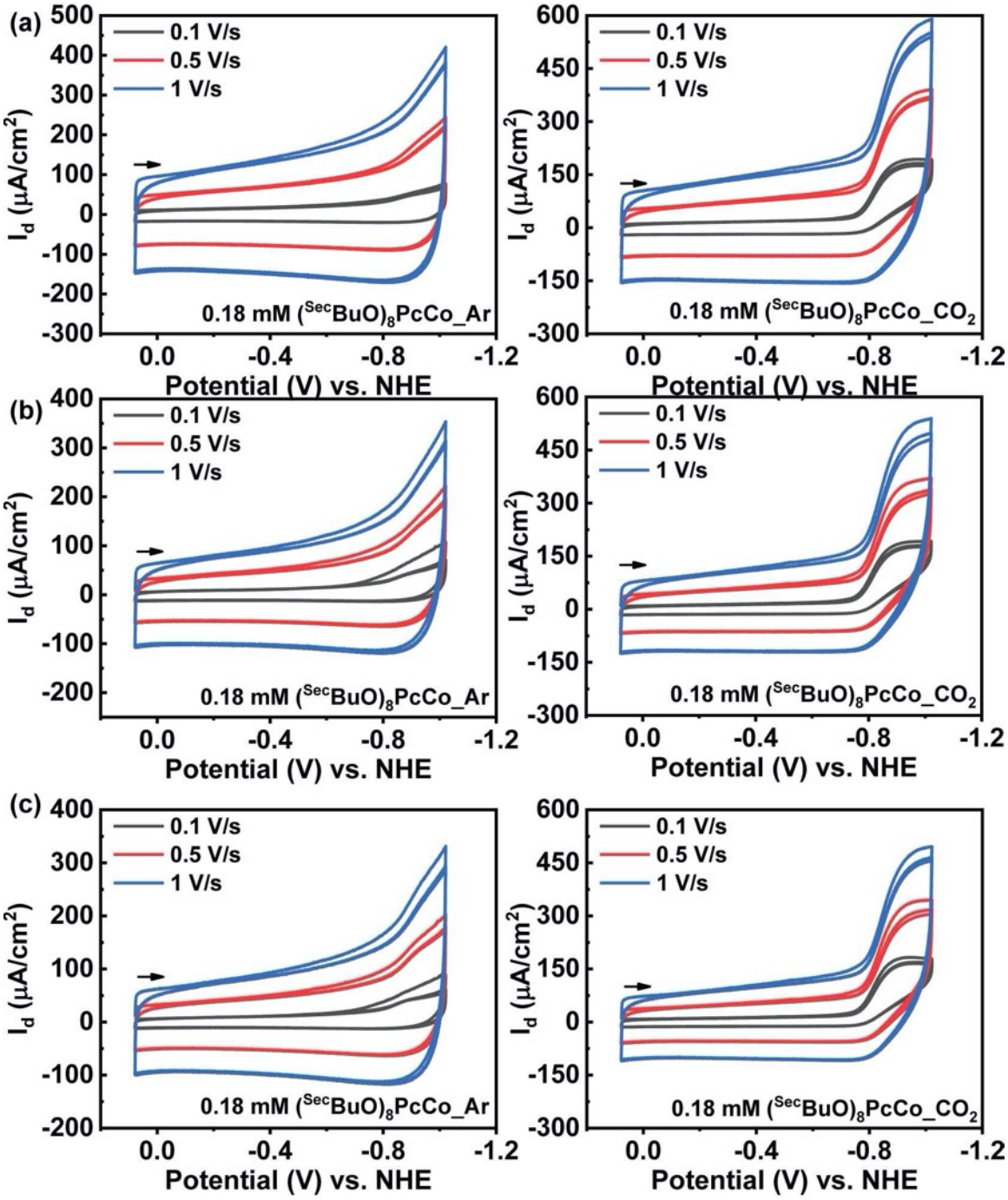

Figure S50. (a) Run 1, (b) Run 2, and (c) Run 3 Scan rate dependent CVs of ^{secBuO}PcCo in 0.18 mM concentration stock solution used to coat working electrodes. On the left the rate dependent CVs are under Ar and on the right the rate dependent CVs are under CO_2 atmosphere. The arrow shown in the plots indicates the scan direction.

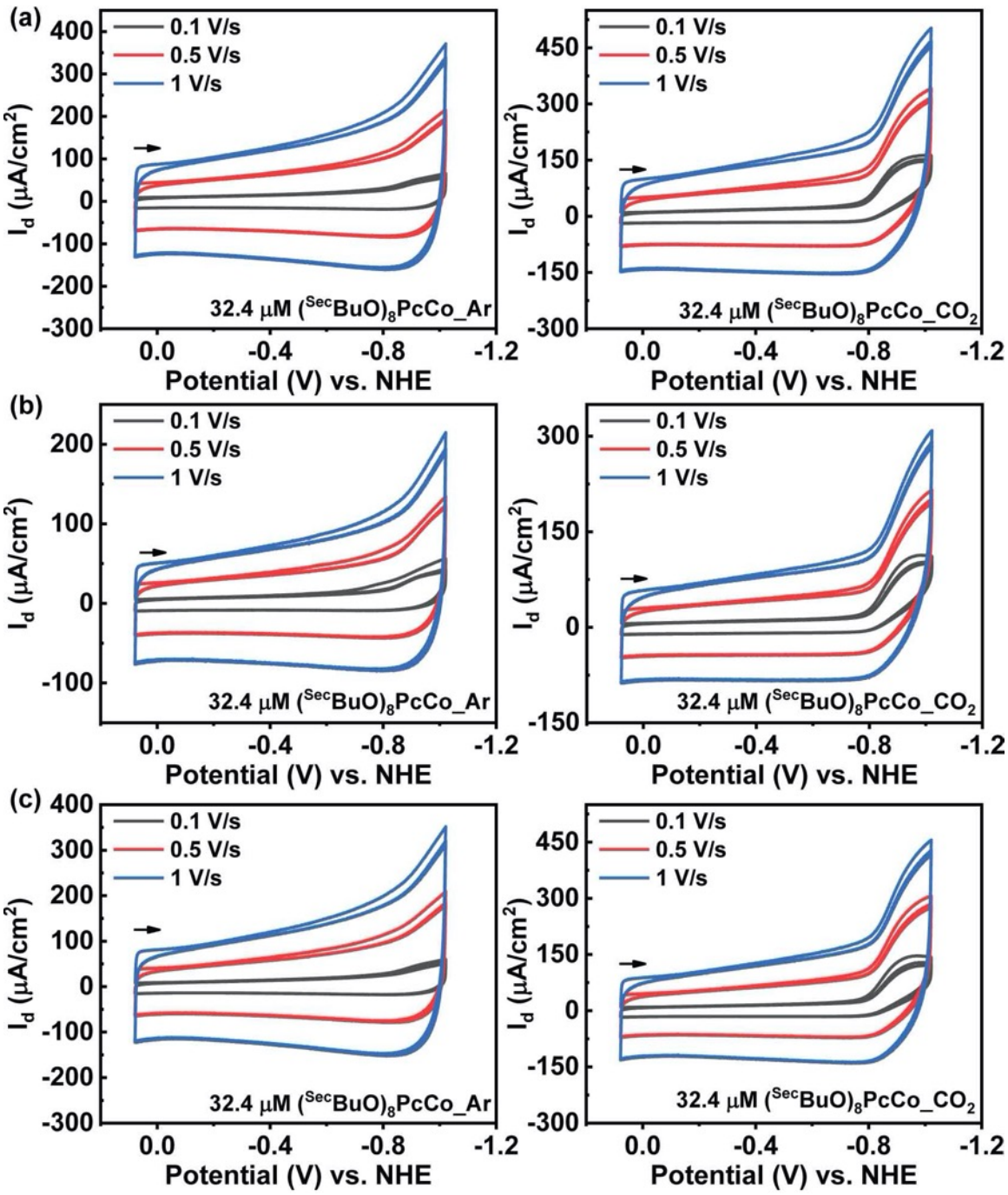

Figure S51. (a) Run 1, (b) Run 2, and (c) Run 3 Scan rate dependent CVs of ^{secBuO}PcCo in 32.4 μM concentration stock solution used to coat working electrodes. On the left the rate dependent CVs are under Ar and on the right the rate dependent CVs are under CO_2 atmosphere. The arrow shown in the plots indicates the scan direction.

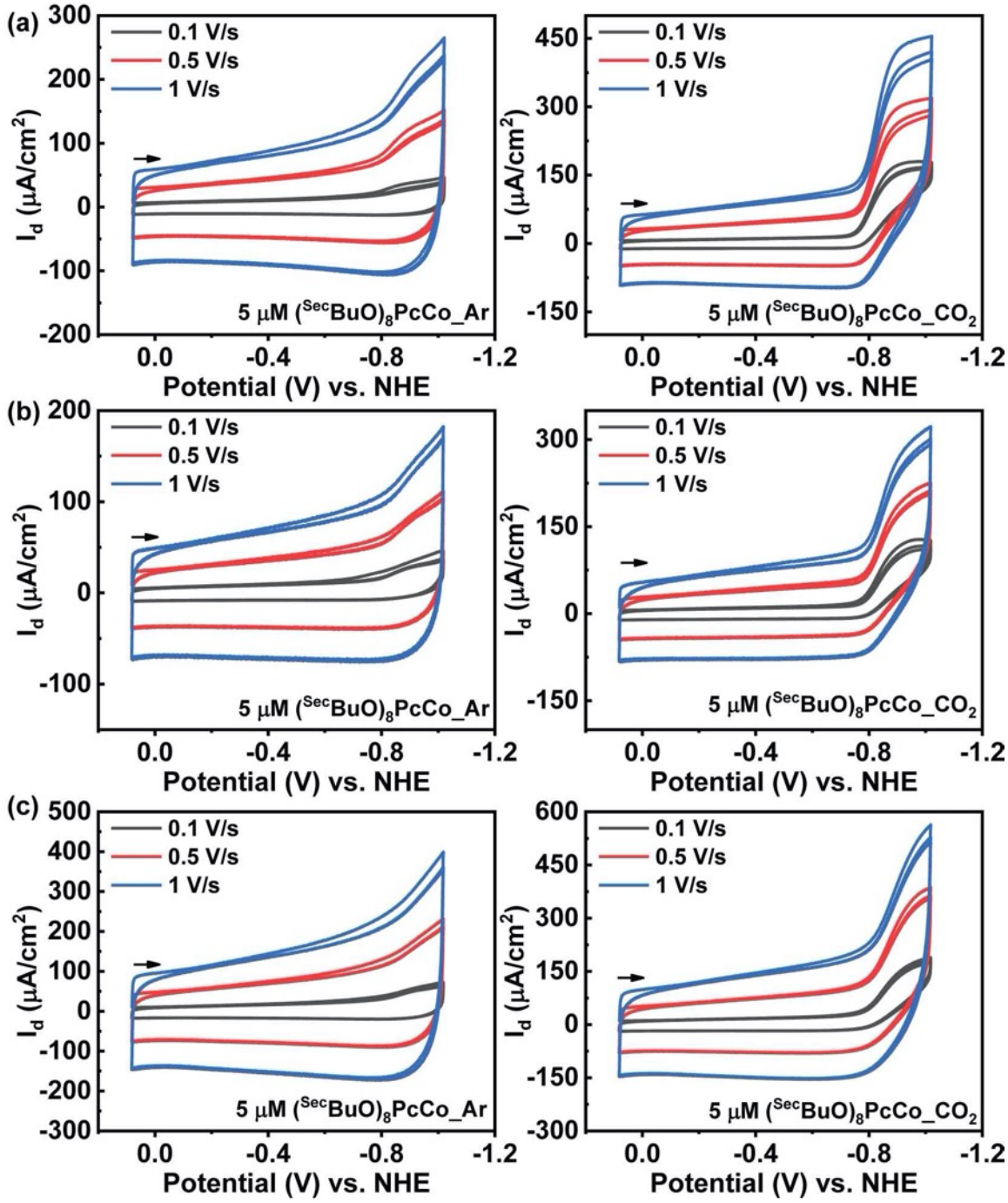

Figure S52. (a) Run 1, (b) Run 2, and (c) Run 3 Scan rate dependent CVs of ^{secBuO}PcCo in 5 μM concentration stock solution used to coat working electrodes. On the left the rate dependent CVs are under Ar and on the right the rate dependent CVs are under CO_2 atmosphere. The arrow shown in the plots indicates the scan direction.

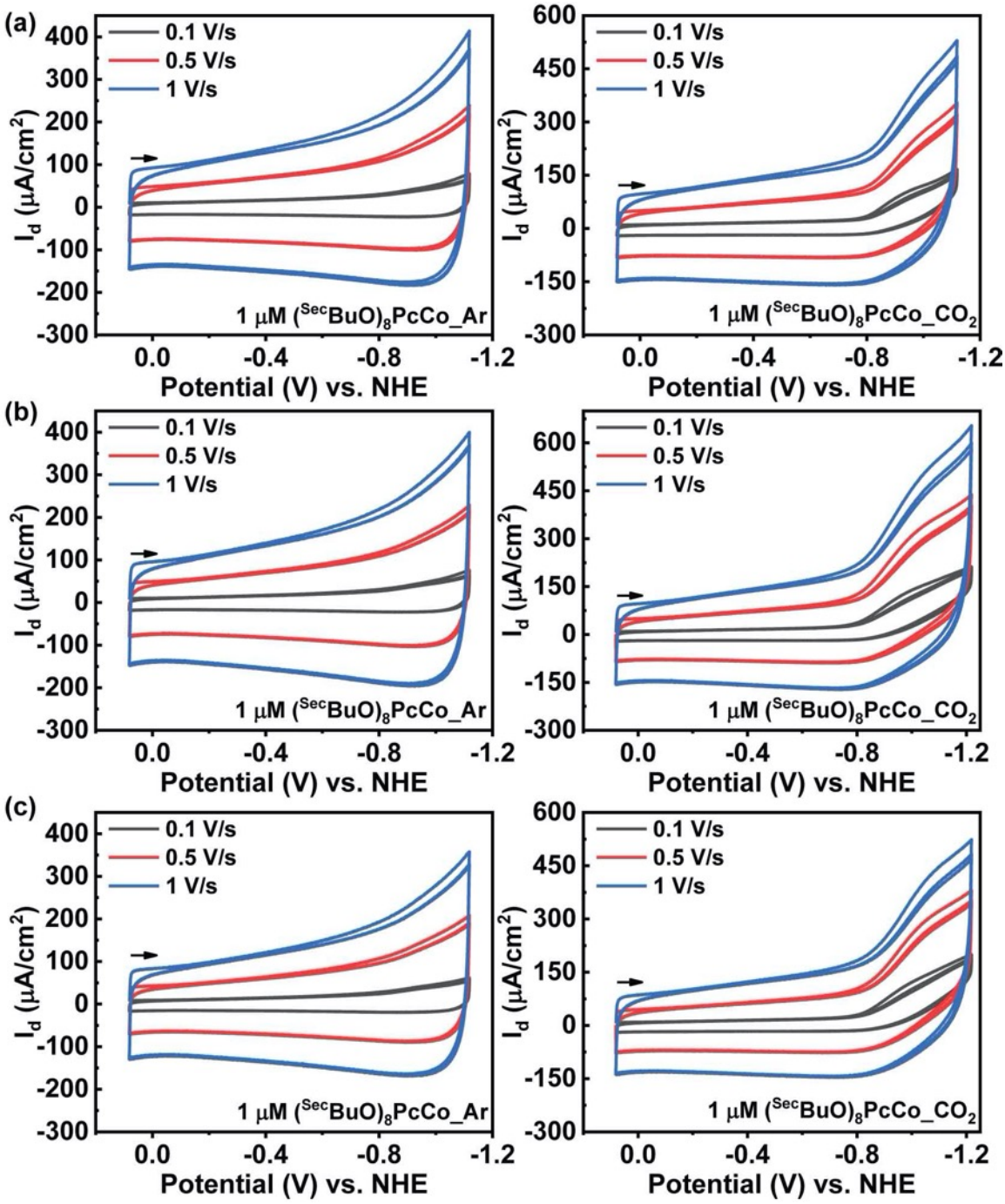

Figure S53. (a) Run 1, (b) Run 2, and (c) Run 3 Scan rate dependent CVs of ^{secBuO}PcCo in 1 μM concentration stock solution used to coat working electrodes. On the left the rate dependent CVs are under Ar and on the right the rate dependent CVs are under CO_2 atmosphere. The arrow shown in the plots indicates the scan direction.

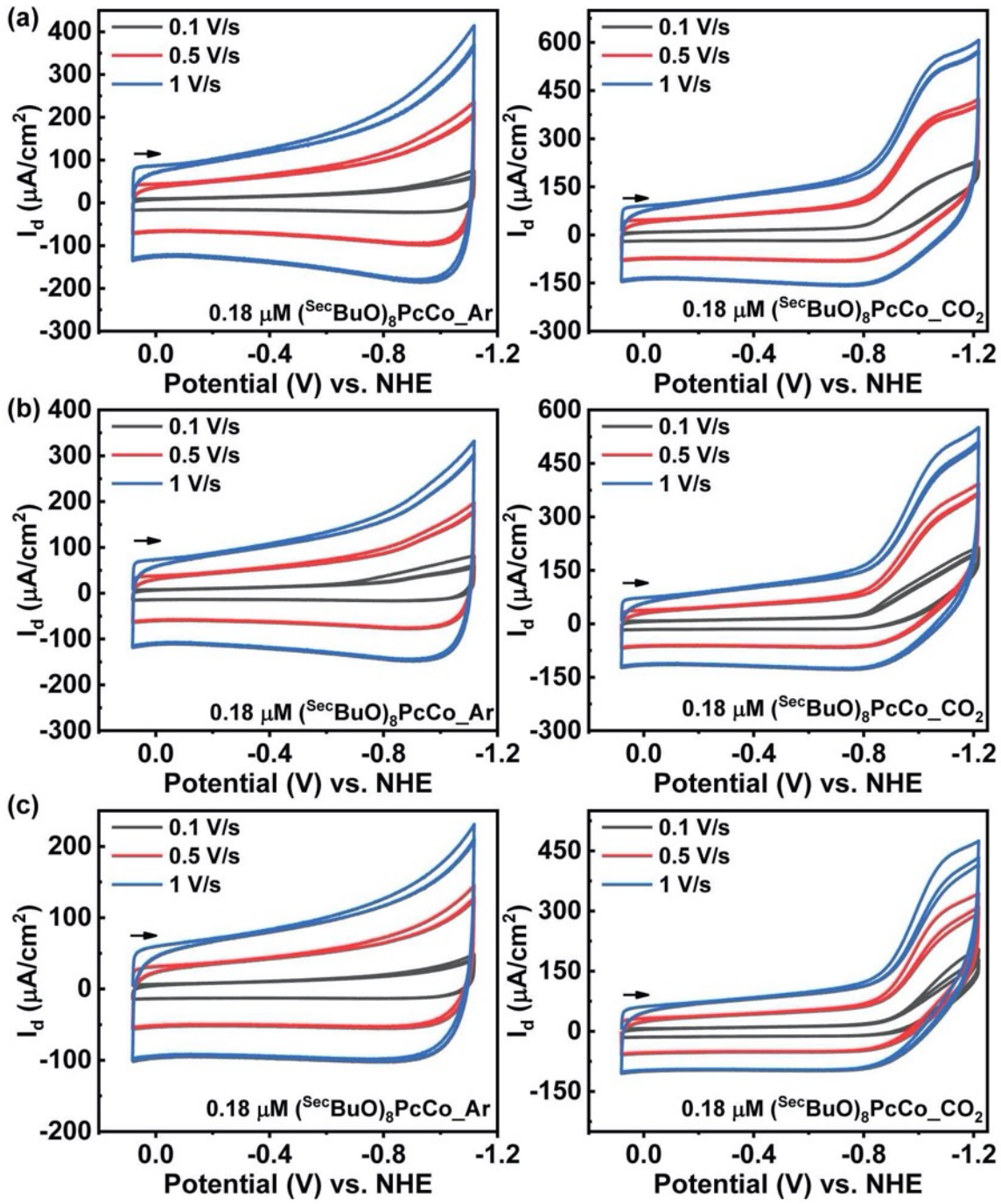

Figure S54. (a) Run 1, (b) Run 2, and (c) Run 3 Scan rate dependent CVs of ^{secBuO}PcCo in 0.18 μM concentration stock solution used to coat working electrodes. On the left the rate dependent CVs are under Ar and on the right the rate dependent CVs are under CO_2 atmosphere. The arrow shown in the plots indicates the scan direction.

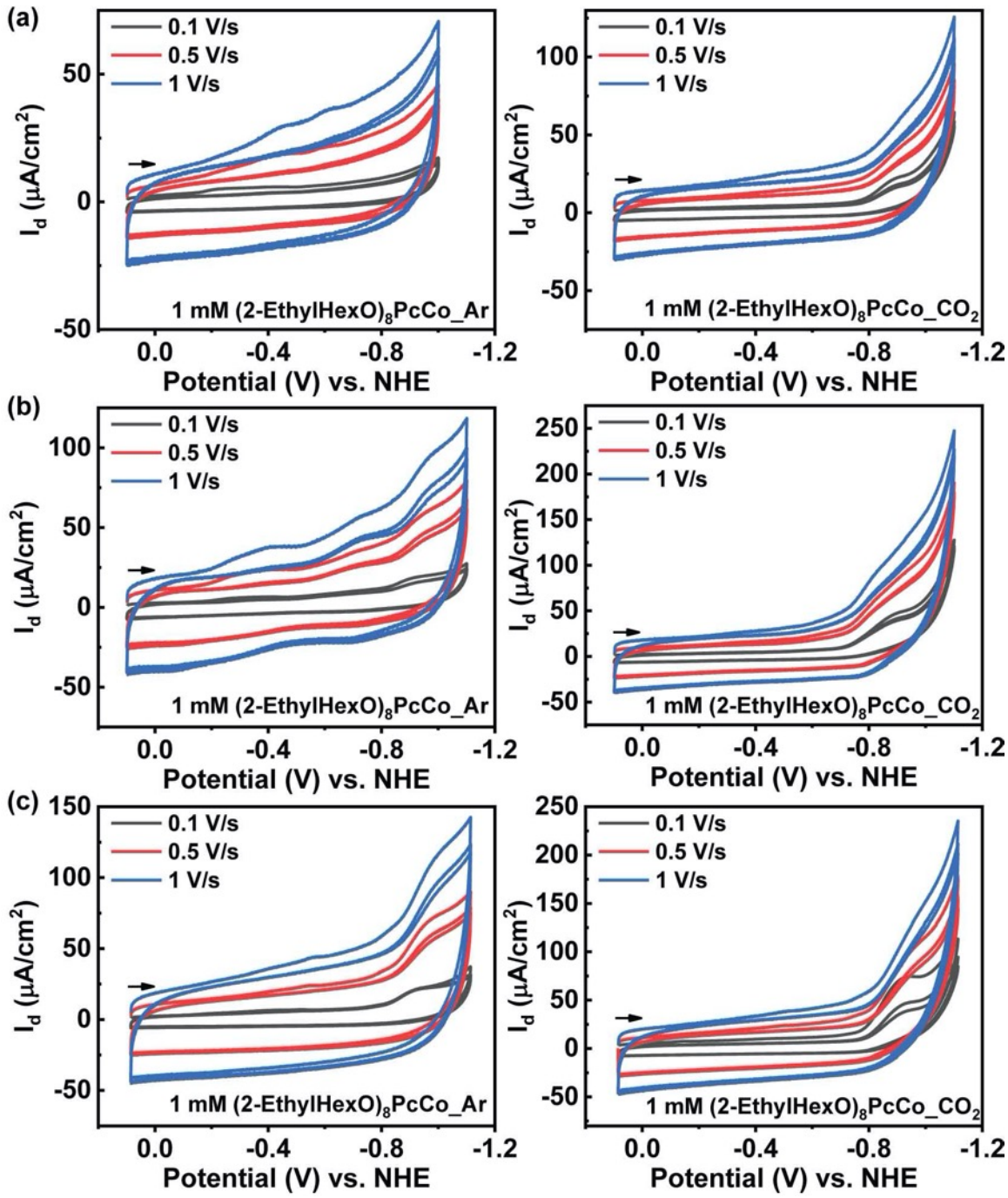

Figure S55. (a) Run 1, (b) Run 2, and (c) Run 3 Scan rate dependent CVs of ^{EtHexO}PcCo in 1 mM concentration stock solution used to coat working electrodes. On the left the rate dependent CVs are under Ar and on the right the rate dependent CVs are under CO_2 atmosphere. The arrow shown in the plots indicates the scan direction.

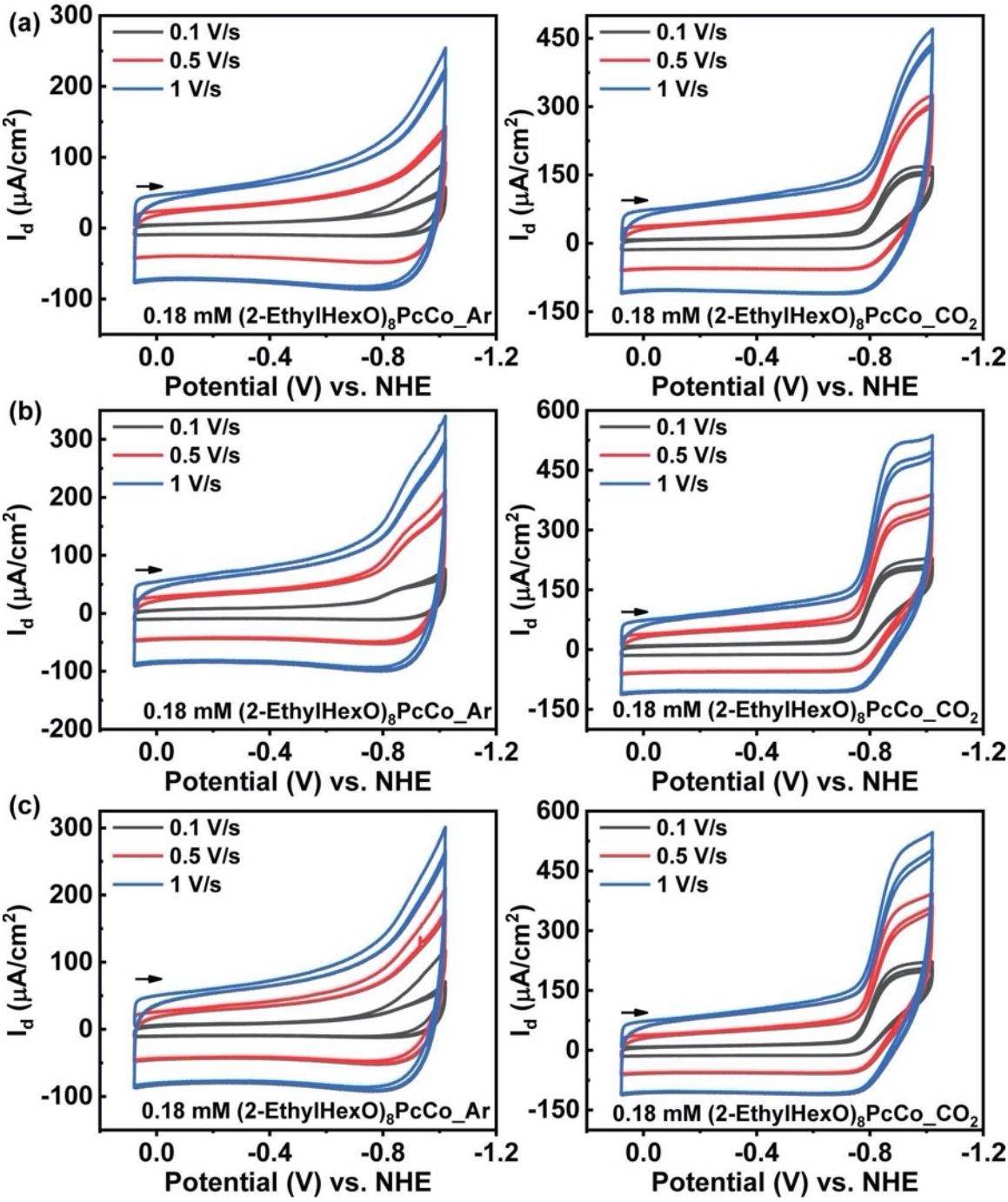

Figure S56. (a) Run 1, (b) Run 2, and (c) Run 3 Scan rate dependent CVs of ^{EtHexO}PcCo in 0.18 mM concentration stock solution used to coat working electrodes. On the left the rate dependent CVs are under Ar and on the right the rate dependent CVs are under CO_2 atmosphere. The arrow shown in the plots indicates the scan direction.

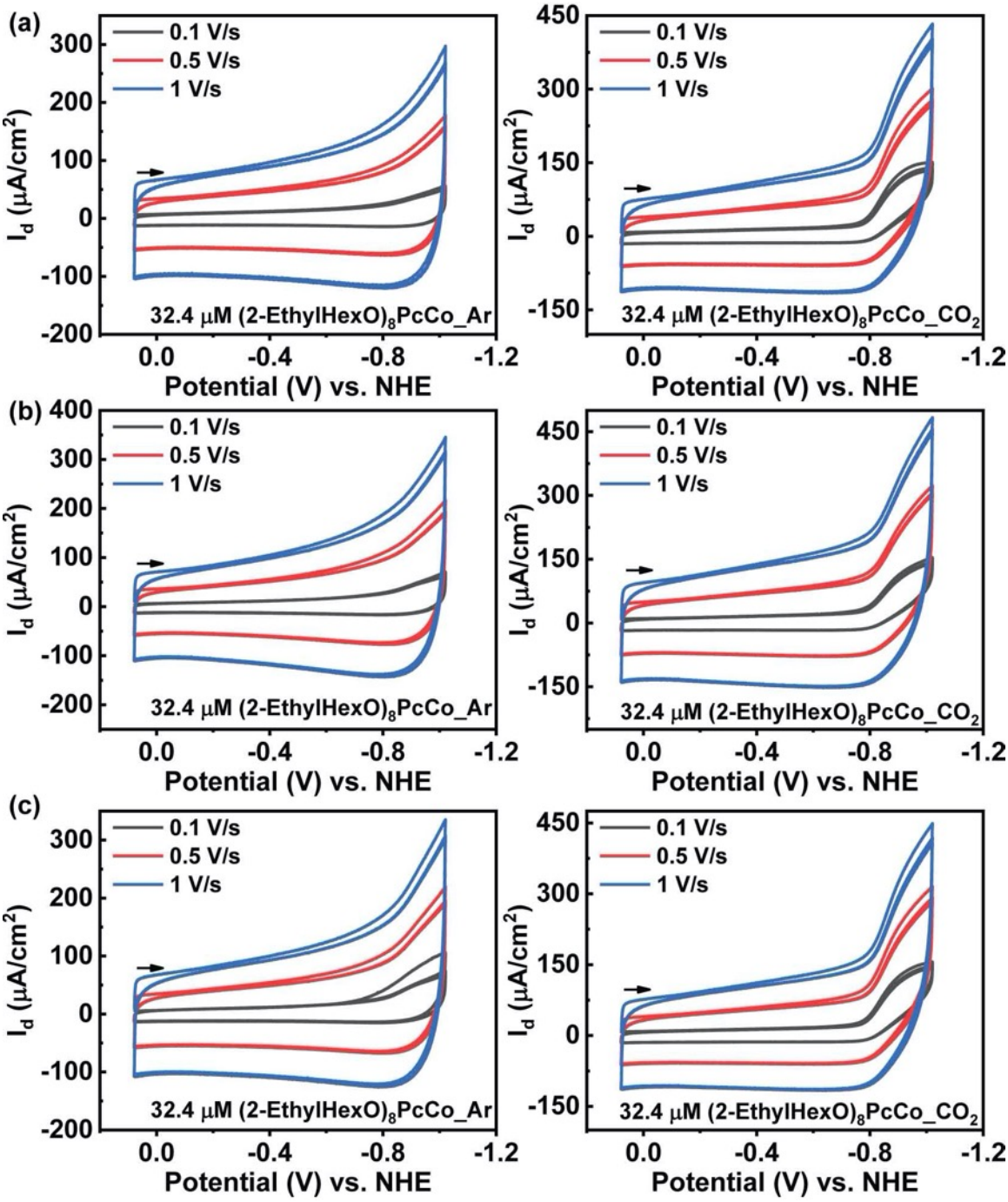

Figure S57. (a) Run 1, (b) Run 2, and (c) Run 3 Scan rate dependent CVs of ^{EtHexO}PcCo in 32.4 μM concentration stock solution used to coat working electrodes. On the left the rate dependent CVs are under Ar and on the right the rate dependent CVs are under CO_2 atmosphere. The arrow shown in the plots indicates the scan direction.

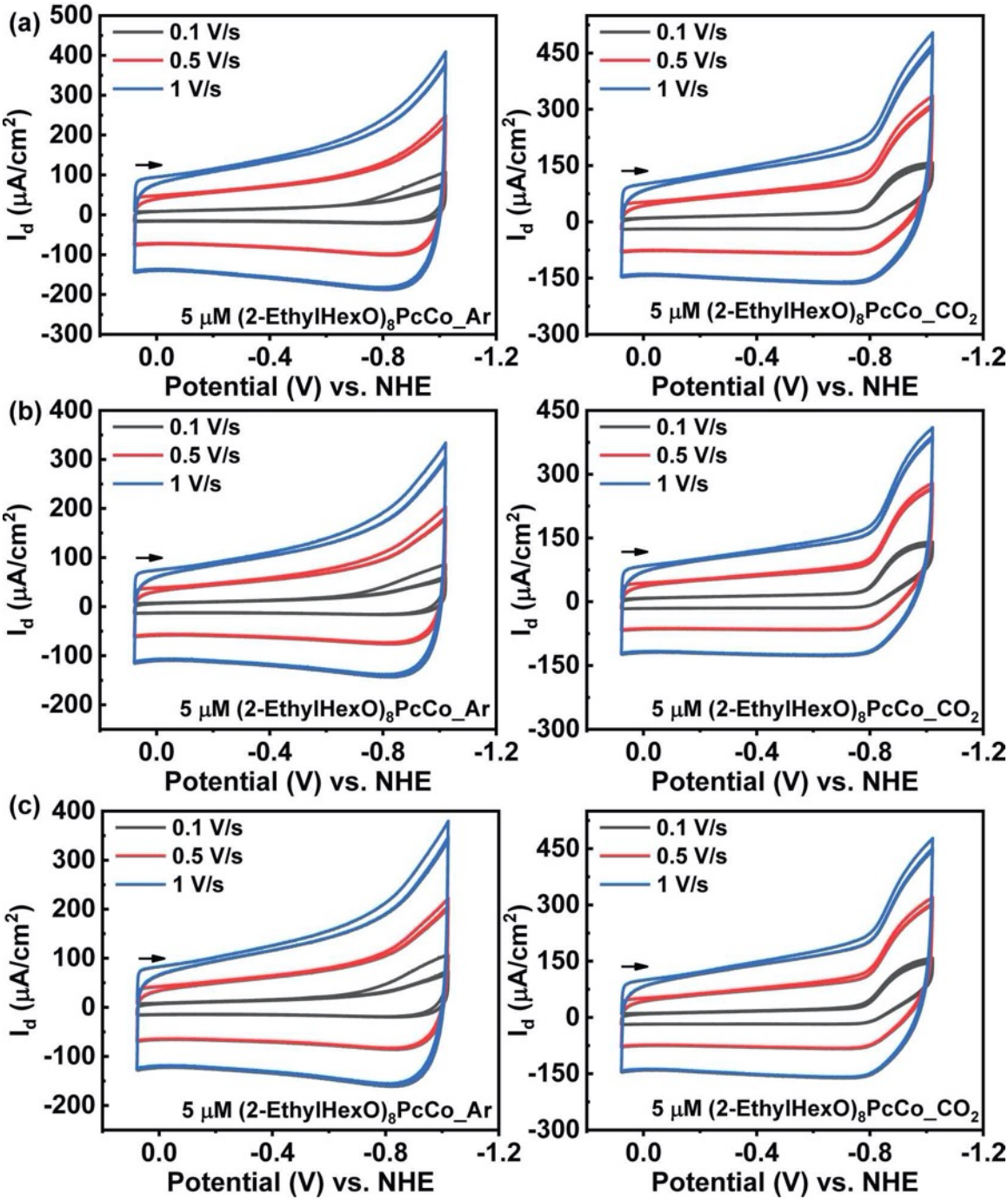

Figure S58. (a) Run 1, (b) Run 2, and (c) Run 3 Scan rate dependent CVs of ^{EtHexO}PcCo in 5 μM concentration stock solution used to coat working electrodes. On the left the rate dependent CVs are under Ar and on the right the rate dependent CVs are under CO_2 atmosphere. The arrow shown in the plots indicates the scan direction.

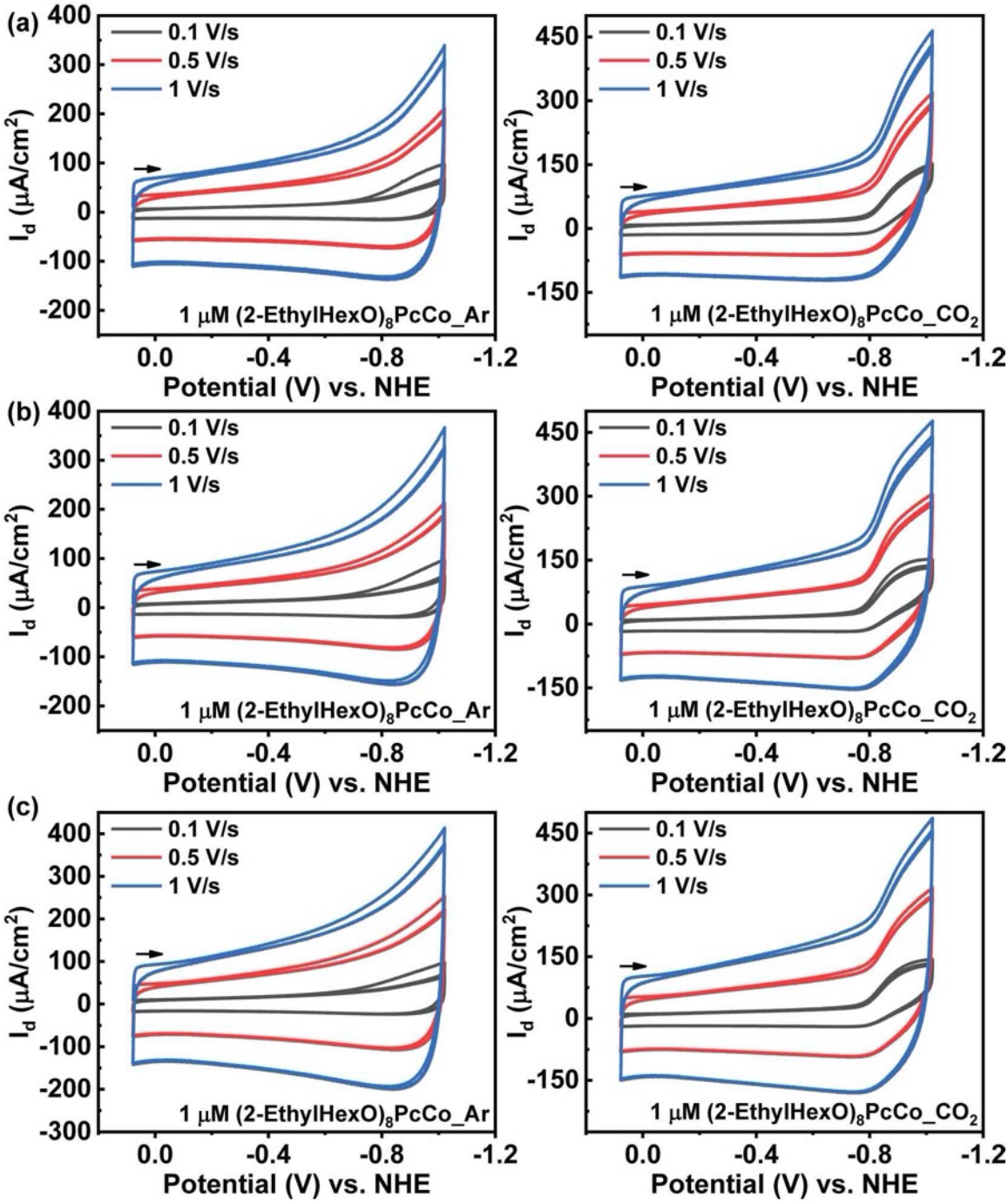

Figure S59. (a) Run 1, (b) Run 2, and (c) Run 3 Scan rate dependent CVs of ^{EtHexO}PcCo in 1 μM concentration stock solution used to coat working electrodes. On the left the rate dependent CVs are under Ar and on the right the rate dependent CVs are under CO_2 atmosphere. The arrow shown in the plots indicates the scan direction.

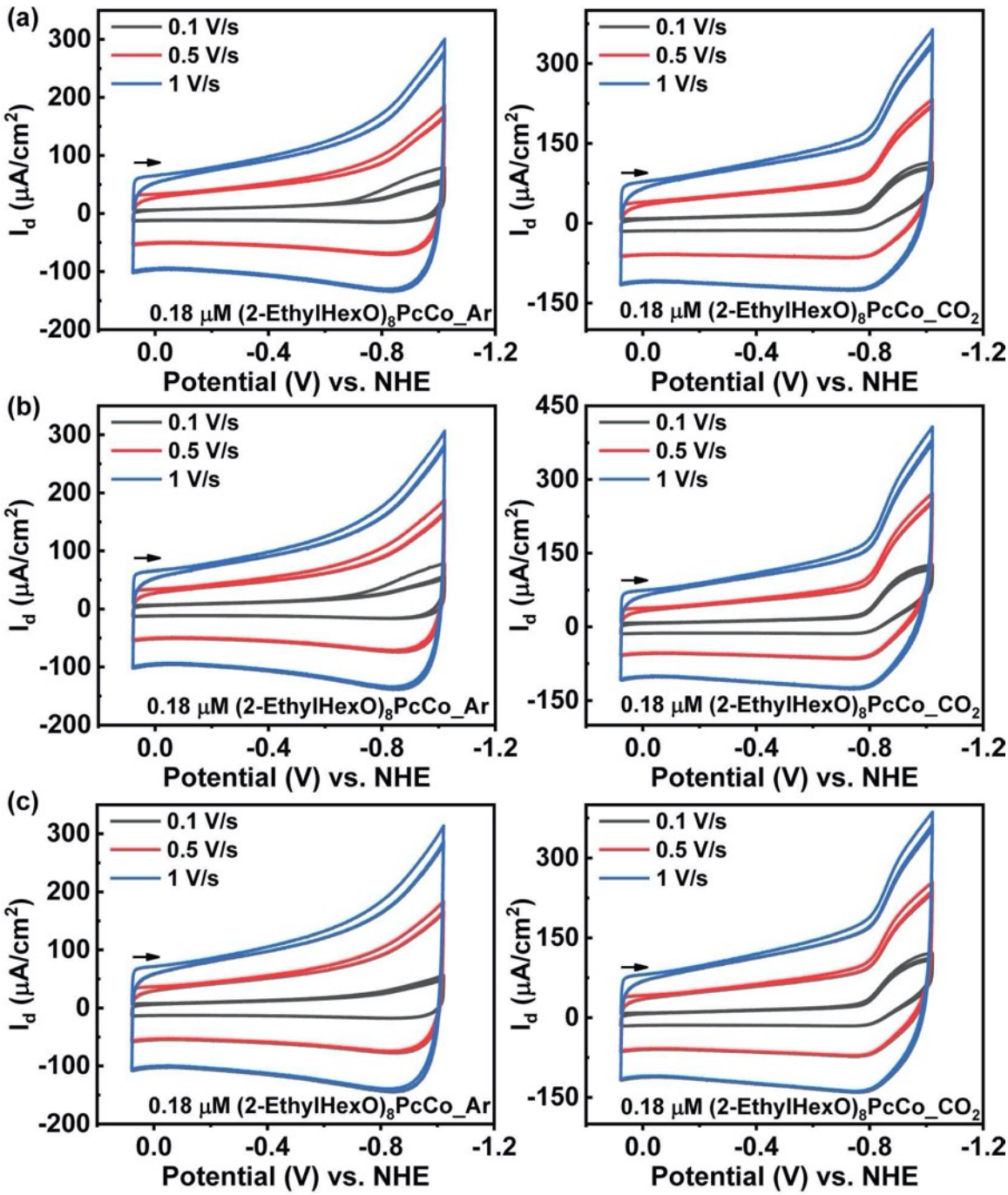

Figure S60. (a) Run 1, (b) Run 2, and (c) Run 3 Scan rate dependent CVs of ^{EtHexO}PcCo in 0.18 μM concentration stock solution used to coat working electrodes. On the left the rate dependent CVs are under Ar and on the right the rate dependent CVs are under CO_2 atmosphere. The arrow shown in the plots indicates the scan direction.

Differential Pulse Voltammetry (DPV)

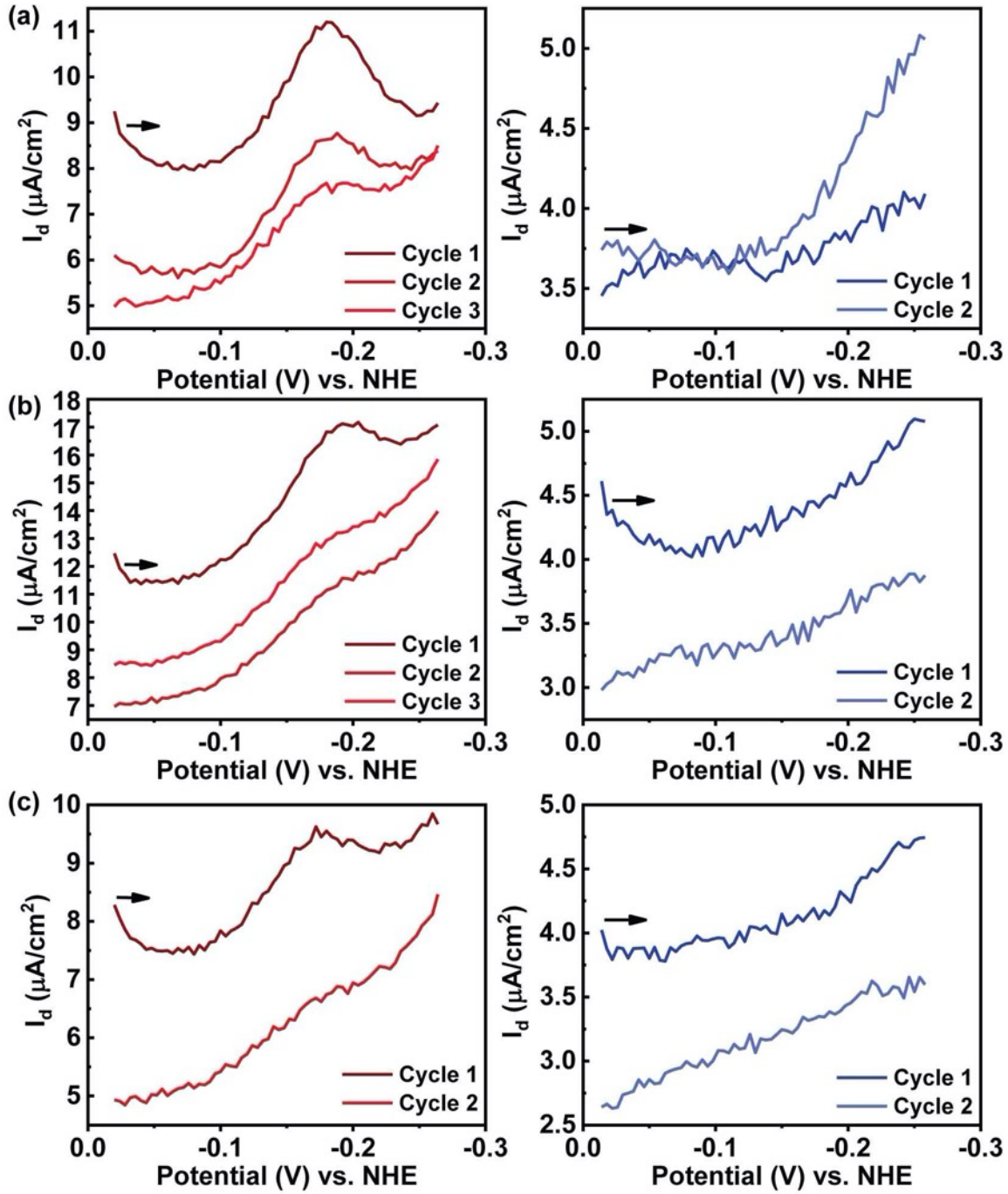

Figure S61. DPV of 32.4 μM deposition concentration of ^{secBuO}PcCo in red and ^{EtHexO}PcCo in Blue for (a) first Run, (b) second Run, and (c) third Run under an atmosphere of Ar. The arrow indicates the direction of scan.

Confirming immobilization of the catalysts on BPG electrodes

To understand if the catalysts are adsorbed on the surface of the electrodes, or if they are freely diffusing in the solution, scan rate dependent CVs of the compounds were obtained, based on the following equation[5]:

$$i_p = \frac{n^2F^2}{4RT}\upsilon A\Gamma^*$$

Where i_p (A) is peak current, n is the number of electrons transferred in the redox event, υ (V/s) is the scan rate, A (cm^2) is the electrode surface area, and Γ^* is the surface coverage of the adsorbed species. The cathodic peak current of Co^{II}/Co^{I} reduction was measured at different scan rates. Plots of peak current (i_p) versus scan rate (υ) were made and there is a linear relationship between peak current and scan rate for each of the CoPc complexes, indicating that the catalysts are adsorbed on the surface of the electrode.

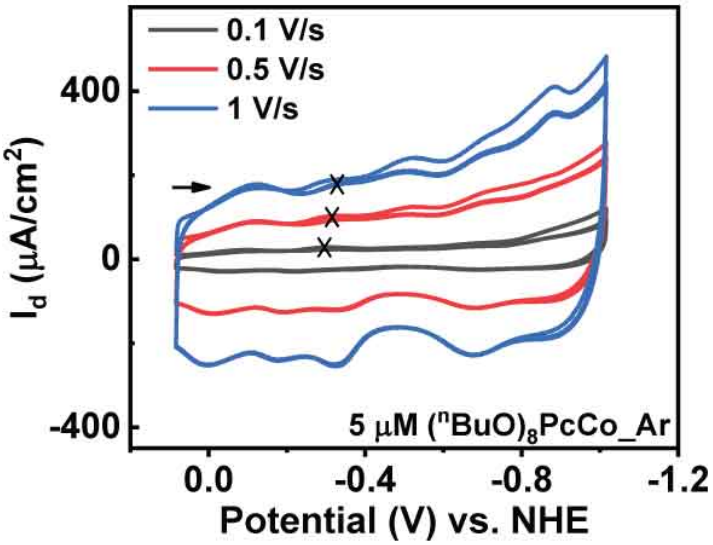

Figure S62. Rate dependent CVs of 5 μM ^{nBuO}PcCo under Ar atmosphere at 0.1, 0.5 and 1 V/s. The cross indicates the point taken from each CV to plot the peak current versus scan rate.

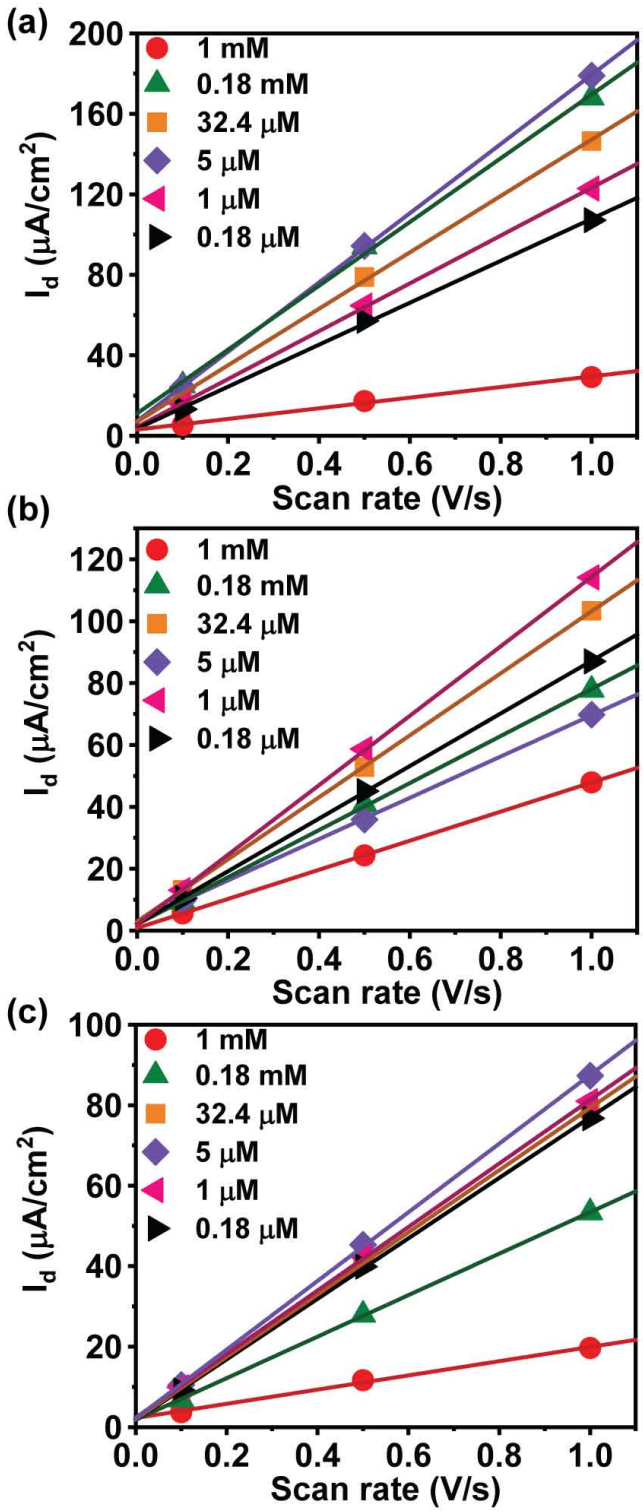

Figure S63. The linear fit of cathodic peak current versus scan rate at different deposition concentrations for (a) ^{nBuO}PcCo, (b) ^{secBuO}PcCo, and (c) ^{EtHexO}PcCo.

Comparing Current Density and Loading

The current density for deposited ^{RO}PcCo under CO_2 and Ar atmosphere was measured in each concentration at the half plateau current's potential ($E_{cat/2}$). For each loading of the catalyst, three replicate CVs were used to derive the average current density enhancement (Table S1). Most deposition concentrations showed relatively large standard deviations. It is likely that the drop-casting method resulted in uneven films and therefore differences in active species concentration. Furthermore, mass transport effects can become more important at higher loadings, resulting in lower current densities, and more difficulties in reproducing the films.

Active Species Concentrations of the catalysts

Table S1. The active concentration of Co^{II}/Co^{I} for different loadings of ^{RO}PcCO

^{nBuO}PcCo					
Deposition Concentration	Loading (mol/cm^2)	Average $\Gamma_{cat} \times 10^{-12}$ (mol/cm^2)	Run 1 $\Gamma_{cat} \times 10^{-12}$ (mol/cm^2)	Run 2 $\Gamma_{cat} \times 10^{-12}$ (mol/cm^2)	Run 3 $\Gamma_{cat} \times 10^{-12}$ (mol/cm^2)
1 mM	5.5×10^{-8}	2.77 ± 0.55	2.51	3.40	2.40
0.18 mM	9.88×10^{-9}	3.73 ± 1.86	1.77	5.46	3.97
32.4 µM	1.8×10^{-9}	3.75 ± 1.43	2.10	4.64	4.51
5 µM	2.8×10^{-10}	6.17 ± 2.53	7.51	3.25	7.74
1 µM	5.6×10^{-11}	3.30 ± 0.24	3.10	3.25	3.56
0.18 µM	1×10^{-11}	0.20 ± 0.03	0.23	0.20	0.16
^{secBuO}PcCo					
Deposition Concentration	Loading (mol/cm^2)	Average $\Gamma_{cat} \times 10^{-13}$ (mol/cm^2)	Run 1 $\Gamma_{cat} \times 10^{-13}$ (mol/cm^2)	Run 2 $\Gamma_{cat} \times 10^{-13}$ (mol/cm^2)	Run 3 $\Gamma_{cat} \times 10^{-13}$ (mol/cm^2)
1 mM	5.5×10^{-8}	2.33 ± 0.62	1.67	2.42	2.90
0.18 mM	9.88×10^{-9}	5.47 ± 0.06	5.44	5.45	5.55
32.4 µM	1.8×10^{-9}	3.69 ± 0.72	4.51	3.36	3.20
5 µM	2.8×10^{-10}	1.35 ± 0.22	1.28	1.59	1.19
1 µM	5.6×10^{-11}	N/A	N/A	N/A	N/A
0.18 µM	1×10^{-11}	N/A	N/A	N/A	N/A
^{EtHexO}PcCo					
Deposition Concentration	Loading (mol/cm^2)	Average $\Gamma_{cat} \times 10^{-13}$ (mol/cm^2)	Run 1 $\Gamma_{cat} \times 10^{-13}$ (mol/cm^2)	Run 2 $\Gamma_{cat} \times 10^{-13}$ (mol/cm^2)	Run 3 $\Gamma_{cat} \times 10^{-13}$ (mol/cm^2)
1 mM	5.5×10^{-8}	0.60 ± 0.12	0.47	0.66	0.68
0.18 mM	9.88×10^{-9}	3.59 ± 1.48	2.27	5.19	3.32
32.4 µM	1.8×10^{-9}	3.08 ± 0.53	2.47	3.39	3.39
5 µM	2.8×10^{-10}	1.56 ± 0.25	1.55	1.31	1.81
1 µM	5.6×10^{-11}	N/A	N/A	N/A	N/A
0.18 µM	1×10^{-11}	N/A	N/A	N/A	N/A

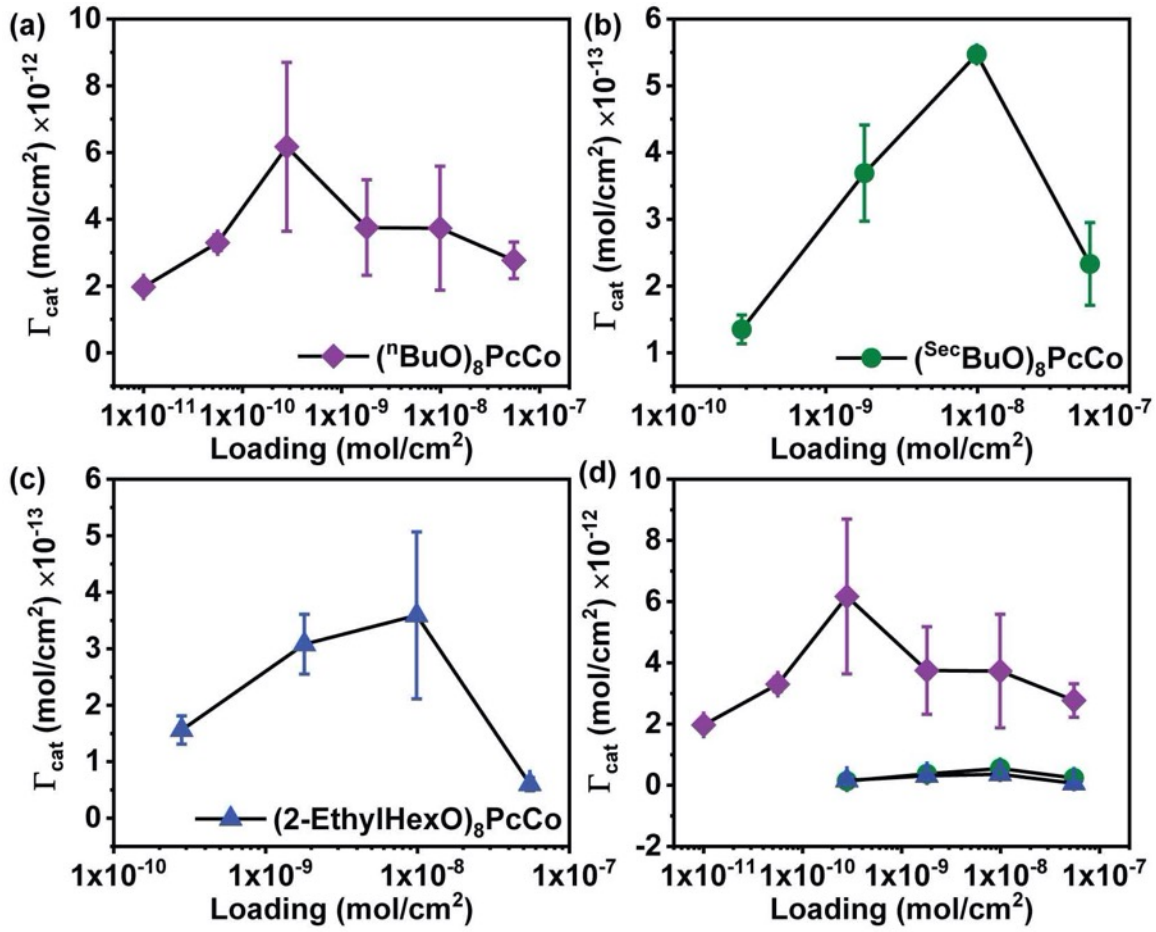

Figure S65. The active concentration of Co^{II}/Co^{I} versus loading for the average of three CV replicates of (a) ^{nBuO}PcCo, (b) ^{secBuO}PcCo, and (c) ^{EtHexO}PcCo, and (d) overlaid plots of the three compounds.

Table S2. The current density difference under CO_2 versus Ar for different loadings of ^{nBuO}PcCo, ^{SecBuO}PcCo, and ^{EtHexO}PcCo.

^{nBuO}PcCo					
Deposition Concentration	Loading (mol/cm^2)	Average I_d (μA/cm^2)	Run 1 I_d (μA/cm^2)	Run 2 I_d (μA/cm^2)	Run 3 I_d (μA/cm^2)
1 mM	5.5×10^{-8}	67.8 ± 23.5	45.0	66.3	92.0
0.18 mM	9.88×10^{-9}	57.8 ± 3.9	57.6	54.0	61.8
32.4 μM	1.8×10^{-9}	58.2 ± 6.0	53.0	56.8	64.8
5 μM	2.8×10^{-10}	86.6 ± 4.2	87.8	81.8	90.0
1 μM	5.6×10^{-11}	71.3 ± 3.0	72.7	67.9	73.4
0.18 μM	1×10^{-11}	45.3 ± 8.3	42.5	54.7	38.8
^{SecBuO}PcCo					
Deposition Concentration	Loading (mol/cm^2)	Average I_d (μA/cm^2)	Run 1 I_d (μA/cm^2)	Run 2 I_d (μA/cm^2)	Run 3 I_d (μA/cm^2)
1 mM	5.5×10^{-8}	65.3 ± 5.7	61.2	62.9	71.8
0.18 mM	9.88×10^{-9}	50.9 ± 3.0	48.5	54.3	49.9
32.4 μM	1.8×10^{-9}	29.4 ± 6.0	35.8	23.8	28.6
5 μM	2.8×10^{-10}	44.0 ± 11.7	56.4	33.1	42.4
1 μM	5.6×10^{-11}	27.3 ± 7.1	19.2	32.3	30.3
0.18 μM	1×10^{-11}	42.0 ± 11.0	54.3	33.1	38.7
^{EtHexO}PcCo					
Deposition Concentration	Loading (mol/cm^2)	Average I_d (μA/cm^2)	Run 1 I_d (μA/cm^2)	Run 2 I_d (μA/cm^2)	Run 3 I_d (μA/cm^2)
1 mM	5.5×10^{-8}	8.0 ± 6.0	1.0	11.8	11.1
0.18 mM	9.88×10^{-9}	64.2 ± 13.0	49.2	70.6	72.8
32.4 μM	1.8×10^{-9}	35.6 ± 2.2	38.1	34.4	34.3
5 μM	2.8×10^{-10}	30.0 ± 1.2	28.8	30.1	31.2
1 μM	5.6×10^{-11}	27.4 ± 5.5	30.5	30.6	21.1
0.18 μM	1×10^{-11}	21.4 ± 4.1	16.8	24.4	23.1

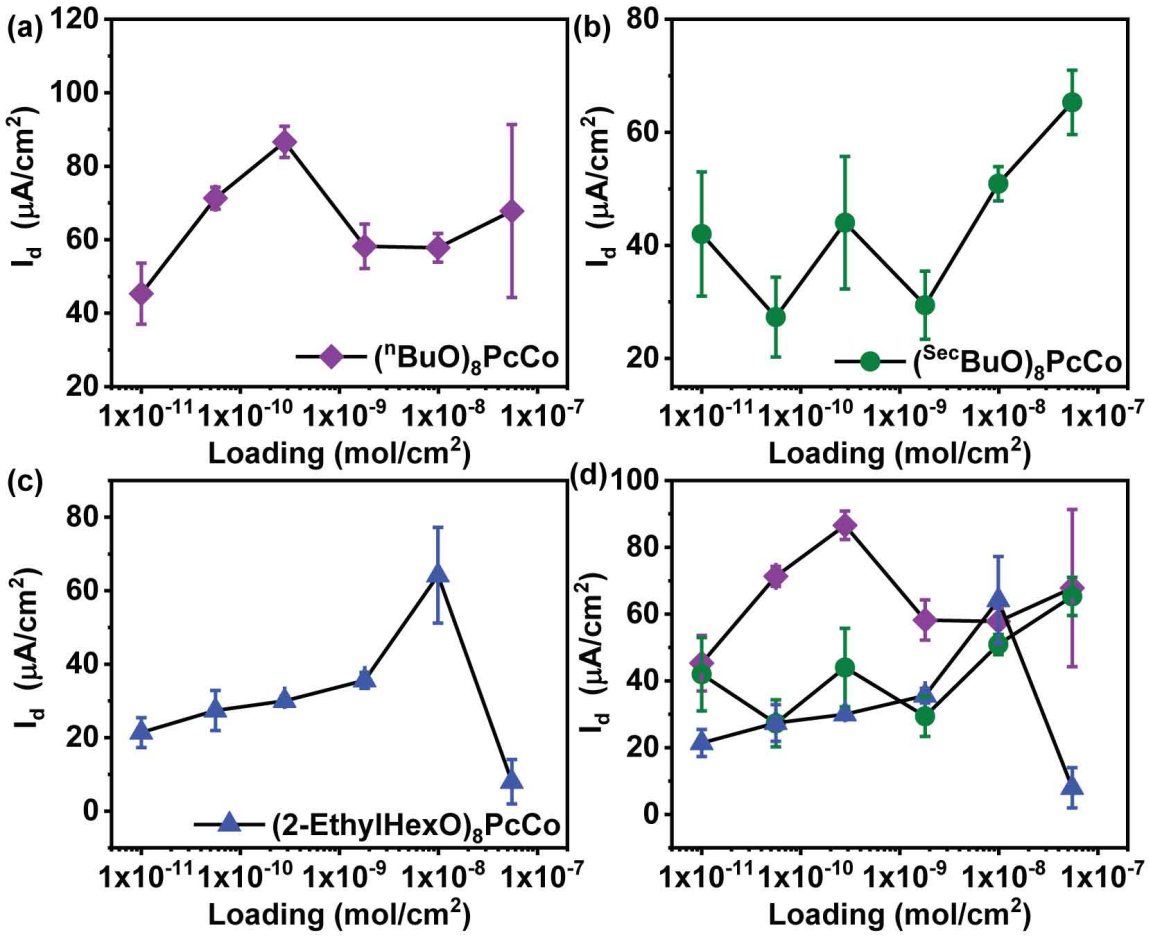

Figure S65. Average current density enhancement versus loading for the average of three CV replicates of (a) ^{nBuO}PcCo, (b) ^{secBuO}PcCo, and (c) ^{EtHexO}PcCo, and (d) overlaid plots of the three compounds.

Stability of the Catalyst Films

To assess the stability of catalyst films during CV experiments, three sequential CV cycles were collected. In general, the second and third cycle are superimposable, indicating the stability of the catalysts on the surface of the electrode and there is no need to repeat the CV. If the second and third cycle, were not superimposable, the CV was performed again. As shown in Figure S73, the cycles in the second run are superimposable to the first run indicating the stability of the catalysts on the surface of the BPG working electrodes both in sequential CV runs and in runs carried out after different wait times.

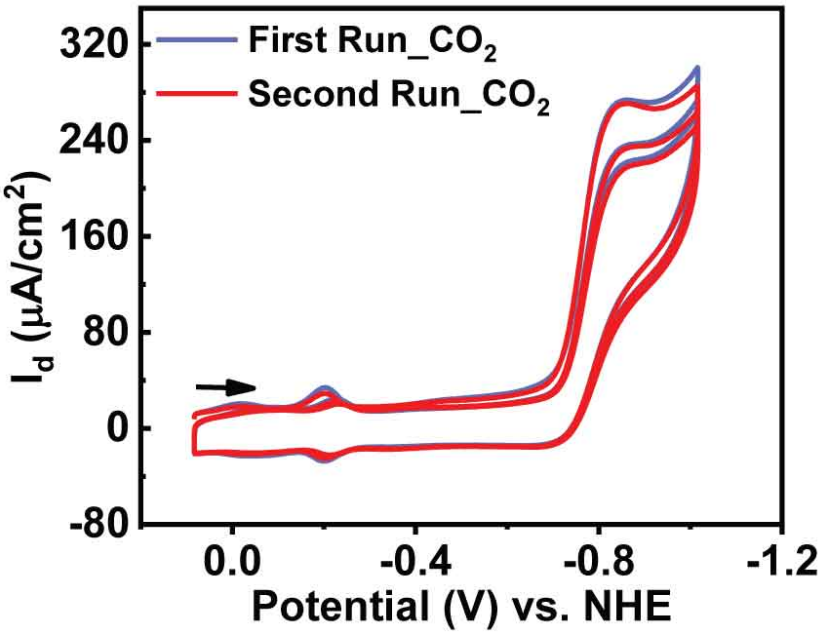

Figure S66. Comparison of the CV peaks for the first and second runs for a 5 μM stock solution of ^{nBuO}PcCo deposited on BPG electrode under CO_2 atmosphere. In each run, three CV cycles were performed.

The stability of the catalysts was evaluated by running CPE experiments for each catalyst. All experiments were carried out with an applied of –0.96 V vs. NHE under CO_2 atmosphere. After an initial decrease in current, the current response remained constant for 2 hours, indicating the stability of the catalysts over time (Figure S74).

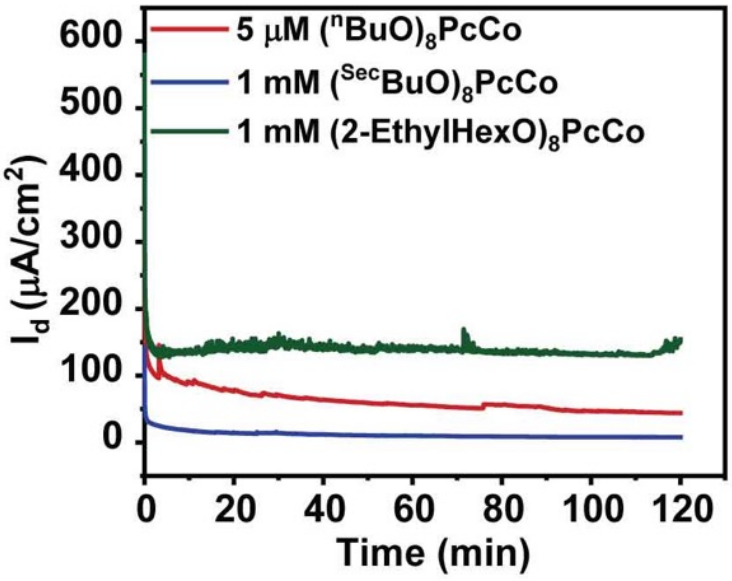

Figure S67. CPE experiments carried out at –0.96 V vs. NHE for 2 hours on BPG electrodes under CO_2 atmosphere.

NMR spectra of reaction products

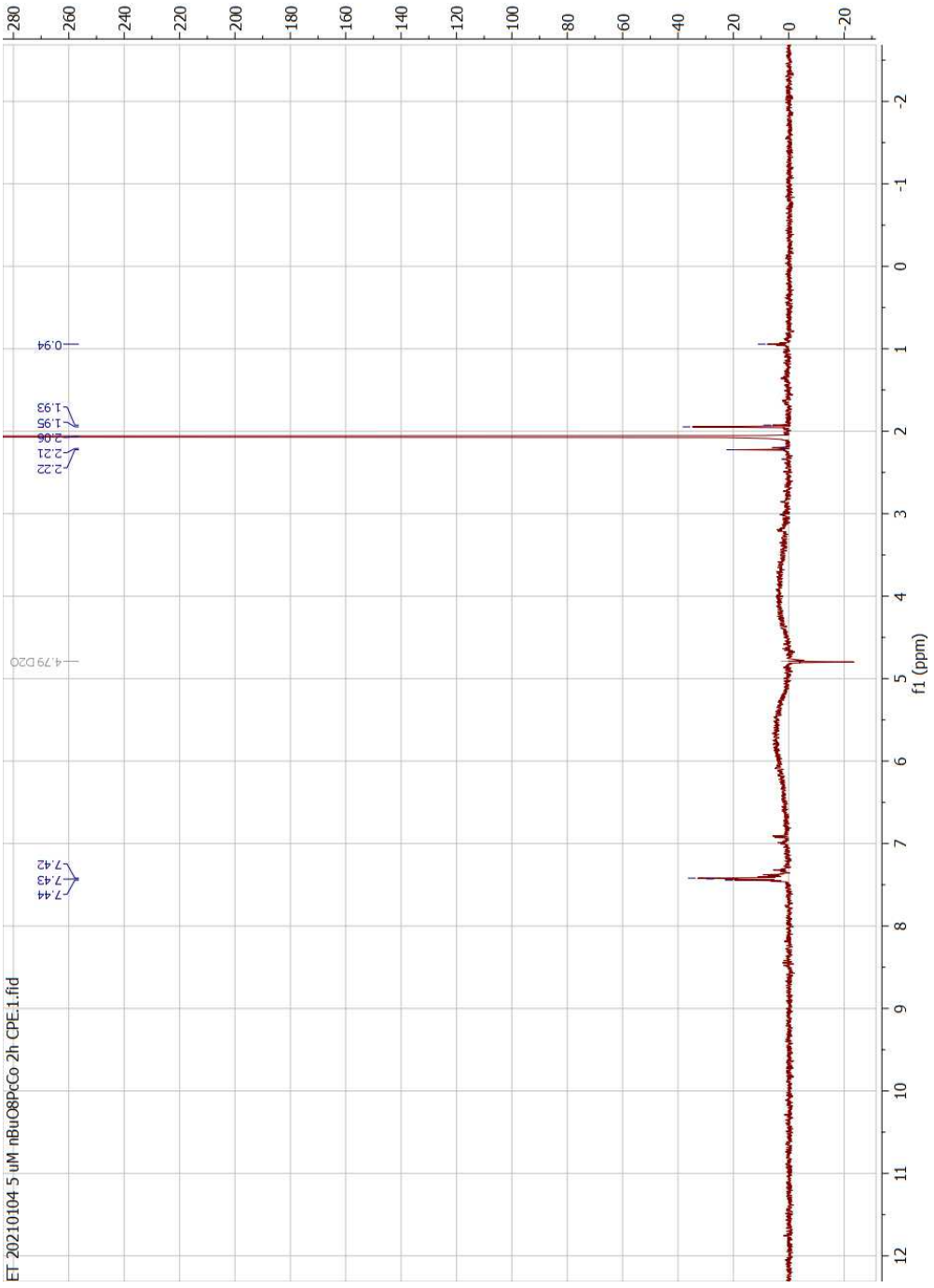

Figure S68. Water suppression ^{1}H NMR spectrum of (^{n}BuO)$_8$PcCo after two hour CPE. The NMR solution contains 90% electrolyte solution after electrolysis and 10% D_2O. Only trace organic material is detected after electrolysis and none correspond to common CO_2 reduction products.

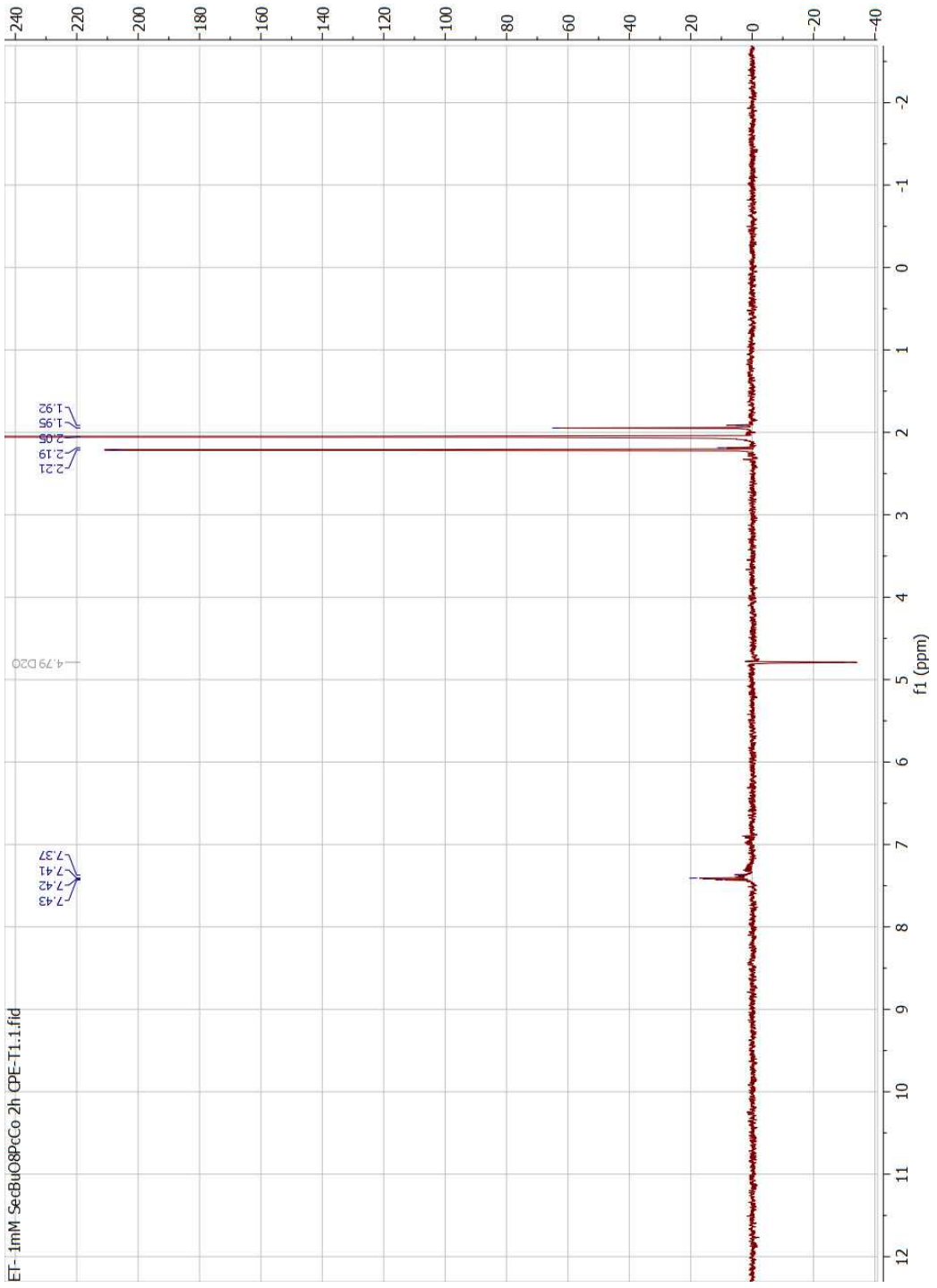

Figure S69. Water suppression ^{1}H NMR spectrum of (^{Sec}BuO)$_8$PcCo after two hour CPE. The NMR solution contains 90% electrolyte solution after electrolysis and 10% D_2O. Only trace organic material is detected after electrolysis and none correspond to common CO_2 reduction products.

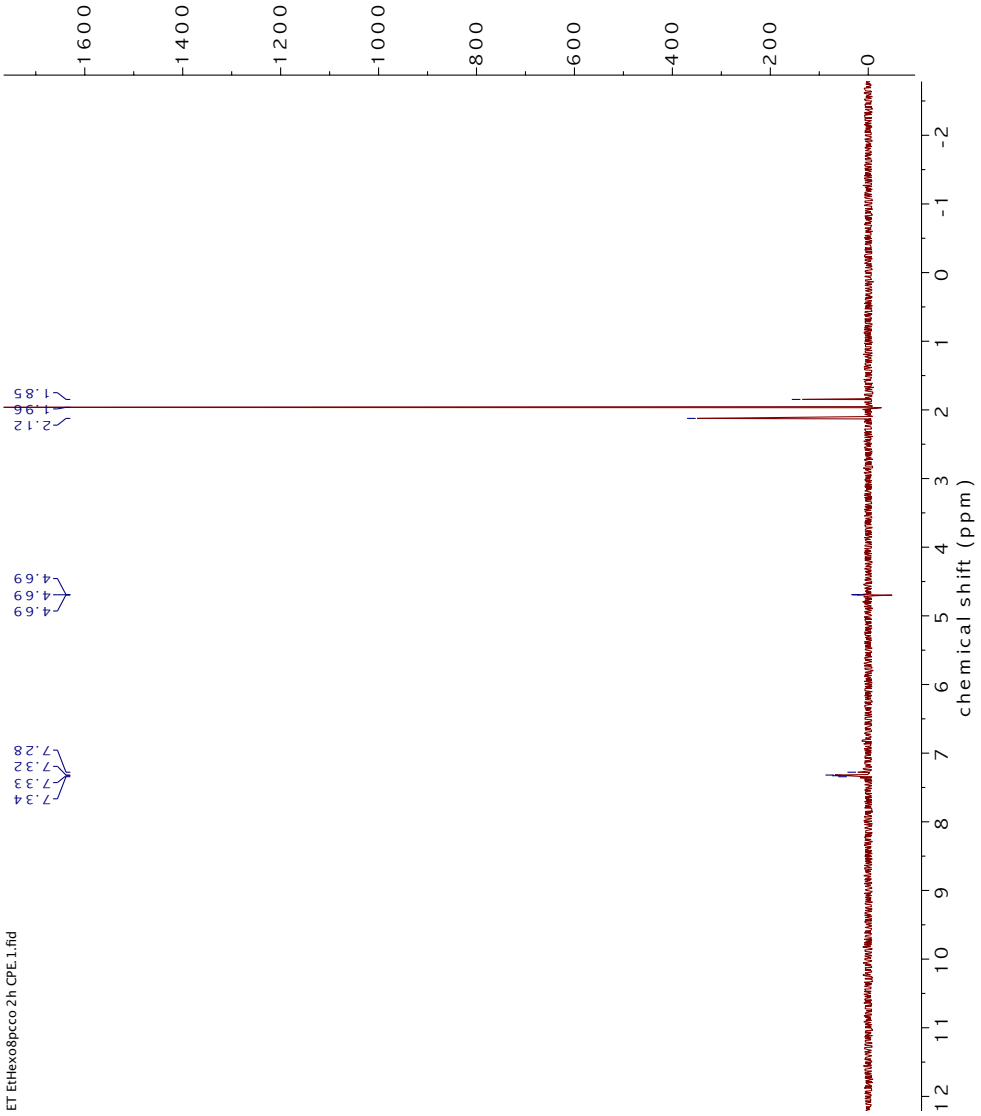

Figure S70. Water suppression ^{1}H NMR spectrum of $(EtHexO)_8PcCo$ after two hour CPE. The NMR solution contains 90% electrolyte solution after electrolysis and 10% D_2O. Only trace organic material is detected after electrolysis and none correspond to common CO_2 reduction products.

FOWA for the ^{RO}PcCo Catalysts

In the heterogeneous system used in this thesis, the catalyst is adsorbed on the surface of the electrode and does not diffuse to the bulk solution. In this case, the current (i) only depends on the apparent rate of reaction (k) and the diffusion of the substrate and the product (CO_2, CO) between the electrode and the electrolyte solution. Here, it is assumed that the gradient of both CO_2 and CO are constant as well as the bulk concentration of the substrate (CO_2).

Under these assumptions, the overall rate constant of the catalysts in each loading were calculated using the Foot-of-the-Wave Analysis (FOWA) for heterogeneous systems following Equation 2.3. This formula is the modified version of this formula found for heterogeneous systems for water oxidation reaction by Llobet and co-workers.[6]

$$\frac{i}{Q} = \frac{k}{1+e^{[f(E-E^{0,ap})]}} \quad (2.3)$$

i is the current under CO_2,

Q is moles of electrons associated with one electron transfer (found by taking the area under the metal couple redox peak under Ar),

k is the pseudo-first order rate constant,

f is the ratio of F/RT (F/RT = 38.94), where F is Faradaic constant, R is the universal gas constant, and T is the absolute temperature,

E is the potential under CO_2,

$E^{0,ap}$ is the apparent potential for metal redox couple peak under Ar.

For extracting the rate constants, the linear fit of i/Q versus [1/[1+e(F(E-$E^{0,ap}$)/RT)]] in the foot of the wave, where there is negligible catalyst depletion and/or side phenomena (e.g., substrate consumption, mass transfer effects), was used. The slope of the linear fit directly gives the rate constant. Rate constants with high variance were observed in some cases, which may be due to differences in the calculated active species concentration or current density enhancement as described in previous sections. The variance can be quite large (e.g., up to a factor of 2 in some

cases). Some rate constants were not calculated for the concentrations of 1 μM and 0.18 μM since these concentrations were too dilute to observe the metal redox peak necessary for calculating Q.

Table S3. Rate constants for three Runs for each catalyst loading for ^{nBuO}PcCo, ^{secBuO}PcCo, and ^{EtHexO}PcCo.

^{nBuO}PcCo					
Deposition Concentration	Loading (mol/cm^2)	Average k (s^{-1})	Run 1 k (s^{-1})	Run 2 k (s^{-1})	Run 3 k (s^{-1})
1 mM	5.5×10^{-8}	59 ± 20	82	49	47
0.18 mM	9.88×10^{-9}	410 ± 290	750	200	280
32.4 μM	1.8×10^{-9}	420 ± 68	480	440	350
5 μM	2.8×10^{-10}	190 ± 57	230	210	120
1 μM	5.6×10^{-11}	220 ± 87	290	230	120
0.18 μM	1×10^{-11}	930 ± 150	1000	1000	760
^{secBuO}PcCo					
Deposition Concentration	Loading (mol/cm^2)	Average k (s^{-1})	Run 1 k (s^{-1})	Run 2 k (s^{-1})	Run 3 k (s^{-1})
1 mM	5.5×10^{-8}	4100 ± 1000	4800	4500	2900
0.18 mM	9.88×10^{-9}	810 ± 57	850	840	750
32.4 μM	1.8×10^{-9}	550 ± 130	600	400	650
5 μM	2.8×10^{-10}	2300 ± 1200	3600	1300	1900
^{EtHexO}PcCo					
Deposition Concentration	Loading (mol/cm^2)	Average k (s^{-1})	Run 1 k (s^{-1})	Run 2 k (s^{-1})	Run 3 k (s^{-1})
1 mM	5.5×10^{-8}	2000 ± 570	1300	2200	2300
0.18 mM	9.88×10^{-9}	1800 ± 540	1200	2200	2100
32.4 μM	1.8×10^{-9}	730 ± 120	870	650	660
5 μM	2.8×10^{-10}	1300 ± 160	1300	1100	1400

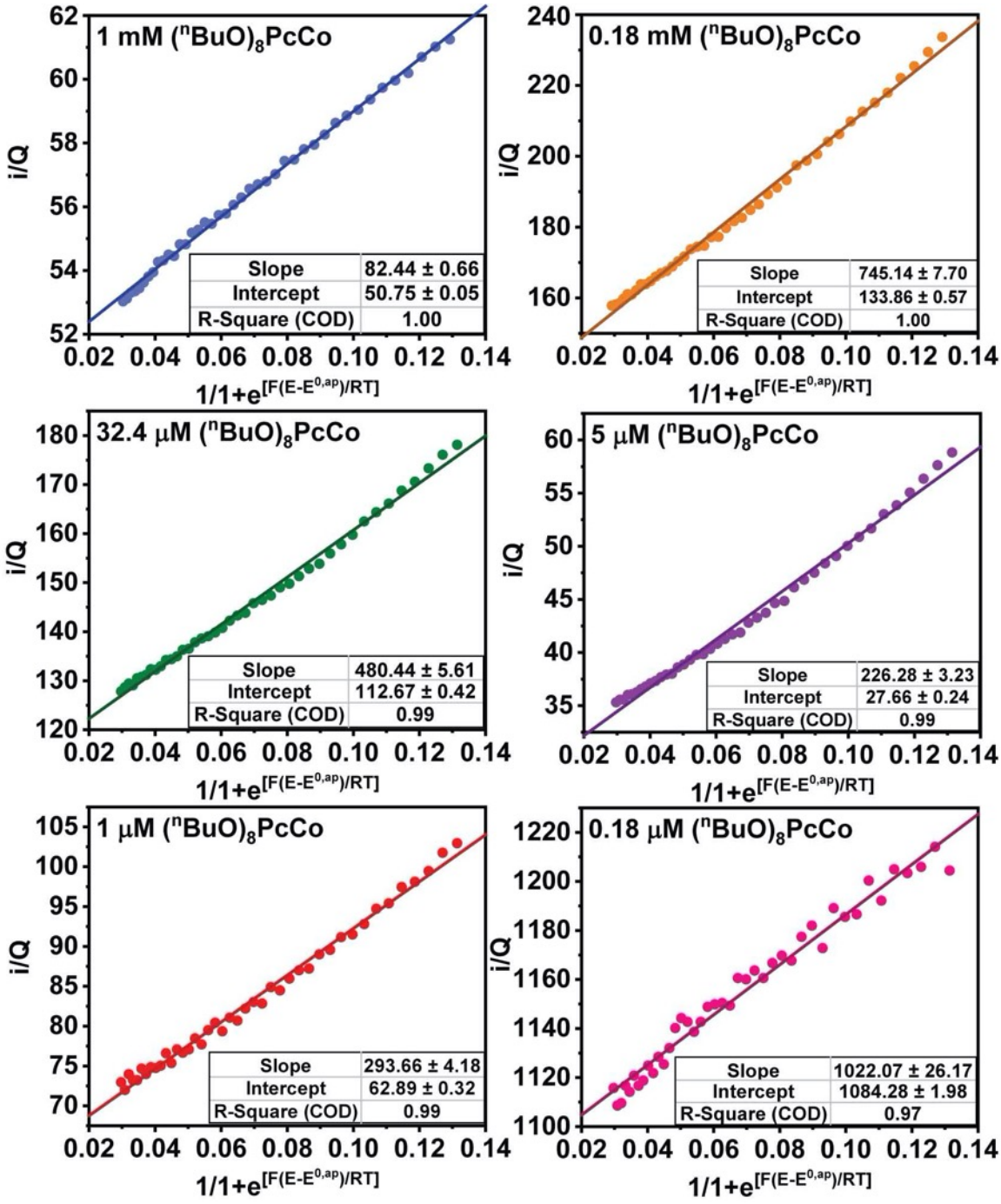

Figure S71. FOW plots for Run 1 of ^{nBuO}PcCo in six different deposition concentrations. Lines indicate the linear fits used to obtain rate constant (k).

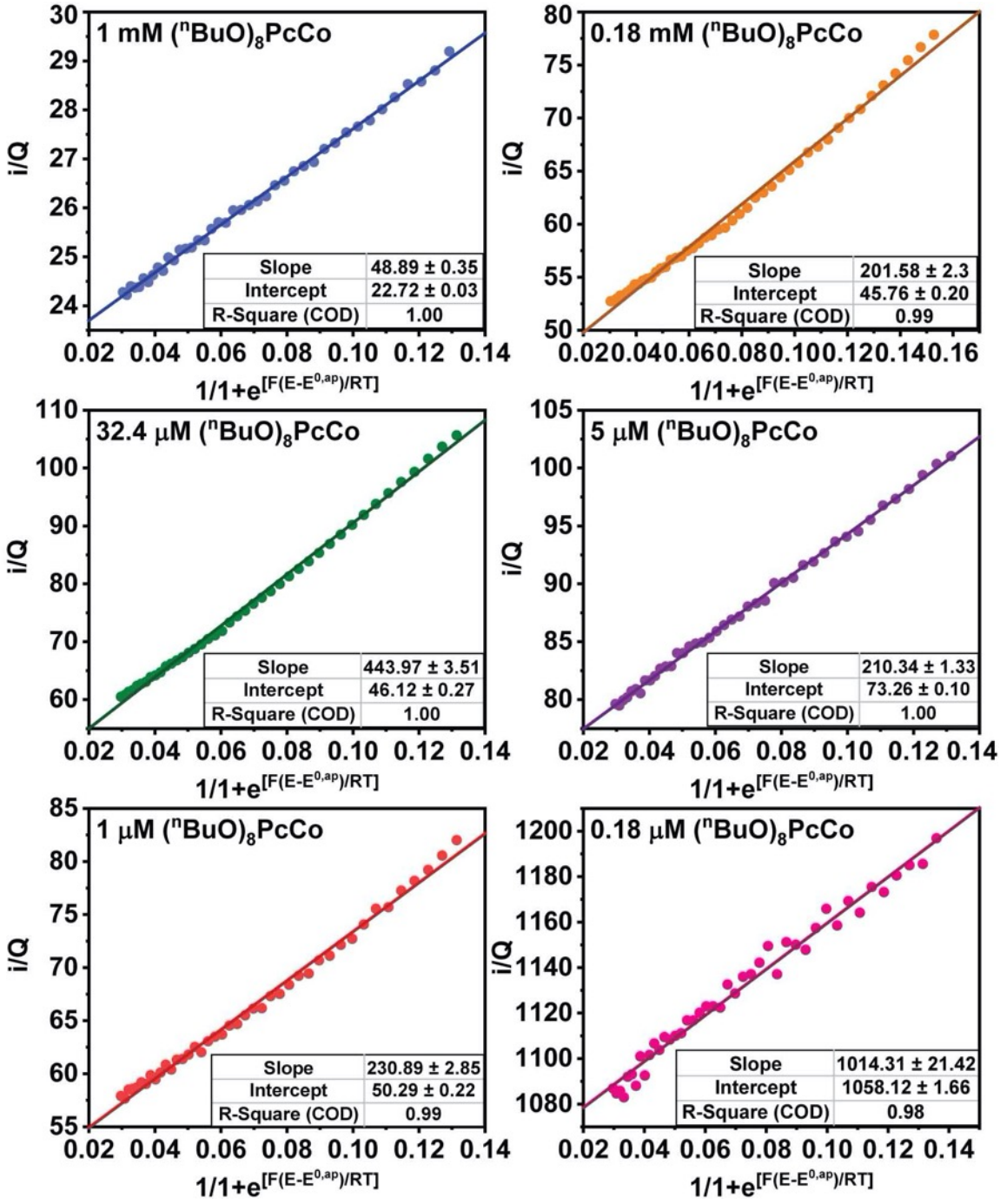

Figure S72. FOW plots for Run 2 of ^{nBuO}PcCo in six different deposition concentrations. Lines indicate the linear fits used to obtain rate constants (k).

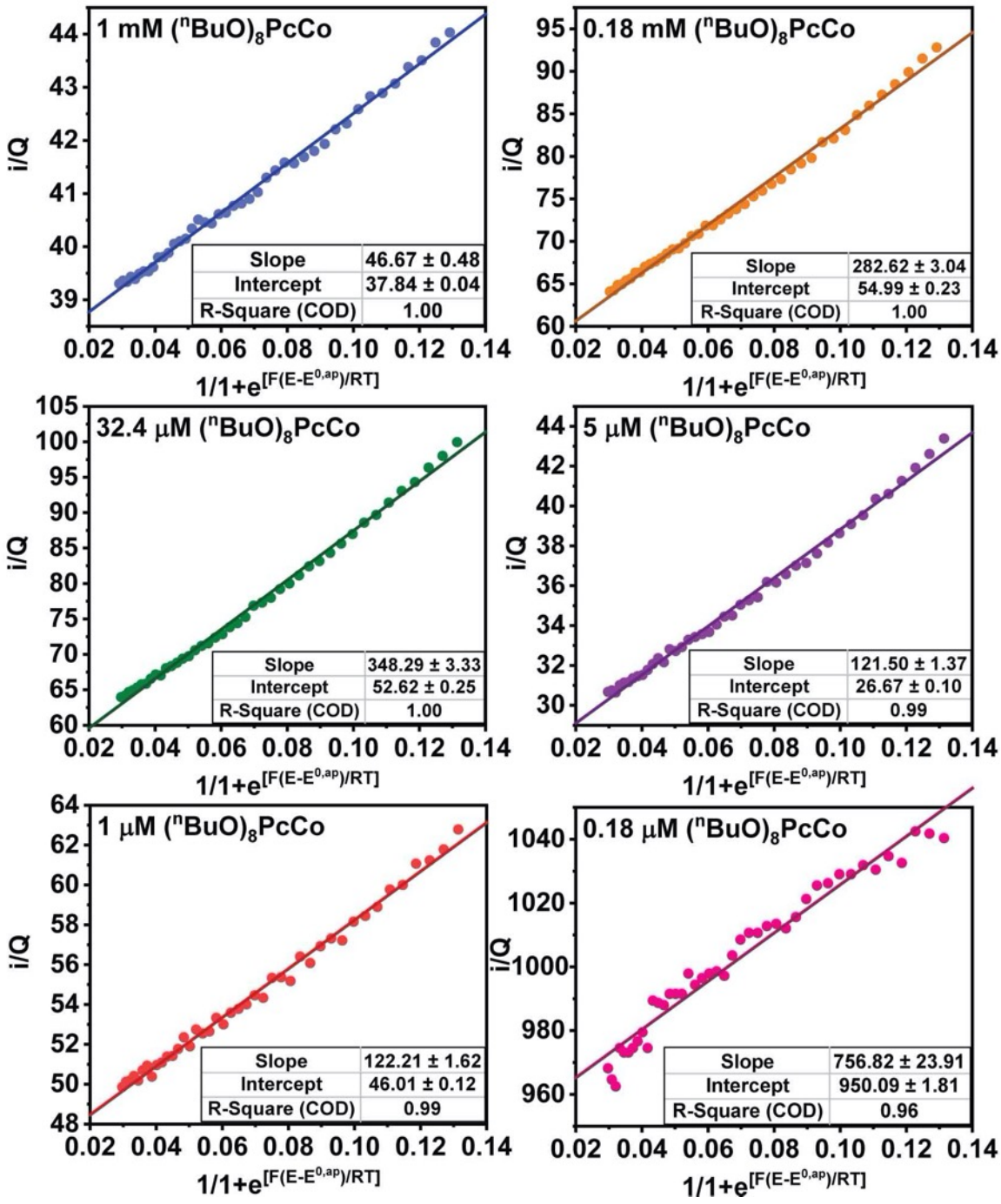

Figure S73. FOW plots for Run 3 of ^{nBuO}PcCo in six different deposition concentrations. Lines indicate the linear fits used to obtain rate constants (k).

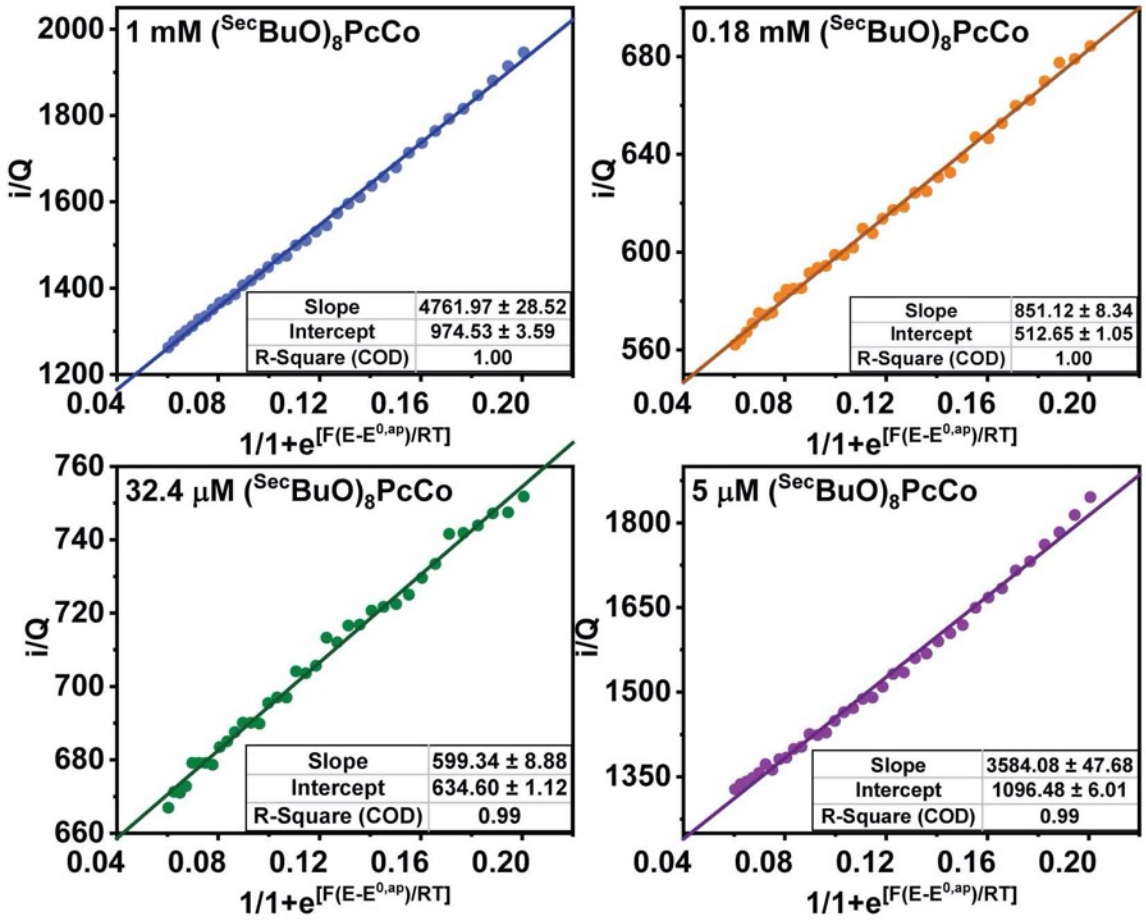

Figure S74. FOW plots for Run 1 of ^{secBuO}PcCo in four different deposition concentrations. Lines indicate the linear fits used to obtain rate constant (k).

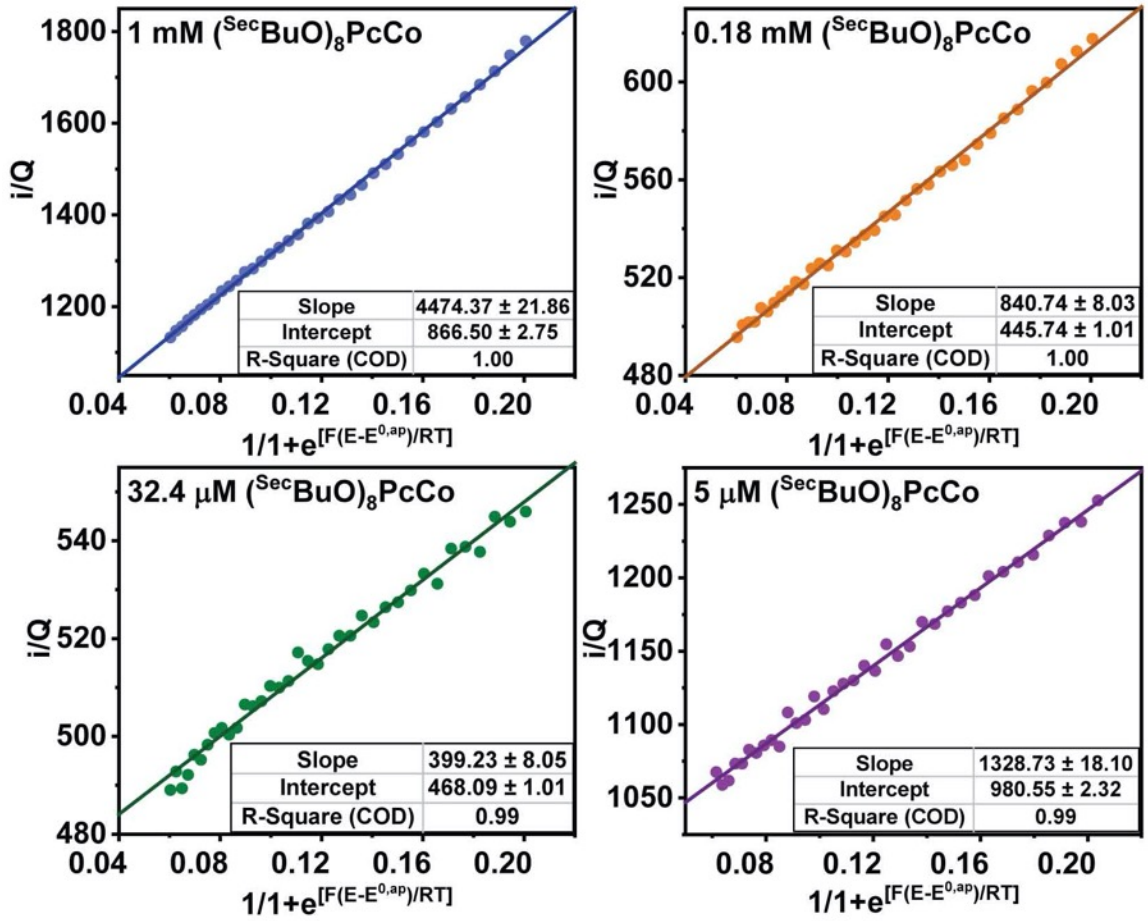

Figure S75. FOW plots for Run 2 of ^{secBuO}PcCo in four different deposition concentrations. Lines indicate the linear fits used to obtain rate constants (k).

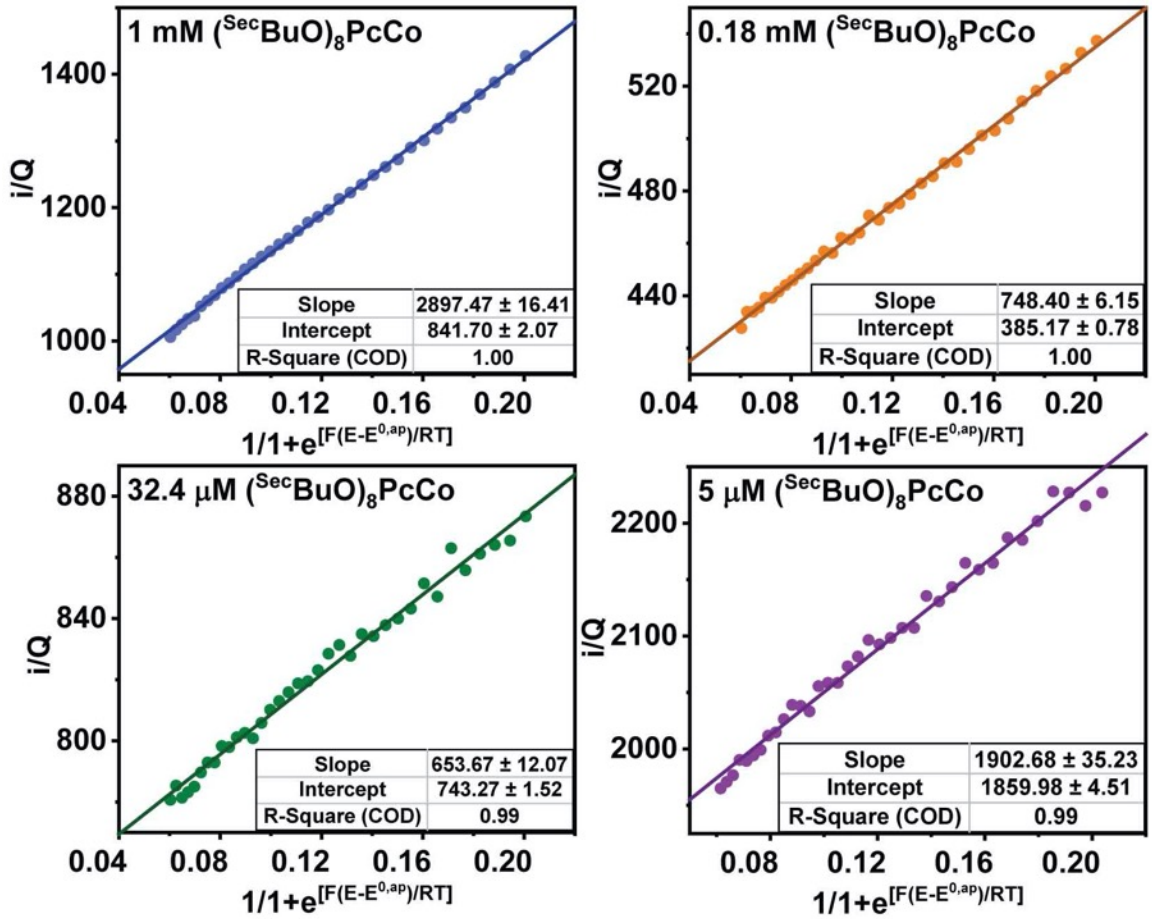

Figure S76. FOW plots for Run 3 of ^{secBuO}PcCo in four different deposition concentrations. Lines indicate the linear fits used to obtain rate constants (k).

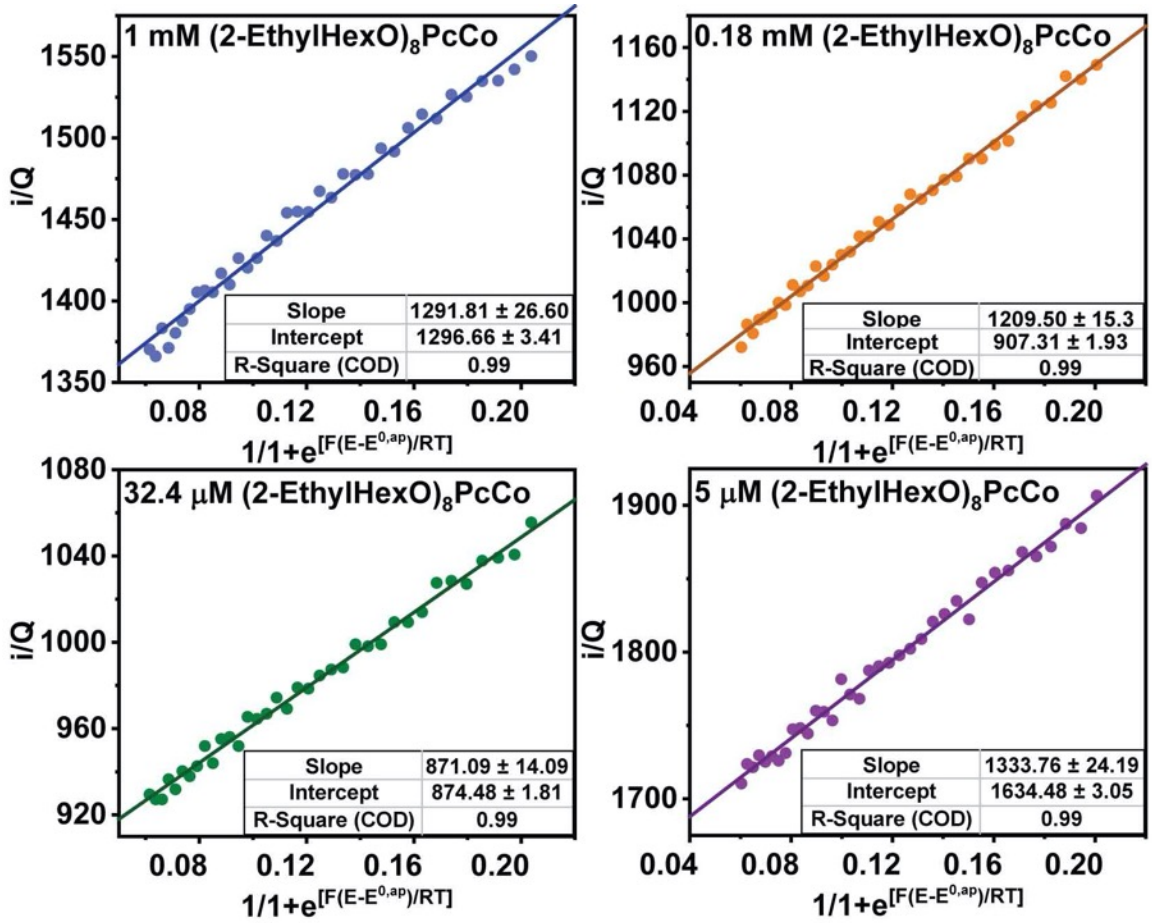

Figure S77. FOW plots for Run 1 of ^{EtHexO}PcCo in four different deposition concentrations. Lines indicate the linear fits used to obtain rate constant (k).

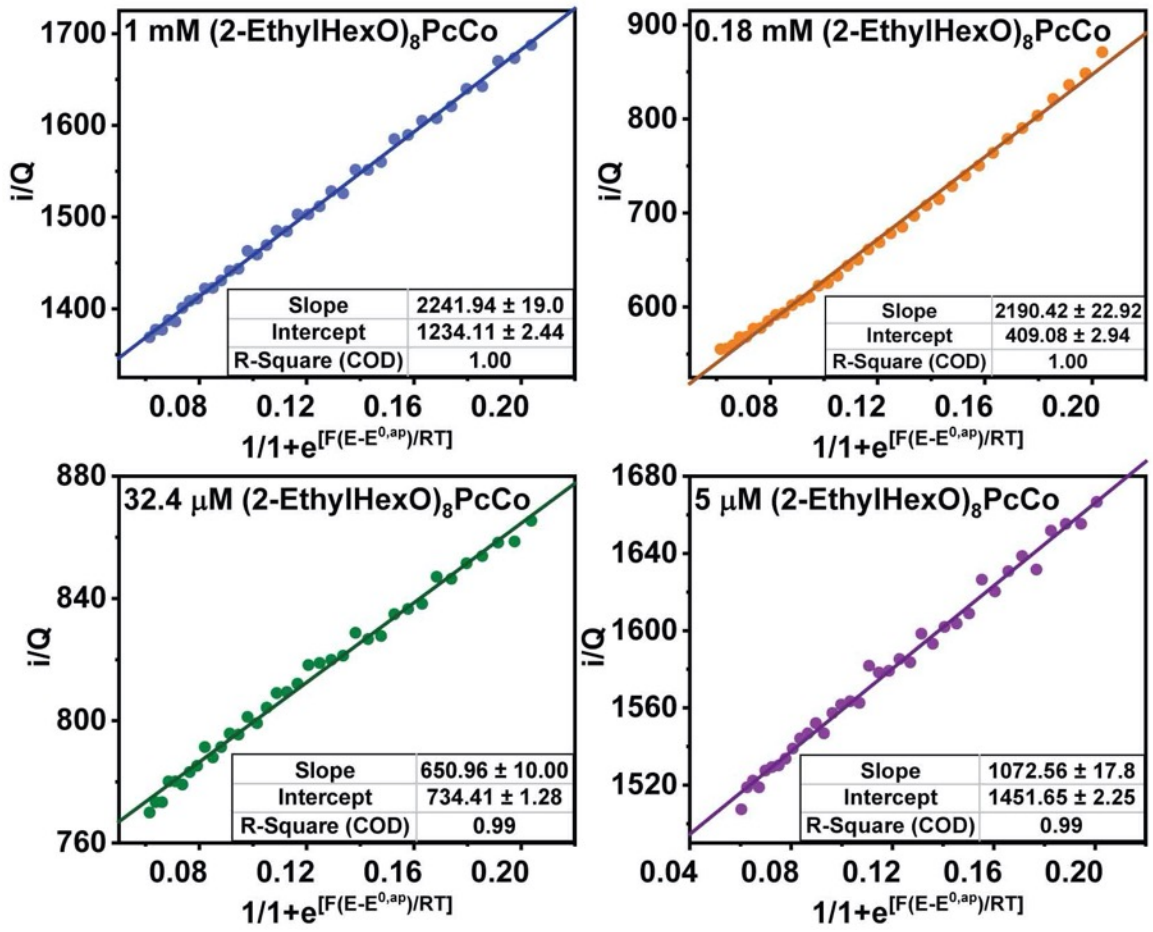

Figure S78. FOW plots for Run 2 of ^{EtHexO}PcCo in four different deposition concentrations. Lines indicate the linear fits used to obtain rate constants (k).

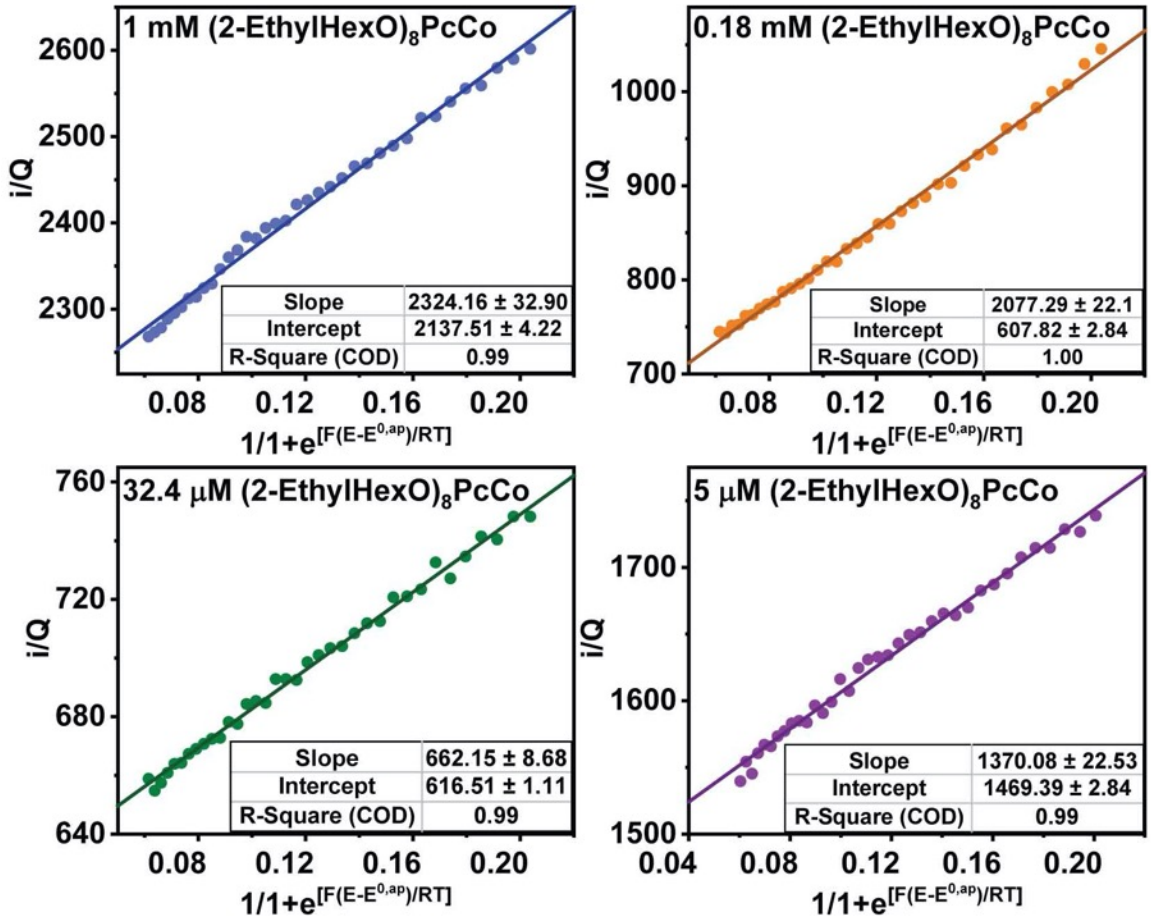

Figure S79. FOW plots for Run 3 of ^{EtHexO}PcCo in four different deposition concentrations. Lines indicate the linear fits used to obtain rate constants (k).

Kinetics parameters from plateau current analysis

$$\frac{i_{cat}}{i_p} = 2.2406 \sqrt{\frac{RT}{nFv} n' k_{obs}}$$

Values of k_{obs} values were calculated for each catalyst using the abov equation where i_{cat} is the maximum current density under CO_2, i_p is the peak current under argon, R, T, anf F have theis usual meanings, n is the number of electrons involved in CO_2 reduction (n = 1), is the scan rate, and n' is the number of catalyst molecules required for catalysis (n' =1). Errors in Table S4 are given to one standard deviation from three independent runs.

Table S4. Summary of k_{obs} values from plateau current analysis (s^{-1}).

	^{nBuO}PcCo	^{secBuO}PcCo	^{EtHexO}PcCo
1000 μM	530 ± 190	620 ± 70	240 ± 130
180 μM	97 ± 4	390 ± 100	580 ± 130
32 μM	63 ± 17	240 ± 40	240 ± 50
5 μM	130 ± 30	440 ±190	190 ± 20
1 μM	380 ± 90	270 ± 50	200 ± 40
0.18 μM	350 ± 90	520 ± 40	180 ± 30

(1) Forsyth, T. P.; Bradley, D.; Williams, G.; Montalban, A. G.; Stern, C. L.; Barrett, A. G. M.; Hoffman, B. M. A Facile and Regioselective Synthesis of Trans-Heterofunctionalized Porphyrazine Derivatives. *J. Org. Chem.* **1998**, *63* (2), 331–336.
(2) Gao, D.; Xu, H.; Yan, T.; Peng, B. The Synthesis of Symmetrically Octa-Substituted Phthalocyanines and Their Physical and Photo-Physical Properties. *Journal of the Chinese Chemical Society* **2001**, *48* (6B), 1189–1196. https://doi.org/10.1002/jccs.200100175.
(3) Cook, M. J.; Dunn, A. J.; Howe, S. D.; Thomson, A. J.; Harrison, K. J. Octa-Alkoxy Phthalocyanine and Naphthalocyanine Derivatives: Dyes with Q-Band Absorption in the Far Red or near Infrared. *Journal of the Chemical Society, Perkin Transactions 1* **1988**, No. 8, 2453–2458. https://doi.org/10.1039/p19880002453.
(4) Abdelkader, A. M.; Cooper, A. J.; Dryfe, R. a. W.; Kinloch, I. A. How to Get between the Sheets: A Review of Recent Works on the Electrochemical Exfoliation of Graphene Materials from Bulk Graphite. *Nanoscale* **2015**, *7* (16), 6944–6956. https://doi.org/10.1039/C4NR06942K.
(5) Bard, A. J.; Faulkner, L. R. Allen J. Bard and Larry R. Faulkner, Electrochemical Methods: Fundamentals and Applications , New York: Wiley, 2001, 2nd Ed. *Russian Journal of Electrochemistry* **2002**, *38* (12), 1364–1365. https://doi.org/10.1023/A:1021637209564.
(6) Matheu, R.; Neudeck, S.; Meyer, F.; Sala, X.; Llobet, A. Foot of the Wave Analysis for Mechanistic Elucidationand Benchmarking Applications in Molecular Water Oxidation Catalysis. https://doi.org/10.1002/cssc.201601286.